The role of serotonin in behavior

Shining light on the *maestro* of the brain

Patrícia Marçal Alves Correia

Dissertation presented to obtain the
Ph.D degree in Biology | Neuroscience

Instituto de Tecnologia Química e Biológica António Xavier | Universidade Nova de Lisboa

Research work coordinated by:

Champalimaud Foundation

FCT Fundação para a Ciência e a Tecnologia
MINISTÉRIO DA EDUCAÇÃO E CIÊNCIA

FUNDAÇÃO CALOUSTE GULBENKIAN
Instituto Gulbenkian de Ciência

Oeiras,
October, 2015

INSTITUTO DE TECNOLOGIA QUÍMICA E BIOLÓGICA ANTÓNIO XAVIER /UNL
Knowledge Creation

This work was developed in the context of the International Neuroscience Doctoral Programme (INDP) of the Champalimaud Research Programme, Champalimaud Center for the Unknown, Lisbon, Portugal. The project entitled "The role of serotonin in behavior: shining light on the maestro of the brain" was carried out at Instituto Gulbenkian de Ciência, Oeiras, Portugal and at the Champalimaud Research Programme, Champalimaud Center for the Unknown, Lisbon, Portugal, under the scientific supervision of Zachary Mainen, Ph.D, and under the guidance of the Thesis Committee composed by Rui Costa, Ph.D, and Marta Moita Ph.D. This work was supported by the fellowship SFRH / BD / 332774 / 2007 from Fundação para a Ciência e Tecnologia, Portugal.

À mudança

Acknowledgments

Esta longa expedição começou com a entrada no programa de doutoramento (PGCN), ainda em fase de criação. Obrigada aos nove que me acompanharam e com quem descobri as maravilhas do cérebro, em particular à Maria, à Margarida e ao Zé, pelas aventuras partilhadas. Um agradecimento especial ao Zach, Rui e Marta, por acreditarem em nós e por terem dedicado imensa energia (juntamente com outros) para criar o que é hoje o INDP e o Champalimaud Neuroscience Programme (CNP).

The next stop was San Francisco. Thank you Loren. It is known how important *baby steps* are for the future development. I am so thankful that my memorable first steps in neuroscience were given in your lab. Thank you Maggie, Caleb and the rest of the lab for your guidance and constructive support. Obrigada Rita Tavares por teres tornado esta etapa ainda melhor.

Back in Lisbon, it was an immense privilege to be part of the CNP construction. Thank you Zach for your eternal creative spirit, the inspirational out-of-the-box thinking, the *wings* and freedom that forced me to grow. Susana, Marta e Rui pelo apoio, força e motivação que sempre me transmitiram. To the lab for the conceptual discussions and the unifying moments. To Guillaume, Eran, Masa and Eric for the scientific guidance. To the 5-HT team for the shared suffering in the unknown moments. Sara por teres sido a minha 5-HT buddy. To Dhruba and Madalena for precious help. André, aquelas conversas. Gil, pela (improvável) cumplicidade. Rita pela tua criatividade contagiante e pelas

nossas aventuras fora da caixa (PS-isto não pára aqui). Maria, por seres a minha *irmã* científica nesta expedição e amiga no restante.

To all the CNP, for the magical moments. To Alfonso, for coordinating the INDP in the last years. To the CNP Admin unit, especially Teresa, for making all the bureaucracy easy. To Inês Soeiro and Ana Nunes for the valuable organization skills. To all the CNP Platforms for making sure everything runs smoothly in the lab.

I am very thankful also to the main institutions that supported my PhD: Instituto de Tecnologia Química e Biológica / Universidade Nova de Lisboa, Instituto Gulbenkian de Ciência, Fundação para a Ciência e Tecnologia and Fundação Champalimaud. It was an extraordinarily stimulant opportunity for the beginning of my career.

Por fim, constantes ao longo desta viagem... Obrigada aos meus pais, pelos genes que me deram e pelo amor, apoio e força que recebo cada dia. À minha irmã, pelo sempre. Aos meus amigos, pela vida além da ciência. À Catarina, por me obrigar a fazer *zoom out* nos momentos mais cinzentos. À Constança, por me relembrar a importância da investigação fundamental.

A Mario, per la rivoluzione in questa spedizione e por seres a minha casa.

Resumo

A serotonina (5-hydroxytryptamine, 5-HT) é um neuromodulador fundamental, envolvido em diversas funções cerebrais e doenças, incluindo a depressão e a ansiedade. No entanto, a função específica que a 5-HT desempenha no comportamento, permanece um mistério. Atualmente, existem três teorias principais que procuram explicar a ação deste complexo neuromodulador no cérebro: 1) inibição comportamental; 2) hipótese sensorio-motora; 3) ação de recompensa. A vasta literatura sobre o sistema serotonérgico apresenta resultados ambíguos e, por vezes, contraditórios, devido, em parte, às limitações metodológicas das abordagens existentes de farmacologia e de fisiologia.

A fim de ultrapassar esta limitação técnica, desenvolvemos uma estratégia nova de optogenética para controlar especificamente neurónios de 5-HT no núcleo dorsal da rafe (DRN), a principal fonte de projeção de 5-HT para o prosencéfalo. Numa primeira fase, validaram-se e otimizaram-se os parâmetros de estimulação, a fim de ativar especificamente os neurónios de 5-HT no DRN, *in vitro* e *in vivo* (Dugué *et al*. 2014). Posteriormente, aplicou-se esta metodologia para testar se a ativação rápida e específica dos neurónios de 5-HT no DRN interferia com respostas sensoriais num teste mecano-sensorial. Foi descoberto que a ativação dos neurónios de 5-HT no DRN promovia uma diminuição rápida e reversível da resposta do animal ao estímulo sensorial. Os resultados demonstram uma nova evidência concordante com

ambas as teorias, de inibição comportamental e da hipótese sensorio-motora.

Para apurar a função da serotonina no comportamento, usou-se a mesma metodologia optogenética para avaliar o papel da 5-HT no movimento. Foi realizado um conjunto de experiências, com a finalidade de testar o efeito da ativação dos neurónios de 5-HT no DRN em diversas tarefas comportamentais, incluindo a arena aberta (*open field*) e testes de coordenação motora. A estimulação dos neurónios de 5-HT no DRN induziu a uma diminuição drástica da velocidade dos animais que se moviam na arena, sem quaisquer efeitos nas medidas clássicas de ansiedade. Por outro lado, usando a mesma metodologia, não foram observadas modificações significativas na coordenação motora dos animais, usando os testes do *rotarod* e *LocoMouse*.

Em seguida, para explorar o efeito da 5-HT em ações de recompensa, foi testado um protocolo de estimulação, confinado a uma sub-região da arena. Não foram observados quaisquer efeitos de reforço positivo ou negativo. Estes resultados revelam que a ativação de neurónios de 5-HT no DRN é suficiente para inibir o movimento dos animais, sem afectar a sua coordenação motora, e induzir estados de ansiedade ou respostas de reforço positivo/negativo.

Estudos prévios propuseram que a 5-HT desempenha um papel inibitório no comportamento sexual masculino. Para aprofundar esta questão, foram ativados os neurónios de 5-HT no DRN de ratinhos macho, enquanto os animais interagiam sexualmente com fêmeas da mesma espécie. A estimulação não produziu

mudanças significativas no número e na duração de montas, no número de intromissões, nos intervalos entre montas e no tempo de ejaculação. Postulou-se que a modulação serotonérgica do comportamento sexual poderá envolver outras áreas específicas do cérebro, formas alternativas de ativação, ou afectar aspetos mais subtis do comportamento.

A técnica de optogenética permite controlar o efeito da 5-HT no comportamento, de forma especifica e rápida. Com base nos resultados obtidos e, aqui apresentados, propõe-se que a 5-HT desempenha uma função inibitória no comportamento, excepto quando o animal se encontra num estado de motivação elevada, como, por exemplo, durante a interação sexual ou durante a corrida para obter recompensa.

Os estudos publicados nesta dissertação prestam um contributo fundamental às investigações já realizadas até ao momento com resultados pertinentes que permitem distinguir o papel deste neuromodulador na inibição do comportamento, para além de fomentarem a realização de outros trabalhos de investigação que promovam o conhecimento das funções da 5-HT no campo das neurociências.

Abstract

Serotonin (5-hydroxytryptamine, 5-HT) is a major neuromodulator linked to a disparate set of brain functions and disorders including depression and anxiety, but its fundamental roles in behavior remain a mystery. Three main theories for 5-HT function attempt to unravel how this complex neuromodulator acts in the brain: 1) behavioral inhibition, 2) sensorimotor hypothesis and 3) reward action. The vast literature in the 5-HT field is hard to reconcile and presents ambiguous results, due in part to the limitations of traditional pharmacological and physiological methods.

We developed an optogenetic strategy to specifically target and manipulate 5-HT neurons in the dorsal raphe nuclei (DRN), the main source of 5-HT to the forebrain. We started by optimizing and validating the DRN 5-HT photostimulation parameters, both *in vitro* and *in vivo* (Dugué et al. 2014). We then employed this approach to test if transient and specific activation of DRN 5-HT neurons in behaving mice interfered with sensory responses in a mechanosensitivity assay. We found that activation of DRN 5-HT neurons displayed a rapid and reversible decrease in the animal's responses to plantar stimulation. Our findings provided a new level of evidence for both the sensorimotor hypothesis and the behavioral inhibition theory.

To further explore the role of 5-HT in behavior, we used the same optogenetic strategy to study the function of 5-HT in movement. We performed a set of experiments examining the effects of

optogenetic activation of DRN 5-HT neurons in both an unconstrained environment and in a series of tasks to assess motor coordination. We found that photostimulation of DRN 5-HT neurons induced a dramatic decrease in speed of mice running in an open field arena, with no effects in the classical measures of anxiety. In contrast, using the same optogenetic approach, we found no evidence of motor coordination impairment in the accelerating rotarod and linear track locomotion tests. Next, we confirmed the absence of an appetitive or aversive effect of DRN 5-HT activation, in a task with photostimulation constrained to a sub-region of the open field, under non-rewarding or non-punishment conditions. These results provide direct evidence of sufficiency of DRN 5-HT activation in inhibiting movement, without affecting motor coordination and anxiety-like parameters or promoting reinforcing responses.

Finally, we investigated the role of 5-HT in male sexual behavior, where it has been proposed to have an inhibitory effect. We optogenetically activated DRN 5-HT neurons, in sexually aroused males and found no significant changes in number and duration of mounts, intromissions, inter-mount intervals and latency to ejaculate. We hypothesized that 5-HT modulation of male sexual behavior might involve other specific pathways and/or alternative forms of activation, or it may affect more subtle aspects of the behavior.

Optogenetic techniques allowed us to access the effect of 5-HT transients in behavioral actions at a very fast timescale. Based on our findings, we proposed that 5-HT acts in the brain with an

inhibitory function, unless the animal is already engaged in a highly motivated state (eg. mating, or running to get reward). The present series of studies contribute to 5-HT research in neuroscience, advancing the current understanding of 5-HT function and more specifically clarifying its role in behavioral inhibition.

Abbreviations list

5-HT	5-hydroxytryptamine, serotonin
AAVs	Adeno-associated viruses
AOM	Acousto-optical modulator
ChR2	Channelrhodopsin-2
DRN	Dorsal raphe nuclei
GABA	γ-Aminobutyric acid
GPCR	G protein coupled receptors
MRN	Median raphe nuclei
ROI	Region of interest
SERT	Selective 5-HT transporter
SSRIs	Serotonin reuptake inhibitors
TPH	Tryptophan hydroxylase
VTA	Ventral tegmental area
WT	Wild type
YFP	Yellow fluorescent protein

Figure Index

Supplemental Figure Index

Table Index

Contents

1 General Introduction

The flutes start gently rising. In a very precise moment the violin initiates and immediately after, the contrabassoon. Innumerous sounds are playing in a non-synchronous way, yet with coordination and harmony. Who is maintaining this organization, silencing the oboe, while activating the tuba? Who communicates with all instruments, ensuring a healthy orchestra?

1.1 Serotonin: the *maestro* of the brain

Serotonin (or 5-hydroxytryptamine, 5-HT) is one of the main *conductors* of the brain. Discovered by the Italian scientist Vittorio Erspamer (Vialli & Erspamer 1937), 5-HT was noticed for causing smooth muscle contraction in the gastrointestinal tract. It was years after its characterization (Rapport et al. 1948) that 5-HT was proposed to be a neurotransmitter (Brodie & Shore 1957), the third one to be found.

5-HT, together with other neuromodulators like dopamine, acetylcholine and norepinephrine have the fundamental role of modulating different neuronal populations, ensuring a balanced functioning of the whole brain *orchestra*. In detail, 5-HT has a crucial role in regulating a huge variety of brain processes, including sleep, movement and social behaviors. However, the exact mechanism of 5-HT action in behavior is still enigmatic.

The present work has investigated the role of 5-HT in diverse behavioral contexts, by employing a combination of optogenetic and behavioral approaches.

In the following sections, we will: explore the anatomical organization and neurophysiology of the serotonergic system (**1.2 Serotonergic system**); review some of the main theories proposed for 5-HT function (**1.3 Theories and hypothesis of 5-HT**); consider the different methodological challenges to study 5-HT in the brain (**1.4 Technical barriers**); and suggest how to overcome these limitations, by applying optogenetic approaches

to investigate the role of 5-HT in behavior (**1.5 Optogenetics: the new neuroscience era**).

1.2 Serotonergic system

5-HT is a biogenic monoamine produced through the hydroxylation of tryptophan and its subsequent decarboxylation (Clark et al. 1954). The vast majority of body's 5-HT is located in the periphery, mainly stored in platelets and enterochromaffin cells. Within the central nervous system, 5-HT is synthesized and stored in the presynaptic neurons. Upon neuronal depolarization, 5-HT is released into the synaptic cleft. It can bind to postsynaptic 5-HT receptors or 5-HT autoreceptors on the presynaptic membrane (Cerrito & Raiteri 1979). Binding of 5-HT to the autoreceptor acts as a negative feedback against further release of 5-HT into the synaptic cleft (Cerrito & Raiteri 1979). The highly selective 5-HT transporter (SERT) located on the presynaptic membrane is responsible for removing 5-HT from the synaptic cleft. Once transported into the presynaptic neuron, 5-HT is recycled back into presynaptic vesicles where it is protected from metabolism.

The serotonergic system is incredibly complex, featuring seven families of 5-HT receptors (5-HT$_{1–7}$; Hoyer et al. 1994), further divided into a total of at least seventeen 5-HT receptors (Bockaert et al. 2010). The 5-HT receptor is a phylogenetically ancient receptor (evolved over 750 million years ago) and is present in

the lowest of invertebrates as well as the higher mammals (Peroutka & Howell 1994). Most 5-HT receptors are G-protein coupled receptors (except for 5-HT_3 which is a ligand-gated ion channel; Derkach et al. 1989) and exhibit heterogeneity with both excitatory and inhibitory functions.

Within the central nervous system, 5-HT is located in nine groups of neurons isolated in the pons and midbrain (Dahlstroem & Fuxe 1964). The raphe nuclei constitute the major 5-HT area in the brain, with both ascending 5-HT fibers projecting to the forebrain and descending fibers that extend to the medulla and spinal cord (Dahlstroem & Fuxe 1964). Raphe nuclei are evolutionarily conserved across fish, amphibians, up to mammals. In rodents, the more posterior raphe nuclei provide serotonergic innervation to the spinal cord, the brainstem itself, and some cerebellar areas. The more anterior nuclei, dorsal (DRN) and median raphe (MRN) provide extensive serotonergic innervation to the forebrain and midbrain. DRN and MRN together constitute 80% of the serotonergic innervation to the forebrain (Azmitia & Segal 1978). In detail, DRN fibers are widely distributed throughout the forebrain, including ventral midbrain, lateral hypothalamus, midline thalamus, amygdala, striatum and most of the cortex. In contrast, MRN projects preferentially to the hippocampus, septum and other forebrain structures lying on or close to the midline (Vertes & Linley 2008).

DRN constitutes approximately 50% of the total 5-HT neuronal population in the brain (Steinbusch 1981; Descarries et al. 1982), being the structure with highest density of 5-HT neurons. Apart

from the vast set of projections, DRN also receives afferents from many brain structures, including cortical, limbic and brainstem areas. Recent studies using rabies tracing strategies, combined with cell-type-specific cre-driver mouse lines, confirm 5-HT DRN inputs from prefrontal cortex, lateral habenula, ventral striatum and lateral hypothalamus, highlighting the diversity of the serotonergic brain map (Weissbourd et al. 2014; Pollak Dorocic et al. 2014; Ogawa et al. 2014).

The complexity of 5-HT is not limited to receptor's subtypes and anatomical organization. DRN comprises also a variety of other cell types, including dopamine, GABA, glutamate and other neuropeptides (Araneda et al. 1980). In fact, 5-HT neurons represent only about one third of the DRN neurons (Jacobs & Azmitia 1992). Given such diversity, it is not surprising that electrophysiological recordings from DRN putative 5-HT neurons show a wide variety of responses (Jacobs & Azmitia 1992; Veasey et al. 1997; Ranade & Mainen 2009).

In summary, DRN is the major container of 5-HT, with impressive morphological, anatomical and neurochemical heterogeneity.

1.3 Theories and hypothesis of 5-HT

5-HT is a critical neuromodulator, investigated in diverse animal models, with a variety of different functions. Amongst these, 5-HT is involved in mediating behavioral state changes related with

food deprivation (Groome et al. 1993) and sensitization of defensive reflexes (Sahley 1995) in the leech and locomotion, eating and foraging (Horvitz et al. 1982; Sawin et al. 2000; Flavell et al. 2013) in the nematode *C. elegans*. Furthermore, 5-HT induces behavioral gregarization in the locusts (transformation from solitary to group formation, Anstey et al. 2009) and affects social dominance in the lobster (Kravitz 1988).
In mammals, 5-HT is "*leaving fingerprints in the scene of many crimes*" leading to a disparate set of theories and hypothesis. Some of the most relevant 5-HT theories are going to be reviewed in the following section, with a primary focus on the rodent literature (since the original studies here described use the mouse as animal model).

1.3.1 5-HT in behavioral inhibition

Brodie and Shore originally proposed a general role for 5-HT in behavioral inhibition, in contrast with the presumed excitatory role of norepinephrine (Brodie & Shore 1957). Subsequent studies focused on the hypothesis that 5-HT constrains the response of organisms to external stimuli (usually aversive) and that 5-HT absence potentiates that response (Soubrié 1986; Depue & Spoont 1986). This argument is largely supported by a set of 5-HT depletion studies showing increase pain sensitivity (Tenen 1967), increase exploration or locomotor activity (Gately et al. 1985; Eagle et al. 2009), increase startle behavior (Davis & Sheard 1974; Davis et al. 1980), increase the output of operant behavior suppressed by punishment (reviewed in Dayan & Huys

2009), increase aggression (Vergnes et al. 1986) and facilitation of male sexual behavior (Dewsbury & Davis 1970; Dewsbury et al. 1972).

Consistent with the behavioral inhibition theory is the set of studies relating 5-HT with impulse control, one of which from our lab (Fonseca et al. 2015). DRN neurons are active while rats wait for delayed rewards and delayed reward predictive cues (Miyazaki et al. 2011) and blocking DRN 5-HT activity increases premature responding (Miyazaki et al. 2012). More recently, it was confirmed with optogenetic techniques that activation of DRN 5-HT neurons suppresses impatient responses (Miyazaki et al. 2014; Fonseca et al. 2015) .

Another line of research found 5-HT encoding aversive outcomes very attractive, giving rise to the 5-HT and dopamine opponency theory, with observations at the anatomical, physiological and biochemical levels (Deakin & Graeff 1991; see also Cools et al. 2011 for review). The opponency hypothesis has also been formally extended to a computational version (Daw & Daw 2002; Dayan & Huys 2008). Dopamine has long been associated with behavioral rewards, having two main behavioral functions: 1) motor facilitation or activation and 2) reward-driven learning, through reward prediction error signaling (Schultz et al. 1997). Under the opponency hypothesis, 5-HT is suggested to play a negative functional counterpart of DA with two proposed roles: 1) mediation of behavioral inhibition and 2) mediation of aversive learning or negative prediction errors (reviewed in Dayan & Huys

2009). However, diverse behavioral and clinical studies using 5-HT and dopamine manipulations demonstrate a rather cooperative function between these two neuromodulators (reviewed in Boureau & Dayan 2011). More recently, the opponency framework has been experimentally tested in classical conditioning learning paradigms, by monitoring DRN 5-HT activity with electrophysiological recordings (Cohen et al. 2015) and bulk fluorescence imaging (Matias et al. submitted). While the first study reveals that 5-HT neurons respond to reward predicting cues and punishments, the latter shows that, similar to dopamine, 5-HT neurons are activated by prediction violations. However, unlike dopamine neurons which are activated by better-than-expected outcomes, for 5-HT neurons the valence of these violations is not important. This finding suggests that the opponency theory might need to be re-interpreted in a different manner. It will be important to further explore this theory, extending it to different behavioral contexts, also without the conditional learning component. Social behaviors, in detail male-female sexual interactions, are good candidates for testing the opponency hypothesis, as dopamine and 5-HT seem to play a crucial role in maintain a balanced sexual cycle (reviewed in Pfaus 2009). However, the nature of the modulation and the exact pathways involved in this interaction are still lacking experimental support.

1.3.2 5-HT in sensorimotor function

A second major theory of 5-HT function is based in the sensorimotor hypothesis. Jacobs first proposed that the main role of 5-HT is to facilitate motor output and suppress ongoing processing of sensory input during motor behavior (reviewed in Jacobs & Fornal 1997). Initial evidence to support this theory comes from the finding that 5-HT activity is silent during REM sleep, a state of movement paralysis (Lai & Siegel 1988). Moreover, 5-HT infusion into the forebrain reduces the acoustic startle reflex in rats, but enhances this response when infused onto the spinal cord (Davis et al. 1980). The positive link between 5-HT and motor output became more clear with subsequent electrophysiological studies, correlating raphe neurons with central pattern generators (Martín-Cora et al. 2000; see also Clark et al. 2004 for review). Although most of the putative 5-HT motor control is associated with the more caudal raphe nuclei neurons, Jacobs suggests an involvement of the cat DRN neurons in oral-buccal behavior patterns, such as chewing, licking, biting, grooming (Fornal et al. 1996). In the same experiment, DRN activity seems to be resistant to somatosensory stimuli, but surprisingly silent during orientation to a strong external stimulus (sudden opening of a door). These results motivated Jacobs to propose that 5-HT neurons tonically inhibit sensory processing and facilitate motor output (reviewed in Jacobs & Fornal 1997). The sensory interaction part of this hypothesis receives further confirmation (Müller et al. 2007; Pum et al. 2008) and it is supported by the findings that boosting 5-HT activity attenuates pain responses (Reyes-Vazquez et al. 1989; Wang & Nakai 1994).

Studies examining the effect of 5-HT release on sensory processing reveal that raphe electrical stimulation inhibits somatosensory responses in the neocortex (Sheibani & Farazifard 2006; Mantz et al. 1990), thalamus (Dong et al. 1991), and brainstem (Chiang et al. 1989). Furthermore, local application of broad-spectrum 5-HT receptor agonists attenuates odor-evoked olfactory receptor neurons activity, supporting the idea that 5-HT suppresses olfactory inputs (Petzold et al. 2009). More recently, a study from our lab also described that DRN 5-HT activation attenuates firing of anterior piriform cortex neurons (Lottem et al. submitted).

Overall, the sensorimotor hypothesis also considers a general inhibitory role for 5-HT. Although it sketches a relatively coherent scenario of the physiological effects of 5- HT, it still lacks a coherent connection to behavior itself. Unlike the behavioral inhibition theory (more specifically the dopamine opponency hypothesis), the sensorimotor theory also gives no insight into why 5-HT would be an important modulator of mood, emotion or any other of its psychoactive properties. These two theories, while not completely inconsistent, remain to be further connected.

1.3.3 5-HT in reward

An alterative theory suggests a role for 5-HT in reward and reinforcing behaviors. This hypothesis is based on the evidence that putative 5-HT neurons in the DRN respond to reward (Nakamura et al. 2008; Ranade & Mainen 2009; Bromberg-

Martin et al. 2010; Inaba et al. 2013; Cohen et al. 2015; Matias et al. submitted) and that 5-HT depletion impairs reward processing (Rogers et al. 2003; Seymour et al. 2012). A more recent study shows that optogenetic activation of DRN 5-HT neurons positively reinforces several behaviors (Liu et al. 2014). Again, as with any other 5-HT theory, when a function is proposed, other findings prove it wrong. Two studies used a similar optogenetic approach, but failed to observe 5-HT reinforcing effects (Miyazaki et al. 2014; Fonseca et al. 2015). It was even proposed that the rewarding effect in the DRN is preferentially non-serotonergic (McDevitt et al. 2014), thus suggesting that different subsets of DRN neurons might have different effects in behavior. In fact, in Liu et al.'s study, the authors claim to affect also glutamatergic, besides 5-HT neurons in DRN (Liu et al. 2014; reviewed in Luo et al. 2015). It seems critical to further investigate the role of specific DRN 5-HT neurons in appetitive behaviors, using unconstrained behavioral paradigms.

In agreement with the 5-HT reward theory and its complexity is the collection of psychopharmacological data implicating 5-HT in animal models of depression and anxiety (Leonard 1987; Graeff et al. 1996; Maier & Watkins 2005). In humans, selective 5-HT reuptake inhibitors (SSRI) have been demonstrated to be effective in treating major depression and are the most popularly prescribed class of antidepressant drugs. SSRIs act by inhibiting 5-HT uptake and thus increasing synaptic levels of 5-HT. Dietary depletion of tryptophan leads to clinical relapse in depressed

patients who were successfully treated with SSRIs (Delgado et al. 1991; Heninger et al. 1996), thus suggesting that enhanced 5-HT transmission is necessary to maintain the therapeutic effectiveness of antidepressants.

Efforts to model human affective disorders in animals comprise both animal models of depression and animal behavioral tests sensitive and selective for detecting antidepressant drugs (Willner 1990). The forced swimming test (Porsolt et al. 1978) is one of the most frequent behavioral assays used to measure potential antidepressant activity. Effects of SSRIs were reported either to be active, inactive, or active only at high doses in this behavioral test (reviewed in Borsini 1995). A recent study using optogenetic methods shows that activating the pathway that connects medial prefrontal cortex with DRN has a robust impact in forced swimming behavior (Warden et al. 2012).

Another commonly used behavioral test is the open field assay (Seibenhener & Wooten 2015). Originally designed to score defecation as a measure of animals' 'emotionality' (Hall 1934), the open field provides an initial screen for anxiety-related behavior in rodents (Bailey & Crawley 2009). Once again, pharmacological manipulations reveal all possible combinations: 5-HT promotes, reduces, or has no effect in anxiety-like behaviors (see Prut & Belzung 2003 for review). A recent optogenetic study shows no involvement of DRN in anxiety, whereas photostimulation of MRN induces anxiolytic behavior (Ohmura et al. 2014). Open field studies are frequently combined

with other behavioral tests and significant effort has been made to overcome the complexity of the serotonergic system and pinpoint its mechanism in anxiety circuitry. As an example, the receptor 5-HT1a is expressed both in 5-HT (auto-receptor) and non-5-HT neurons (hetero-receptor). The importance of both neuronal populations has been highly debated, and it seems that 5-HT1a auto-receptors are necessary, but not sufficient, to modulate anxiety (Piszczek et al. 2013). Further studies manipulating the activity of 5-HT neurons should help shine light on the exact role of 5-HT in anxiety-like behaviors.

In summary, you have been guided through three main theories for the role of 5-HT in behavior: 1) behavioral inhibition, 2) sensorimotor and 3) reward functions. However, these three dots are still very challenging to connect. Behavioral inhibition can help explain the 5-HT connection to depression and anxiety, but prediction of aversive outcomes seems opposite to reward coding. The sensorimotor hypothesis focus on a different data set, giving insight on 5-HT physiological function, but lacks behavioral connection.

In the present set of studies, we aimed to experimentally test these theories in spontaneous behaviors, as general locomotion and sexual behavior. We hypothesize that behavioral inhibition is the best candidate theory to describe the role of 5-HT in behavior, but possibly with different mechanisms of action.

1.4 Technical barriers

Despite the valuable efforts of numerous pharmacological, physiological and genetic experiments, the role of 5-HT in behavior is not well understood. The reason for such mystery is in part the heterogeneity of the 5-HT system, but also the technical limitations of most of the methods employed so far.

While pharmacological experiments provide reasonable specificity for 5-HT, they lack temporal resolution, acting like modulators rather than controllers of 5-HT function. This is problematic because transient bursts of activity in 5-HT neurons are likely to be important to 5-HT function (Nakamura et al. 2008; Ranade & Mainen 2009). The sensitivity of receptors to the time course of transmitter concentration depends on their affinity, with higher affinity receptors, which unbind transmitter more slowly, being more sensitive to slow, tonic changes. Therefore, low-affinity 5-HT receptors (including 5-HT1a) and high-affinity receptors (including 5-HT2a) will be more sensitive to phasic and tonic 5-HT levels respectively (Glennon et al. 1995). Because 5-HT1a and 5-HT2a receptors have opposite effects on signal transduction pathways, tonic manipulations of 5-HT may in fact have the opposite effect of phasic signals (reviewed in Dayan & Huys 2009). Consequently, different affinity receptors may influence similar 5-HT-mediated responses, but in very different ways, such as the role of 5-HT1a and 5-HT2c receptors in anxiety (Glennon & Lucki 1988).

Another common approach is to use knockout mouse lines. While an animal model lacking 5-HT neurons is non-viable, it is possible to create viable knockouts lacking a particular 5-HT receptor (Stark et al. 2007). Although behavioral changes can be observed in these lines, the impact cannot be easily attributed to the specific loss of that receptor subtype, given the many compensatory changes in 5-HT neurons and other neurotransmitter systems involved. Additionally, this genetic manipulation affects the expression of the 5-HT receptors throughout the brain.

Electrical stimulation is another used method that allows a targeted manipulation to the raphe nuclei neurons, providing also temporal specificity. The results of some electrical stimulation studies are in agreement with the inhibition theory, producing cessation of ongoing appetitive behavior, "freezing" responses and/or sedation (Kostowski et al. 1969; Graeff et al. 1978). However, others have produced equivocal or even contradictory effects, such as increased arousal (Jacobs et al. 1973). Electrical stimulation of the raphe nuclei also inhibits neural activity in sensory systems (Sheibani & Farazifard 2006; Dong et al. 1991; Mantz et al. 1990), but the behavioral effects on sensory processing have not been assayed. The ambiguity and diversity of results with electrical stimulation of the raphe nuclei are likely to be due to its lack of cellular or neurochemical specificity. The importance of this issue is especially critical because 5-HT neurons are embedded in heterogeneous networks containing

abundant non-5-HT neurons, including dopaminergic and GABAergic neurons. Electrical stimulation may also activate the dense nerve fascicles containing descending and ascending spinal tracts (Fardin et al. 1984).

In order to overcome these technical limitations, a new method has emerged, hopefully to shine light on the mysteries of 5-HT functions.

1.5 Optogenetics: the new neuroscience era

I was fortunate to develop my thesis during an evolutionary memorable moment for neuroscience: the optogenetics boom. The introduction of genetically-based methods for stimulating, silencing and monitoring neuronal activity has been an exciting breakthrough discovery for the field. Most notable among the (now) vast list of optogenetic tools is the photosensitive protein channelrhodospin-2 (ChR2, Nagel et al. 2003). ChR2 is a light-gated monovalent cation channel isolated from a green algae, which opens upon exposure to blue light (activation maximum at 470 nm). Light can be delivered to ChR2- expressing neurons either directly from the surface or through fiber optics inserted in desired brain regions (Han & Boyden 2007). The efficacy of ChR2 to drive neurons has been confirmed in acute slices (for example, Aravanis et al. 2007; Arenkiel et al. 2007; Zhang et al. 2007; Wang et al. 2007) and *in vivo* electrophysiological recordings (for example, Lima et al. 2009; Arenkiel et al. 2007).

A growing number of recent studies have shown that behavioral responses can be evoked by light in mice engineered to express ChR2 in specific brain regions and/or neuronal types (for an overview see Boyden 2015; Deisseroth 2015). The use of ChR2 provides considerable advantages compared to the previous described manipulations, since it allows for selective, rapid and reversible activation of genetically defined populations of neurons embedded in complex circuits.

The mysterious 5-HT system (as well as other neuromodulatory systems) owns the most important flavors for the application of optogenetic methods: clear genetic specification and compact localization of the 5-HT neurons. There are now available two mouse lines (Scott et al. 2005; Zhuang et al. 2005) and two viruses lines (Benzekhroufa et al. 2009a; Benzekhroufa et al. 2009b) to allow specifically targeting of 5-HT neurons. Indeed, such tools have recently placed the 5-HT system in the spotlight and several groups are studying the effect of stimulating various types of DRN neurons on several behavioral tasks (reviewed in Luo et al. 2015).

Throughout this thesis, ChR2 was used to specifically activate DRN 5-HT neurons. Because inactivation of ChR2 and autoinhibition of 5-HT neurons may limit the efficiency of photostimulation, we optimized the stimulation parameters (frequency, amplitude and duration of pulses) *in vitro* and *in vivo* (**Chapter 2**). After validation of the stimulation parameters, we

tested some 5-HT theories, by applying optogenetic perturbations in diverse behavioral assays (**Chapter 2-4**).

1.6 Thesis expedition *guide*

My primary motivation was to explore the "whats" and the "hows" of 5-HT in the brain and behavior. This *expedition* started with the implementation of an optogenetic strategy to study the serotonergic system, a novel method at that moment. We validated and optimized the photostimulation conditions to activate DRN 5-HT neurons in behaving animals (**Chapter 2**, Dugué et al. 2014) and kept this tool for the rest of the *trip*. Next, we tested the effect of 5-HT in spontaneous movement, using the open field test, where animals freely behave, in no reward and no punishment conditions. We found that DRN 5-HT activation induced a dramatic decrease of speed in the animals (**Chapter 3**). The effect was robust throughout many days and did not seem to affect motor coordination, anxiety-like or aversive and appetitive responses. Finally, we went on a preliminary journey to investigate the role of 5-HT in sexual behavior, an ethological relevant behavior. We confirmed the existence of variability in biology and challenged the role of DRN 5-HT neurons in male copulatory behavior (**Chapter 4**). We were able to narrow down some "whats", leaving space for future explorations to resolve the "hows" of 5-HT in behavior (**Chapter 5**).

2 Optogenetic recruitment of dorsal raphe serotonergic neurons acutely decreases mechanosensory responsivity in behaving mice

Results published: Dugué GP, Lorincz ML, Lottem E, Audero E, Matias S, Correia PA, Léna C, and Mainen ZF. (2014) Optogenetic recruitment of dorsal raphe serotonergic neurons acutely decreases mechanosensory responsivity in behaving mice. PLoS ONE 9(8): e105941. doi:10.1371/journal.pone.0105941

Author contributions: Guillaume Dugué (GD), Clément Lená (CL) and Zachary F. Mainen (ZFM) designed the experiments. GD, Magor M Lorincz (MML), Eran Lottem (EL), Enrica Audero (EA), Sara Matias (SM) and Patrícia A. Correia (PAC) performed the experiments. GD, CL and ZFM analyzed the data. GD, CL and ZFM contributed to the writing of the manuscript.

2.1 Abstract

The inhibition of sensory responsivity is considered a core serotonin function, yet this hypothesis lacks direct support due to methodological obstacles. We adapted an optogenetic approach to induce acute, robust and specific firing of dorsal raphe serotonergic neurons. *In vitro*, the responsiveness of individual dorsal raphe serotonergic neurons to trains of light pulses varied with frequency and intensity as well as between cells, and the photostimulation protocol was therefore adjusted to maximize their overall output rate. *In vivo*, the photoactivation of dorsal raphe serotonergic neurons gave rise to a prominent light-evoked field response that displayed some sensitivity to a 5-HT1A agonist, consistent with autoreceptor inhibition of raphe neurons. In behaving mice, the photostimulation of dorsal raphe serotonergic neurons produced a rapid and reversible decrease in the animals' responses to plantar stimulation, providing a new level of evidence that serotonin gates sensory-driven responses.

2.2 Introduction

The influences of central serotonin (5-hydroxytryptamine or 5-HT) impact a wide range of brain functions, from the control of autonomic responses (Audero et al. 2008; Richerson 2004) to the regulation of complex emotional behaviors (Lucki 1998; Cools et al. 2007). These diverse influences may be systematized by

considering possible core neurophysiological functions. Among these, serotonergic neuromodulation has long been implicated in the inhibition of sensory responsivity (Hurley et al. 2004; Davis et al. 1980), an idea chiefly supported by gain-of-function experiments. Pharmacological enhancement of 5-HT function inhibits primary afferent neurotransmission *in vitro* (Choi et al. 2012; Chen & Regehr 2003), dampens sensory and nociceptively-evoked firing *in vivo* (Petzold et al. 2009; Waterhouse et al. 1990; Yoshida et al. 1984; Reyes-Vazquez et al. 1989) and decreases acoustic startle responses and their pre-pulse inhibition (Davis et al. 1980; Geyer et al. 2001). Similarly, electrical microstimulation of the dorsal raphe nucleus (DRN), one of the largest sources of ascending 5-HT projections (Abrams et al. 2004), reduces forebrain sensory and nociceptively-evoked activity (Petzold et al. 2009; Yoshida et al. 1984; Reyes-Vazquez et al. 1989; Iwayama et al. 1989; Kayama et al. 1989; Andersen & Dafny 1982) and elevates vocalization thresholds to noxious stimuli (Fardin et al. 1984).

Despite these observations, technical limitations have impeded a deeper understanding of the underlying mechanisms. Pharmacological upregulation of 5-HT pathways neither mimics phasic 5-HT release nor takes into account the effect of co-released substances (Trudeau 2004; Gras et al. 2002), and may exhibit paradoxical effects due to autoreceptor-mediated negative feedback (Fornal et al. 1994) and drug-induced plastic changes (Riad et al. 2001). Electrical stimulation, while spatially and temporally precise, can produce non-specific effects by activating

non-5-HT neurons and fibers-of-passage (Fardin et al. 1984). To overcome these technical limitations, we optimized and validated a direct and specific optogenetic stimulation of DRN serotonergic neurons in mice. We then employed this strategy to test whether transient and specific activation of DRN 5-HT neurons in behaving mice can indeed interfere with sensory responsivity in a simple test of mechanosensitivity.

2.3 Results

2.3.1 In vitro photostimulation of virally transduced dorsal raphe 5-HT neurons

To overcome the limitations of previous studies and explore the specific functions of DRN 5-HT projections, we targeted channelrhodopsin-2 fused to YFP (ChR2-YFP) to DRN 5-HT neurons using a viral expression strategy. Adeno-associated viruses (AAVs) carrying a Cre-activated expression cassette for ChR2-YFP were injected into the DRN of SERT-Cre mice (Gong et al. 2007) (**Figure 2.1A-B**). The specificity of this approach was assessed using anti-tryptophan hydroxylase (TPH) immunocytochemistry (**Figure 2.1C-E**). TPH immunoreactivity was observed in 93.9 ± 2.0% of ChR2-YFP cells (n = 3 brains, respectively 287/308, 293/305 and 507/549 counted ChR2-YFP-positive cells also positive for TPH), confirming that this method yields 5-HT neuron-specific expression. The photosensitivity of ChR2-YFP neurons was assessed in acute DRN slices (**Figure**

2.1F-G). Non-fluorescent cells displayed no photoevoked spike or current in response to the highest irradiance tested (1.5–10.4 $mW \cdot mm^{-2}$, n = 7). In contrast, all ChR2-YFP cells fired in response to brief (6 ms) light pulses (n = 34), with an average photostimulation threshold of 0.26 ± 0.47 $mW \cdot mm^{-2}$ (calculated for a subset of n = 21 cells; **Figure 2.1G-I**).

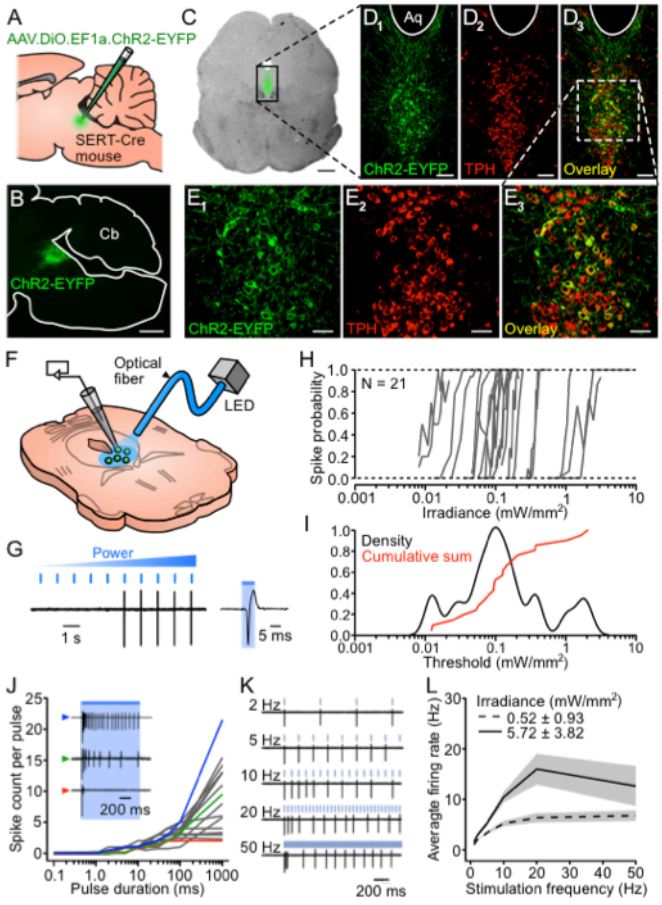

Figure 2.1. Specificity of ChR2-YFP expression in DRN 5-HT neurons and efficiency of photostimulation *in vitro*.
(**A**) Schematics of viral injections. (**B**) Fluorescence picture of a parasagittal slice showing restricted ChR2-YFP expression in the DRN. (**C**) Superimposed fluorescence and brightfield images of a ChR2-YFP-expressing coronal slice.

Bar: 500 mm. (**D1–3**) Confocal pictures of the area delimited by a black rectangle in C. Aq: aquaduct. Bar: 100 mm. (**E1–3**) Magnified view of the area delimited by a white rectangle in D3. Bar: 50 mm. (**F**) Schematics of patch-clamp recordings in DRN slices. (**G**) Left: example of a loose cell- attached recording illustrating the protocol used to assess photo- stimulation thresholds (PTs). Right: blow-up of the trace showing a single photoevoked spike. (**H**) Spike probability versus incident irradiance for 21 cells. (**I**) Kernel density estimate of the distribution of logarithmically-scaled PTs (black) and superimposed normalized cumulative sum (red). (**J**) Spike count per pulse versus pulse duration for 17 cells at twice their PT. Inset: representative firing profiles of 3 different cells identified in the graph by colored arrowheads. (**K**) Response of a ChR2-YFP cell to trains of repeated light pulses (6 ms) at various frequencies (irradiance set at twice its PT). (**L**) Average firing rate (± SEM, shaded area) during a 5 s train versus photostimulation frequency at twice the PT (dashed line; n = 29, 28, 25 and 18 cells for 1–2, 5–10, 20 and 50 Hz respectively) and at a higher irradiance (~5 $mW \cdot mm^{-2}$; solid line, n = 14 and 13 cells for 1–20 and 50 Hz respectively).

Longer pulses (1 s) at twice the photostimulation threshold evoked firing profiles ranging from non- to fully-inactivating (**Figure 2.1J**). Firing evoked by repeated photostimulation (6 ms pulses at 1–50 Hz) generally adapted over time (**Figure 2.1K**). During 5 s photostimulation trains, ChR2-YFP cells could reliably (spike probability > 0.85) follow up to 2 Hz at twice their photostimulation threshold and up to 10 Hz at a higher irradiance (~5 $mW \cdot mm^{-2}$). However the maximal average firing rates for these two irradiances (6.8 ± 4.6 Hz, n = 18 and 16.0 ± 11.4 Hz, n = 14) were attained with 50 and 20 Hz photostimulations respectively (**Figure 2.1L**). Therefore irradiances one order of magnitude above photostimulation threshold are required to induce firing rates comparable to those observed in behaving animals during phasic episodes of increased DRN firing (Fornal et al. 1996; Miyazaki et al. 2011; Walletschek & Raab 1982).

2.3.2 In vivo photostimulation of dorsal raphe 5-HT neurons

In order to estimate how far from the fiber tip ChR2-YFP neurons could be recruited *in vivo*, we measured the spread of blue light in the DRN of hemisected brains (**Figure 2.2A-B**); see Methods). Light intensity decayed in an exponential fashion away from the fiber tip, with a space constant of 199 ± 35 μm (n = 3; **Figure 2.2C-D**).

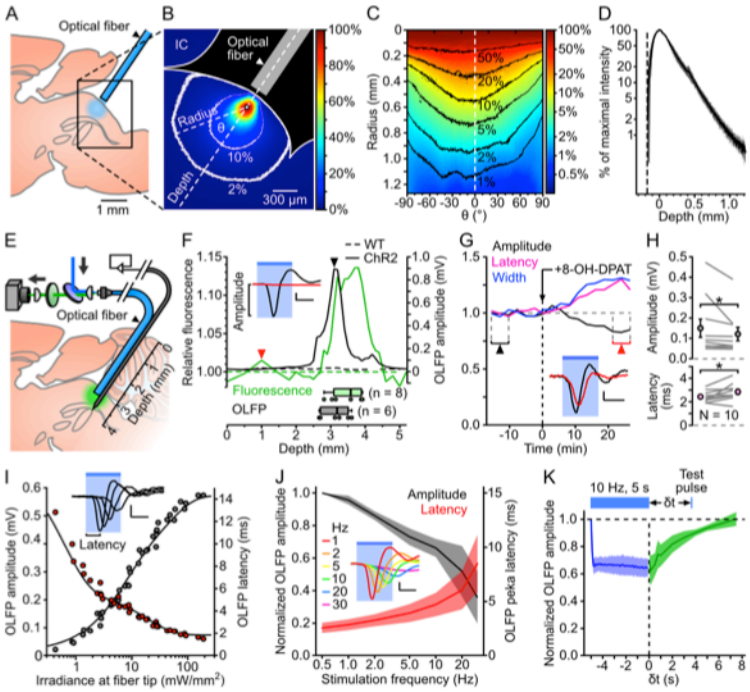

Figure 2.2. Photostimulation of DRN 5-HT neurons in vivo
(**A**) Schematics of the experiment used to assess the spread of blue light in the DRN. (**B**) Example image of DRN illumination. The intensity is color-coded relative to the pixel of maximal intensity (white dot). The 10 and 2% contour lines are shown in white. IC: inferior colliculus. (**C**) Circular profile plot calculated from B, showing pixel intensities along concentric lines centered on the brightest pixel. (**D**) Average intensity profile (± SD, shaded area; n = 3 brains) along the fiber axis. The depth and intensities are calculated relative to the brightest pixel. (**E**) Schematics of the setup used to map YFP fluorescence and photoevoked firing in vivo. (**F**) Example of a combined electrophysiological and fluorescence mapping experiment in a ChR2-YFP-

expressing SERT-Cre (ChR2, solid lines) and a wild-type (WT, dotted lines) mouse. Top: normalized fluorescence (green, left axis) and OLFP amplitude (black, right axis) profiles plotted against the optrode position. Bottom: boxplots showing the optrode position at the point of maximal fluorescence (green, n = 8 mice) and largest OLFP amplitude (grey, n = 6 mice). Inset: average OLFP for the ChR2 mouse at the locations marked by the arrowheads. (**G**) Example showing the time course of the effect of the 5-HT1A receptor agonist 8-OH-DPAT on the OLFP amplitude (black), latency (purple) and width (blue). Bin: 158 s. Inset: average OLFP before (black) and after (red) 8-OH-DPAT injection (taken from the periods indicated by arrowheads). (**H**) Top: OLFP amplitude before and after 8-OH-DPAT injection (mean ± SD: 1506121 mV and 1216105 mV respectively, n = 10). Bottom: OLFP peak latency before and after 8-OH-DPAT injection (mean ± SD: 2.460.5 ms and 2.860.7 ms, n = 10). Changes are significant in both cases (P = 0.037 and P = 0.030 respectively, paired Wilcoxon rank sum test). Error bars represent the SEM. (**I**) Example illustrating the dependence of the OLFP amplitude (grey points) and latency (red points) on the irradiance at the fiber tip. The sum of two exponential functions was fitted to each curve (black lines). Inset: superimposed OLFPs for 0.2, 0.7, 1.6 and 6.0 $mW \cdot mm^{-2}$. (**J**) Normalized average (6 SD, shaded area) OLFP amplitude (black, left axis) and latency (red, right axis) versus photostimulation frequency (n = 7 mice). (**K**) Average OLFP amplitude recovery curve (green; ± SD, shaded area) assessed by delivering test pulses at variable intervals (dt) after 10 Hz, 5 s trains of 6 ms light pulses (n = 4 mice). Blue: average amplitude during the trains.

The volume of tissue receiving more than 2% of the irradiance at the brightest point extended 1.65 ± 0.21 mm, > 1.00 and 1.23 ± 0.10 mm in the antero-posterior, medio-lateral and fiber axes respectively (n = 3). We then probed the response of DRN 5-HT neurons *in vivo* by advancing a custom optrode toward the DRN of anaesthetized animals, while intermittently shining light pulses. The tissue fluorescence (**Figure 2.2E**) displayed a peak 3.48 ± 0.43 mm below the cerebellar surface (n = 8), which correlated spatially with a prominent multiphasic photoevoked potential (OLFP, optically-evoked local field potential; **Figure 2.2F**). Systemic administration of the 5-HT1A receptor agonist 8-OH-DPAT, a drug commonly employed to inhibit 5-HT cell firing by activating local autoreceptors (Fornal et al. 1994), blunted the

OLFP amplitude and prolonged its latency (**Figure 2.2G-H**). The OLFP peak amplitude and latency displayed a graded dependence on the irradiance at the fiber tip (**Figure 2.2I**), approaching saturation (slope < 10 μV/mW·mm^{-2}) at 117 ± 34 mW.mm^{-2} (n = 9). This dependence could be described as the sum of two exponential functions (τ_{fast} and τ_{slow} of 7.4 ± 6.0 and 53.5 ± 18.7 mW.mm^{-2} accounting for 46% and 54% of the amplitude respectively; τ_{fast} and τ_{slow} of 3.1 ± 5.2 and 29.6 ± 26.2 mW.mm^{-2}, accounting for 70% and 30% of the latency respectively; n = 9). The OLFP waveform also rapidly adapted to trains of repeated photostimulation (reduced amplitude and extended latency with increased stimulation frequency, **Figure 2.2J**), an effect potentially mediated by a combination of factors such as partial inactivation of voltage-dependent sodium channels, ChR2 desensitization, a build-up of afterhyperpolarization currents or the activation of 5-HT1A autoreceptors. The OLFP recovery kinetics, assessed for 10 Hz trains, had a time constant of 2.9 ± 0.5 s (n = 4; **Figure 2.2K**), and full recovery was observed after 8 seconds.

2.3.3 Decreased mechanosensory responsivity of behaving mice during acute dorsal raphe 5-HT neurons photostimulation

Having characterized the specificity and efficacy of the photostimulation of DRN 5-HT neurons, we then tested this methodology in behaving animals using a classical test of

mechanical sensitivity, the von Frey assay (Barrot 2012) (**Figure 2.3A**).

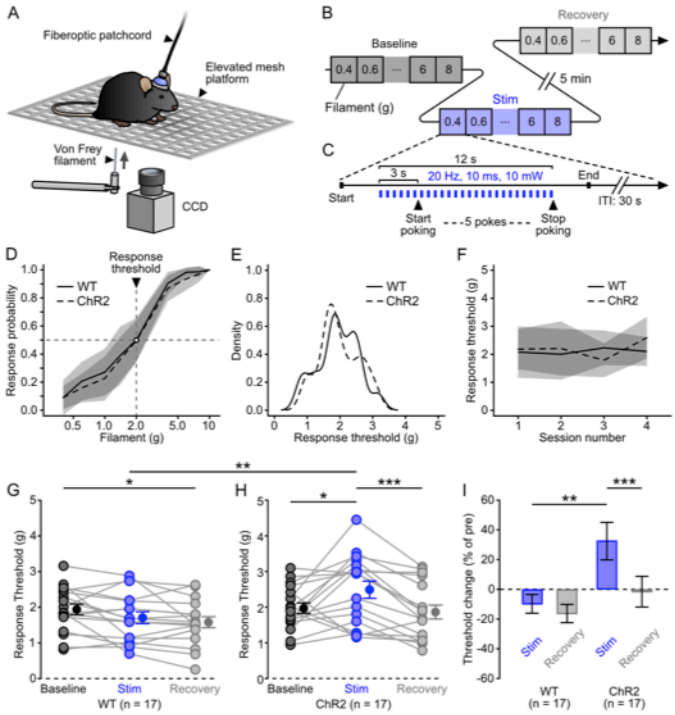

Figure 2.3. Decreased responsivity to mechanical stimuli during DRN 5-HT neurons photostimulation

(**A**) Schematics of the experiment. (**B**) Structure of a session. (**C**) Structure of a trial in the ‘‘stim’’ block. The filament was applied to the hindpaw during a 12 s train of light pulses. (**D**) Average baseline response probability curves for control (infected WTs, solid line, n = 17) and ChR2 (dashed line, n = 17) mice. (**E**) Kernel density estimates of the baseline threshold distribution for control (WT, solid line) and ChR2 (dashed line) mice. (**F**) Average baseline threshold across sessions for control (WT, solid line) and ChR2 (dashed line) mice. (**G–H**) Thresholds for all control and ChR2 mice in the baseline (dark grey), ‘‘stim’’ (blue) and recovery (light grey) blocks. *: P<0.05 (paired Wilcoxon rank sum test); ***: P<0.001 and **: P<0.01 (unpaired Wilcoxon rank sum test). (**I**) Threshold change for control and ChR2 mice in the ‘‘stim’’ (blue) and recovery (light grey) blocks. ** P<0.01 and *** P<0.001 (paired and unpaired Wilcoxon rank sum test respectively). Shaded areas and error bars represent the SD in all panels.

In this test, a series of calibrated Nylon filaments (von Frey hairs) of ascending stiffness are applied to the plantar surface of the hind paws while monitoring the animal's withdrawal response. Groups of SERT-Cre (ChR2) and littermate wildtype (WT) control mice (n = 17 for both) were infected with the same viral vector. Both groups had the same sex ratio (9 males, 8 females) and were implanted with optical fibers positioned over the DRN.

After a habituation period of 5 days (see Experimental procedures), animals were tested during 3 to 4 sessions, with a maximum of 1 session per day. Each session was divided in 3 blocks, designed to test the animal's sensitivity prior to ("baseline"), in conjunction with ("stim") and after ("recovery") photostimulation (**Figure 2.3B**). For each block, a psychometric curve (response probability versus filament) was calculated and the response threshold was taken as the interpolated filament value corresponding to a response probability of 0.5. Baseline responsivity to ascending forces applied with von Frey hairs (0.4–8 g) to the hind paws did not differ between SERT-Cre and WT mice (**Figure 2.3D-E**), with average response thresholds of 1.93 ± 0.63 g and 1.97 ± 0.61 g, respectively (P = 0.97, unpaired Wilcoxon sum rank test). However in the presence of concomitant photostimulation (a 12 s train of 10 ms light pulses at 20 Hz, ~300 $mW \cdot mm^{-2}$ at the fiber tip, **Figure 2.3B-C**), response thresholds were significantly higher for ChR2 animals than WT controls (2.49 ± 1.00 g vs 1.71 ± 0.69 g, P = 0.0076, unpaired Wilcoxon sum rank test). This difference was no longer observed in the "recovery" block, 5 minutes after the last

photostimulation train (**Figure 2.3G-H**). The effect observed in ChR2 mice during photostimulation corresponded to a significant threshold elevation of 32.5 ± 52.0% (**Figure 2.3I**) which counteracted the slight sensitization observed in WT animals (**Figure 2.3G**). This result shows that acute DRN 5-HT photostimulation induces a transient and fully reversible decrease in responsivity to plantar stimulations in behaving mice.

2.4 Discussion

The initial optogenetic approaches used to study DRN functions employed non-specific promoters (Warden et al. 2012; Varga et al. 2009) or targeted local or distal neurons presynaptic to 5-HT neurons (Warden et al. 2012; Challis et al. 2013). Recently, specific optogenetic stimulation of DRN 5-HT neurons has been achieved using transgenic mouse lines (Ito et al. 2013; Ohmura et al. 2014) or viral injections (Liu et al. 2014) but these studies have not provided a detailed account of optimal photostimulation parameters. Here we devoted substantial efforts to optimizing the yield of direct and specific photostimulation of DRN 5-HT neurons. ChR2-EYFP-expressing cells were sensitive to low irradiance *in vitro* (< 1 $mW \cdot mm^{-2}$, **Figure 2.1H-I**). However high irradiances (> 100 $mW \cdot mm^{-2}$ at fiber tip) were necessary to saturate the photoevoked local field potential *in vivo*, a measure that might prove useful for optimally positioning optical fibers and assessing levels of ChR2-YFP expression in target structures.

Using irradiance of > 250 $mW \cdot mm^{-2}$ at the fiber tip, we estimated that the entire DRN received irradiances over 5–6 $mW \cdot mm^{-2}$, a value at which the output of ChR2-EYFP neurons could be maximized (up to 16 Hz) *in vitro* by using 20 Hz stimulations, despite their strong frequency-dependent adaptation. These parameters are appropriate to attempt to mimic episodes of increased DRN activity, which occur in association with a variety of behavioral conditions such as oro-buccal movements (Fornal et al. 1996) and defensive encounters (Walletschek & Raab 1982), and in relation to reward outcome (Bromberg-Martin et al. 2010) and waiting for delayed rewards (Miyazaki et al. 2011). Such episodes typically last several seconds, during which the activity of DRN neurons can peak up to 10−20 Hz.

Our protocol for DRN 5-HT neuron photostimulation in behaving mice (20 Hz for 12 seconds) evoked robust decreases in behavioral responses to hind paw stimulation. Previous observations have shown that chronic elevation of 5-HT levels can increase response thresholds in rodent models of mechanical allodynia (Ikeda et al. 2009; Xu et al. 2013; Katsuyama et al. 2013). Our result extends this observation by showing that a similar effect can be reversibly induced on a faster timescale in non-pathological conditions by recruiting DRN 5-HT neurons. Whether the threshold calculated using von Frey filaments in naïve animals is a measure of sensory or nociceptive sensitivity is still a debated question (Barrot 2012). Therefore the question whether the stimulation of DRN 5-HT neurons in our conditions primarily acts upon sensory or nociceptive pathways remains

open. Nevertheless, our result helps to resolve the ambiguity of previous gain-of-function experiments testing the influence of DRN output by directly showing that DRN 5-HT neurons can indeed tone down the influence of sensory and/or nociceptive inputs, as opposed to what has been recently observed in zebrafish (Yokogawa et al. 2012).

Given the projection pattern of DRN 5-HT cells (Abrams et al. 2004), this effect is likely to be mediated by the modulation of anterior structures, as suggested by evidence highlighting a role for 5-HT in the modulation of thalamic (Yoshida et al. 1984; Reyes-Vazquez et al. 1989; Kayama et al. 1989; Qiao & Dafny 1988) and cortical (Hurley et al. 2004; Waterhouse et al. 1990) sensory and nociceptive responses. It is not unlikely that other co-released substances may play a role in the observed effect. In particular, a recent study has shown that the glutamatergic phenotype of certain 5-HT neurons seems to be partly responsible for the effects produced by the photostimulation of DRN 5-HT neurons on reward-related behaviors (Liu et al. 2014).

More refined targeting strategies, e.g. retrograde infection (Rothermel et al. 2013) or intersectional genetics (Jensen et al. 2008), will allow the assessment of contributions of specific sub-populations of DRN 5-HT neurons (Abrams et al. 2004). Overall these results provide a new level of evidence for the involvement of DRN 5-HT neurons in gating the access of sensory inputs to behavioral output, a key physiological role which will help constrain larger-scale theories of 5-HT function.

2.5 Experimental procedures

2.5.1 Viral transduction of dorsal raphe neurons and optical fiber implantation

Adult (8–16 weeks) transgenic SERT-Cre (Audero et al. 2008) or wild-type mice (C57BL/6 background, housed in a standard 12:12 hours light-dark cycle) were anaesthetized with isoflurane mixed with O_2 (3% for induction and 0.5–1% for maintenance) or with ketamine xylazine (100 and 5 mg/kg) and placed in a stereotaxic apparatus (David Kopf Instruments). Lidocaine (2%) was injected subcutaneously before incising the scalp and exposing the skull. A craniotomy was drilled over lobule 4/5 of the cerebellum and a pipette filled with a viral solution (AAV2/1.EF1a.DIO.hChR2(H134R)-EYFP.WPRE.hGH, 10^{13} GC/mL, University of Pennsylvania) was lowered to the DRN (Bregma -4.4 to -4.7 mm AP, -2.8 to -2.9 mm DV) with a 34° angle toward the back of the animal (**Figure 2.1A**). The viral solution (1–1.2 μL) was injected using a Picospritzer II (Parker) or a syringe pump (KDS 310 Plus, KD Scientific) at a rate of 0.05–0.06 μL/min. For optical fiber implantation, the skull was cleaned with H_2O_2 and covered with a layer of Super Bond C&B (Morita) before performing the craniotomy. An optical fiber (200 μm, 0.37 NA) housed inside a connectorized implant (M3, Doric Lenses) was inserted in the brain using the same 34° from the back, with the fiber tip positioned 200 μm above the core of the infection along the penetration axis. The craniotomy was covered

with a drop of warm agarose gel (2%) and the implant was secured with dental acrylic (Pi-Ku-Plast HP 36, Bredent). The skin was stitched at the read and front of the implant and the animal was allowed to recover on a heating pad.

2.5.2 In vitro electrophysiological recordings and photostimulation of DRN neurons

2.5.2.1 Slice preparation, recordings and illumination

DRN slices from male and female SERT-Cre mice aged 8-20 weeks (2–4 weeks post-infection) were prepared as follows. Mice were anesthetized with ketamine-xylazine (80 and 8 mg/kg) and perfused through the heart with 15 ml of cold (4°C) ACSF solution containing (in mM) 130 NaCl, 3.5 KCl, 1 NaH_2PO_4, 24 $NaHCO_3$, 1 CaCl, 3 $MgSO_4$, 10 glucose, saturated with 95% O_2 and 5% CO_2. The brain was then quickly removed and sliced (320 μm thickness) using a VT1200s vibratome (Leica). Slices were allowed to recover for 1 h at room temperature in an ACSF solution with a similar ionic composition as the slicing solution but containing (in mM) 3 $CaCl_2$ and 1.5 $MgSO_4$. This solution was used for recordings as well. Slices were next transferred to a recording chamber under an upright microscope (Olympus WI51) and cells were visualized by epifluorescence and IR-DIC videomicroscopy using a CCD camera (Hamamatsu Orca). For loose cell-attached recordings (n = 4 non-fluorescent and 28 fluorescent cells), pipettes (2–4 MΩ) were filled with ACSF, seal resistance was 30–90 MΩ, R_s was compensated to ~50% and

cells were recorded in voltage clamp with 0 pA current injected. For whole cell recordings (n = 3 non-fluorescent and 6 fluorescent cells), pipettes (5–7 MΩ) were filled with (in mM) 126 K-gluconate, 4 KCl, 4 ATP-Mg, 0.3 GTP-Na_2, 10 HEPES and 10 Creatine-phosphate (pH 7.25; 300 mOsm). Recordings were performed at 34°C using a Multiclamp 700B amplifier (Molecular Devices). Signals were filtered at 10 kHz, digitized at 20 kHz and analyzed with SpAcAn, a collection of IGOR Pro routines (www.spacan.net). Photostimulation was performed using a 465 nm LED coupled to a 200 μm, 0.37 NA optical fiber (Doric Lenses) and controlled by pCLAMP (Molecular Devices) via a universal LED driver (Mightex Systems). The optical fiber was held at 34° relative to the vertical axis and positioned above the slice using a PatchStar micromanipulator (Scientifica). The fiber tip was first placed against the slice within the field of view and then retracted axially by a known distance (0.5–2 mm).

2.5.2.2 Calculation of incident irradiance

For each cell, the incident irradiance was calculated by dividing the power measured at the fiber tip (measured with a PM100D powermeter, Thorlabs) by the area of the illuminated zone (**Figure S 2.1**).

Given that the optical fiber was positioned above the slice at an angle, the illuminated area at the slice surface had an elliptic shape and could be calculated using the following equations.

The eccentricity ε of the ellipse can be calculated from the half-angle of divergence of the cone of light (α) and the angle of the fiber relative to the vertical axis (θ):

$$\varepsilon = \frac{\cos(\alpha)}{\cos(\pi - \theta)} \qquad (1)$$

The half-angle of divergence α is defined by the fiber numerical aperture (NA) and the refractive index of the surrounding medium (n):

$$\theta = \sin^{-1}\left(\frac{NA}{n}\right) \qquad (2)$$

The semi-major (a) and semi-minor (b) axis of the ellipse are linked to the eccentricity by the following relation:

$$b = a \times \sqrt{1 - \varepsilon^2} \qquad (3)$$

The semi-major axis can be calculated knowing the axial distance between the cone vertex and the slice (z):

$$\mathrm{a} = z \times \frac{\cos\theta}{2} \times (\tan(\theta + \alpha) - \tan(\theta - \alpha)) \qquad (4)$$

Finally the area of the ellipse is given by the product $A = \pi \times a \times b$, which can be simplified as $A = \pi \times a^2 \times \sqrt{1 - \varepsilon^2}$ using (3). By combining this expression with (1), (2) and (4), we obtain:

$$A = \frac{\pi}{4} \times z^2 \times (\cos\theta)^2 \times (\tan(\theta + \alpha) - \tan(\theta - \alpha))^2 \times \sqrt{1 - \frac{(\cos\alpha)^2}{(\cos(\pi - \theta))^2}}$$

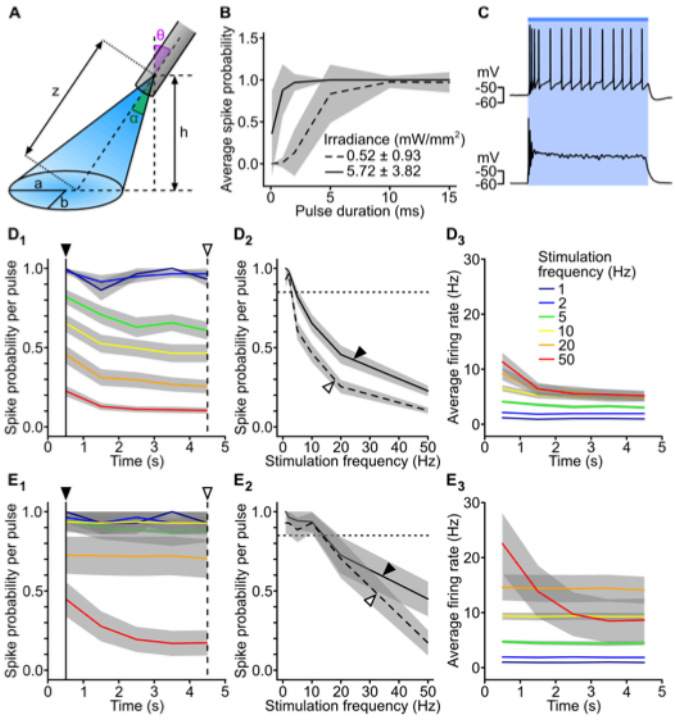

Figure S 2.1. Photostimulation of DRN 5-HT neurons *in vitro*

(**A**) Calculation of the mean incident irradiance. The optical fiber was positioned at an angle (θ) above the slice, with a known axial distance from the slice surface. The cone of light exiting the fiber formed an ellipse onto the slice, whose area can be calculated based on the axial distance between the cone vertex and the slice (z), the fiber angle θ and the divergence half-angle (α) of the fiber (see Methods). (**B**) Average spike probability per pulse as a function of pulse duration for the two irradiance tested (twice the PT, dotted line, n = 17, and maximal irradiance delivered by the LED, dashed line, n = 11). Most cells fired reliably (spike probability > 0.80) for pulses longer than 5 ms at twice their PT (n = 16/17), and for pulses longer than 1 ms at higher irradiance (n = 10/11, 5.1 ± 3.7 mW.mm^{-2}). (**C**) Example traces from two cells recorded in the whole cell configuration and illuminated with a 1 s pulse. Although the two cells had similar input resistances (629 and 565 MΩ) and photostimulation thresholds (0.094 and 0.128 mW.mm^{-2}), one displayed rapid inactivation (bottom) while the other one did not (top). (**D–E**) Firing adaptation during 5 s trains of repeated photostimulation at fixed frequencies, at two irradiance levels: twice the PT (D_1–D_3) and maximal irradiance produced by the LED (~ 5 mW.mm^{-2}, E_1–E_3). The graphs show the average spike probability per pulse as a function of time (D_1 and E_1, bin = 1 s) and as a function of the stimulation frequency (D_2 and E_2) for the first and last time bins (black and white arrowheads), as well as the time course of the average firing rate for various stimulation frequencies (D_3 and E_3). The color code in D_1 and E_1 is the same as

D_3 and E_3. The 0.85 spike probability is marked in D_2 and E_2 by a horizontal dotted line. The numbers of cells averaged for panels D_1–D_3 are n = 29, 28, 25 and 18 cells for 1–2, 5–10, 20 and 50 Hz respectively. The numbers of cells averaged for panels E_1–E_3 are n = 14 and 13 cells for 1–20 and 50 Hz respectively.

2.5.2.3 Photostimulation threshold

The minimum amount of light required to activate ChR2-YFP cells was assessed by delivering brief pulses (6 ms) of increasing power at low frequency (1 Hz; **Figure 2.1G**). Each cell responded in a nearly all-or-none fashion (**Figure 2.1H**) and the photostimulation threshold was defined as the incident irradiance necessary to evoke a spike in half of the trials.

2.5.2.4 Spike count versus pulse duration

Firing profiles were characterized for different pulse durations. Light pulses of increasing duration were delivered in sweeps, each sweep consisting of a series of 0.1, 1, 2, 5, 10, 15, 30, 50, 100 and 1000 ms pulses separated by 1 s.

2.5.2.5 Firing profiles for different photostimulation frequencies

Cells were photostimulated with trains of 6 ms light pulses delivered at 1, 2, 5, 10, 20 and 50 Hz delivered in single sweeps, with an intersweep interval of 1 min.

2.5.2.6 Blue light propagation in the DRN

The spread of blue light in the DRN was assessed *in vitro* using freshly dissected brains. Mice (n = 3) were anaesthetized using pentobarbital and decapitated. The posterior half of the brain was quickly dissected and embedded in 2% agarose gel. Blocks of tissue were then glued and immersed in the chamber of a vibratome (7000 smz 2, Campden Instruments), and trimmed in the parasagittal direction until the aquaduct was exposed. The hemi-cerebellum still attached to the brainstem, was carefully removed by sectioning the cerebellar pedunculi, and the block of tissue was immersed in a petri dish filled with PBS, placed under an upright microscope and imaged through a 5 x objective using a CCD camera (Retiga 4000R, QImaging) (**Figure S2.2**).

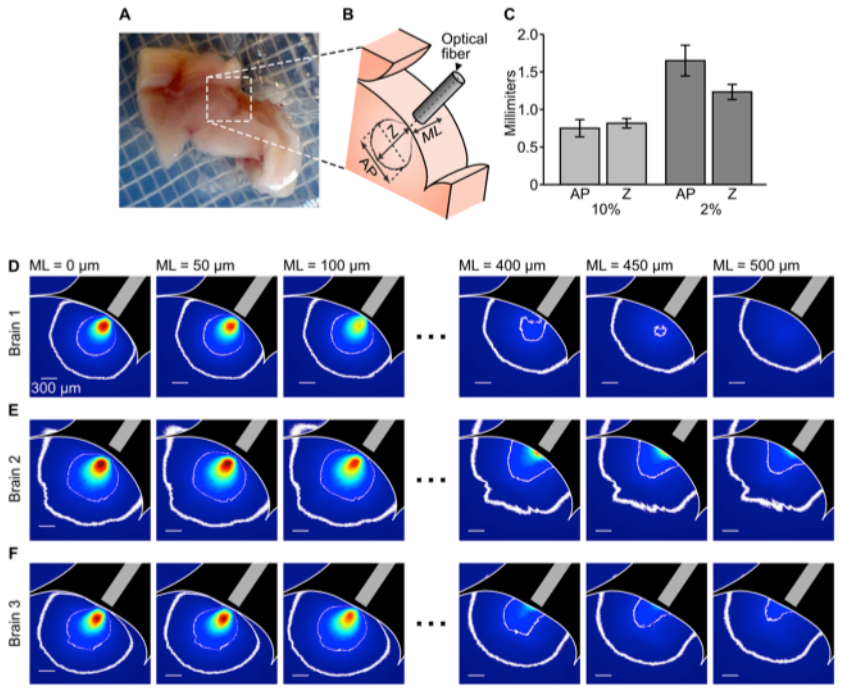

Figure S 2.2. Light propagation in the DRN

(**A**) Picture of a fresh brain hemisected in the sagittal plane (see Methods). The DRN corresponds to the grey matter localized inside the dotted white square. (**B**) Schematics representing the portion of tissue delimited by the white square in A and the optical fiber positioned above it. The spread of light in the tissue was estimated along the axis of the fiber (Z) and along the antero-posterior axis (AP). The fiber was moved medio-laterally (ML) in order to assess how light diffused laterally in the tissue. (**C**) Average dimensions of the volume of tissue receiving more than 10% (light grey) and 2% (dark grey) of the maximal intensity along Z and the AP axis. (**D–F**) Color coded pictures representing the relative pixel intensities for various ML positions of the fiber for the 3 brains examined. The fiber was moved every 50 μm in the ML axis over 500 μm.

Light was delivered through a 200 μm 0.37 NA optical fiber positioned 110 ± 45 μm (n = 3) above the dorsal aspect of the DRN (**Figure S 2.2B**) at the level of the plane of cut. To assess how light spreads laterally in the DRN, the fiber was moved medio-laterally with 50 μm steps (**Figure S 2.2B-F**). Because light is progressively more scattered as it penetrates into the tissue, the brightest pixel was not located at the DRN surface but 172 ± 23 μm below (n = 3). The relative pixel intensity was calculated along concentric circles centered on this point (circular profiles, **Figure 2.2C**) and along the axis of the fiber (linear profiles, **Figure 2.2D**).

2.5.3 Fluorescence mapping of ChR2-EYFP-expressing DRN neurons and electrophysiological recordings of local photoevoked activity in vivo

2.5.3.1 Optical system

Custom optrodes were assembled by gluing a cleaved 200 μm 0.37 NA multimode optical fiber (BFL37-200, Thorlabs) onto a platinum microelectrode (0.8–1.0 MΩ at 1 kHz, FHC). The

optical fiber tip was positioned 300–500 μm above the microelectrode tip. Pulses of light were generated using a laser beam (473 nm, 100 mW DPSS laser, Laserglow) gated by a mechanical shutter (VS14S2ZM1, Uniblitz) and attenuated by a set of neutral density filters. The beam was passed through a 10:90 beamsplitter cube (BS025, Thorlabs) and the resulting 10% beam was collected by a photodiode (SM1PD1A, Thorlabs) for precise light pulse monitoring. The 90% beam was bounced on a dichroic mirror (T495LP, Chroma) and injected into the optical fiber using an aspheric lens (A240, Thorlabs). The fluorescence light travelling back in the fiber was passed through an emission filter (LP02-514-RU, Semrock) positioned after the dichroic mirror and focused onto the sensor of a custom cooled CCD camera using a N-BK7 plano-convex spherical lens (LA1255, Thorlabs). Fluorescence images were analyzed using MATLAB by measuring the average pixel intensity inside the fiber core. All fluorescence measurements were performed in the dark. The fiber intrinsic fluorescence (autofluorescence), assessed with the fiber in the air, accounted for 93 ± 11 % (n = 3) of the average fluorescence measured in the first millimeter of tissue.

The mechanical shutter yielded a minimal pulse duration of 6 ms. Power modulation was achieved using a set of 6 neutral density (ND) filters (transmissions of 0.1, 10, 26, 40, 68 and 81%, measured at 473 nm) positioned inside a filter wheel (FW102C, Thorlabs) and 3 additional filers added in the optical path (transmissions of 10, 32 and 50%). Laser power was set so that the power measured at the fiber tip was 5–6 mW using the 81%

ND filter. The 0.1% ND filter was used for tissue fluorescence measurements (power at the fiber tip of around 10 μW). The 5 other filter wheel positions were used in combination with the 3 additional ND filters to produce 40 different power values for measuring the OLFP dependence on light intensity.

2.5.3.2 Surgery and electrophysiological recordings

Male and female SERT-Cre mice (2–4 weeks postinfection) or wild type littermates were anaesthetized with urethane (1.5 g/kg) and placed in a stereotaxic frame. Incision and craniotomy were performed as described for viral injection. The optrode was lowered in the brain using a 34° angled approach from the cerebellum, using an IVM micromanipulator (Scientifica). The electrophysiological signal was amplified (x1000) and filtered (0.1–10 kHz) by an 1800 AC amplifier (AM Systems), digitized (10 kHz) by a Micro1401-3 interface and acquired using Spike2 (Cambridge Electronic Design). Electrophysiological data were analyzed using IGOR Pro.

2.5.3.3 Properties of the OLFP

The positions of the optrode yielding a maximal fluorescence and OLFP (**Figure 2.2F**) were assessed by fitting Gaussian functions to fluorescence and OLFP amplitude profiles. Fluorescence alone was mapped in 2 mice and combined fluorescence and OLFP profiles were obtained in 6 mice. The sensitivity of the OLFP to a 5-HT1A agonist was tested in 10 mice by sub-cutaneous injection

of 375 μg/kg of 8-OH-DPAT (Tocris). The dependence of the OLFP on the irradiance at the fiber tip was tested by delivering 6 ms light pulses of various intensities at 1 Hz (40 different irradiance values ranging in average from 0.64 ± 0.95 to 191.94 ± 5.73 $mW.mm^{-2}$, 10 repetitions per intensity, n = 9). The effect of repeated photostimulation was assessed using 12 s trains of light pulses (6 ms) delivered at 0.5, 1, 2, 5, 10, 20 and 50 Hz in single sweeps, with an intersweep interval of 1 min. The average OLFP amplitude and peak latency were calculated over the last 4 s of each train. The OLFP recovery rate was assessed using sweeps consisting of a 10 Hz, 5 s trains of light pulses (6 ms) followed by a single test pulse at a variable interval after the train (δt), with an intersweep interval of 30 seconds (**Figure 2.2K**). The recovery rate was fitted using an exponential function. Full recovery was observed after 7.6 s.

2.5.4 Von Frey test

In the von Frey test, a series of calibrated Nylon filaments (von Frey filaments, Bioseb) of ascending stiffness are applied to the plantar surface of each hind paw (avoiding the toes, heel and pads) while monitoring the animal's response. The main response is paw withdrawal but other responses can be observed such as fingers extension. The test allows repeated measures over time with minimal habituation and therefore is well suited for within-animal comparisons and response averaging. Once bent, each filament exerts a constant pressure on the skin (see **Table 2.1** for a chart of theoretical pressures), and repeated measures with the

same filament allow calculating the response probability for this filament.

A total of 34 mice were tested: 17 SERT-Cre mice infected with the Cre-dependent viral vector and 17 wild type littermates (control group) infected with the same virus. Prior to testing, animals were allowed to habituate to the testing box (a 9 x 7 x 14 cm Plexiglas box placed on an elevated metal mesh platform) 5 minutes per day for 5 days. During these habituation sessions, the animals were plugged to a fiberoptic patchcord (Doric Lenses), and the 4.0 g filament was applied 5 times per hind paw. In the testing phase, each animal was subjected to 3 to 4 testing sessions (with a maximum of 1 session per day). All sessions took place during the light period of the light-dark cycle, between 10:00 a.m. and 5:00 p.m. Each session was divided in 3 blocks, designed to test the animal's sensitivity prior to ("baseline"), in conjunction with ("stim") and after ("recovery") photostimulation (**Figure 2.3B**). In each block, filaments ranging 0.4–8 g were applied consecutively in an ascending fashion (each filament was applied 5 times successively to the right and left hind paws), yielding one psychometric curve (response probability versus filament) per block (for each curve the left and right response probabilities were averaged). The threshold was taken as the interpolated filament value corresponding to a response probability of 0.5. The "stim" and "recovery" blocks were separated by a 5 minutes delay. In the "stim" condition, filament application was restricted to the last three quarters of a 12 s photostimulation train (10 ms, 20 Hz, 318 $mW.mm^{-2}$ at the fiber tip; **Figure 2.3C**). The 3 s delay

between photostimulation onset and first filament application are meant to allow the establishment of a potentially slow serotonergic neuromodulatory mechanism. The stimulation parameters were chosen to produce a saturating effect based on our *in vitro* and *in vivo* characterization. Light pulses were generated using a custom system based on an acousto-optic modulator (AOM). AOMs have combined high-precision power modulation and shuttering capabilities. Unlike mechanical shutters, AOMs operate in a totally silent way (AOMs use inaudible acoustic frequencies, typically around 100 MHz) and are therefore well suited for experiments with behaving animals. All sessions were videotaped and analyzed offline. The experimenter was blind to the genotype of the mice throughout both the testing and offline scoring phases.

Table 2.1. Von Frey filaments force scale

Filament target force (g)	Target force (mN)	Theoretical pressure ($g.mm^{-2}$)
0.16	1.6	8.77
0.4	3.9	16.1
0.6	5.9	18.4
1.0	9.8	24.4
1.4	13.7	27.9
2.0	19.6	27.4
4.0	39.2	40.3
6.0	58.8	52.6
8.0	78.4	61.7
10.0	98.0	68.3

3 Optogenetic activation of dorsal raphe serotonergic neurons reduces movement, without affecting motor coordination or inducing reinforcing responses in behaving mice

Manuscript in preparation: Correia PA, Lottem E, Banerjee D, Machado A, Carey M, Mainen ZF. Optogenetic activation of dorsal raphe serotonergic neurons reduces movement, without affecting motor coordination or inducing reinforcing responses in behaving mice.

Author contributions: Patrícia A. Correia (PAC), Eran Lottem (EL) and Zachary F. Mainen designed the experiments. PAC and Dhruba Banerjee (DB) performed the experiments. PAC, EL and DB analyzed the data. Ana Machado (AM) and Megan Carey designed and implemented LocomoMouse setup and AM performed LocoMouse analysis.

3.1 Abstract

Serotonin (5-HT) is a major neuromodulator in the brain, involved in diverse functions and behaviors, including depression and anxiety, but its fundamental actions in behavior are still enigmatic. One prominent theory suggests a general role for 5-HT in promoting behavioral inhibition. Another has suggested 5-HT has a function in reinforcing behaviors. However, how modulation of 5-HT in non-punishment or non-rewarding conditions occurs remains elusive.

In this study, we report that optogenetic activation of 5-HT neurons from the dorsal raphe nuclei (DRN) induced a robust decrease in speed of mice running in an open field arena. The result was very rapid (< 0.5 s) and persisted for many days of stimulation, thus proving not to be related with the novelty of the context. In contrast, using the same optogenetics approach, we found no evidence for motor coordination impairment in the accelerating rotarod and linear track locomotion assays. The movement effect did not induce anxiety-like behaviors in the open field. Furthermore, DRN 5-HT activation constrained to a sub-region of the same arena did not produce either appetitive or aversive responses. These results provide direct evidence of sufficiency of DRN 5-HT activation in decreasing movement, without inducing impairment of motor coordination, anxiety-like responses or reinforcing effects, thus supporting the importance of 5-HT in behavioral inhibition.

3.2 Introduction

Serotonin (5-HT) is a major neuromodulator in the brain, involved in diverse functions and behaviors, including depression and anxiety. One prominent theory suggests a general role for 5-HT in promoting behavioral inhibition (Soubrié 1986), but 5-HT fundamental actions in behavior are still enigmatic. Evidence to support the behavioral inhibition theory comes from a large set of 5-HT depletion studies showing increased locomotor activity (Gately et al. 1985; Eagle et al. 2009), increased startle responses (Davis & Sheard 1974; Davis et al. 1980) and increased output of operant behavior suppressed by punishment (reviewed in Dayan & Huys 2009). Consistent with this hypothesis is a set of data linking 5-HT with impulse control (reviewed in Evenden 1999). Neurons from the dorsal raphe nuclei (DRN, the main source of 5-HT to the forebrain) are active while rats wait for delayed rewards and delayed reward predictive cues (Miyazaki et al. 2011), and blocking DRN 5-HT activity increases premature responding (Miyazaki et al. 2012). More recently, it has been confirmed with optogenetic techniques that activation of DRN 5-HT neurons suppresses impatient responses (Miyazaki et al. 2014; Fonseca et al. 2015). Moreover, increasing 5-HT pharmacologically (Reyes-Vazquez et al. 1989) or optogenetically (Dugué et al. 2014) attenuates responses to painful mechanosensory stimuli.

5-HT has also been associated with reward and reinforcing behaviors (Nakamura et al. 2008; Ranade & Mainen 2009; Inaba et al. 2013; Bromberg-Martin et al. 2010; Liu et al. 2014). The vast literature using selective 5-HT reuptake inhibitors (SSRIs) demonstrates that 5-HT is effective in treating major depression (Leonard 1987; Graeff et al. 1996; Maier & Watkins 2005). Pharmacological studies have suggested a role for 5-HT in anxiety-like behaviors (reviewed in Prut & Belzung 2003), but with inconsistent results. More recently using optogenetic methods, activation of DRN 5-HT neurons produced no effect in anxiety-like parameters, but promoted a decrease in locomotor activity in the elevated plus maze (Ohmura et al. 2014). This result is consistent with 5-HT behavioral inhibition theory, but the nature of the effect remains unclear. One possibility could be that the stimulation of 5-HT is a rewarding signal and in fact a recent study found DRN 5-HT photostimulation to be reinforcing in several behaviors (Liu et al. 2014). This finding is however controversial (McDevitt et al. 2014; Luo et al. 2015), as similar optogenetic methods failed to reproduce reinforcing effects (Miyazaki et al. 2014; Fonseca et al. 2015). Regardless of the inconsistent results, little attention has been given to the function of 5-HT in non-punishment or non-rewarding conditions.

To address these issues, in the present report we performed experiments examining the effects of optogenetic activation of DRN 5-HT neurons in a series of tasks to assess 5-HT's effects in movement, anxiety-like responses, motor coordination and aversive or appetite actions. We found that photostimulation of

DRN 5-HT neurons induced a robust decrease in speed of mice running in an open field arena, with no effects in the classical measures of anxiety. In contrast, using the same optogenetic approach, we found no evidence of motor coordination impairment in the accelerating rotarod and linear track locomotion assays. Finally we confirmed the absence of an appetitive or aversive effect of DRN 5-HT activation, in a task with photostimulation constrained to a sub-region of the open field, under non-rewarding or non-punishment conditions. These results provide direct evidence of sufficiency of DRN 5-HT activation in decreasing movement, without affecting motor coordination or promoting reinforcing responses.

3.3 Results

3.3.1 Optical activation of DRN 5-HT neurons is sufficient to slow down animals in the open field

To study the effect of DRN 5-HT stimulation in movement, we placed adult transgenic mice expressing CRE recombinase under the serotonin transporter promoter (SERT-Cre) and wild-type littermates (WT) in an open field arena and let them freely behave for 30 min (**Figure 3.1A**). To manipulate the activity of DRN 5-HT neurons, we expressed the light-sensitive ion channel channelrhodopsin-2 (ChR2) in DRN 5-HT neurons using an AAV2/9 viral vector (AAV2/9-Dio-ChR2-EYFP) injected into the DRN of SERT-Cre mice (n = 15) or WT (n = 9) and

implanted an optical fiber in the same location (**Figure 3.1B**) (see Dugué et al. 2014 for more details).

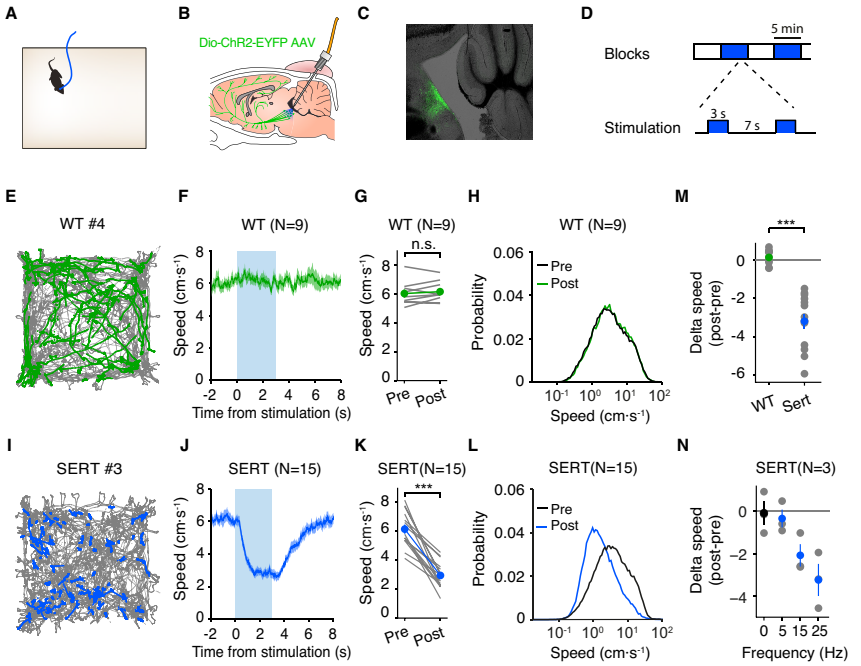

Figure 3.1. DRN 5-HT activation slows down animals in the open field

(A) Schematic drawing of the open field paradigm. Animals were implanted with an optical fiber connected to a blue laser, while freely exploring an open field arena. **(B)** Schematic drawing of the optogenetic approach. DRN neurons are infected with AAV2/9-Dio-ChR2-EYFP. In SERT-Cre mice, 5-HT neurons will express ChR2-YFP (green cells) and can be photoactivated with blue light delivered through an optical fiber implant. **(C)** Fluorescence image of a parasagittal section showing localized ChR2-YFP expression in the DRN. YFP in green. **(D).** Schematic diagram of trial events and photostimulation protocol in the open field. Stimulation alternated between on and off in blocks of 5 min, starting with no stimulation, for a total of 30 min session. Each stimulation trial included 3 s of light on and 7 s of light off. **(E)** Locomotion tracks of an example WT mouse. In grey, all positions visited in the session. In green, the positions visited during the 3 s stimulation trials. **(F)** Speed traces of all stimulation trials, aligned to light onset, for the population of WT mice (n = 9). Averages across mice are shown. The shaded area indicates SEM. **(G)** Speed of pre- and post-stimulation intervals in all photostimulated trials for the population of WT mice (n = 9). Pre-stimulation is the interval of 2 s before light onset and post-stimulation is the interval of 2 s between the first and last

seconds of stimulation (1 s – 3 s). Individual mice shown in grey lines. Averages across mice are shown in filled circles. Error bars indicate SEM. In some cases, the error bars are too small to be visible. n.s., not significant. **(H)** Speed probability distribution of pre- and post-stimulation intervals in photostimulated trials for the population of WT mice (n = 9). **(I)** The same as (E) but for the population of SERT-Cre mice (n = 15). In blue, the positions visited during the 3 s stimulation trials. **(J)** The same as (F) but for the population of SERT-Cre mice (n = 15). **(K)** The same as (G) but for the population of SERT-Cre mice (n = 15). ***$p < 0.001$ with paired t test. **(L)** The same as (H) but for the population of SERT-Cre mice (n = 15). **(M)** Difference between post- and pre-stimulation intervals (delta speed) for photostimulated trials of WT (green) and SERT-Cre mice (blue). Individual mice shown in grey filled circles. ***$p < 0.01$ with two-sample t test. **(N)** Frequency of stimulation dose-dependent decrease in delta speed (difference between post- and pre-stimulation intervals) for a subset of SERT-Cre mice (n = 3). Averages across mice are shown. Error bars indicate SEM.

Histology was performed at the end of testing to confirm ChR2-YFP expression localized to the DRN in SERT-Cre animals (**Figure 3.1C**) and no expression in WT controls (data not shown). After allowing 2–3 weeks for virus expression, we delivered photostimulation at 25 Hz, 5 mW amplitude and 10 ms pulses in 5 min blocks schedule, with photostimulation happening with 3 s light on, interleaved with 7 s light off, during the block of stimulation (**Figure 3.1D**).

DRN 5-HT photostimulation happened heterogeneously in space, as depicted by the locomotion traces for a representative WT (**Figure 3.1E**) and SERT-Cre mouse (**Figure 3.1I**). Optical activation in SERT-Cre, but not WT mice resulted in a robust decrease in movement speed. **Figure 3.1J** shows the mean speed of the stimulated trials for the population of SERT-Cre and WT mice (**Figure 3.1F**). We compared speed before stimulation ('pre' condition, 2 s window before light onset) and during stimulation ('post' condition, second 1 to 3 of light delivery) of the first

exposure session and observed a significant reduction in the post condition for SERT-Cre mice (paired t test, $p=4.80 \times 10^{-7}$, n=15 mice, **Figure 3.1K**). The effect represents a clear change in the distribution of speed, with a mean of 6.14 ± 0.31 cm/s (mean ± S.E.M.) for pre-stimulation and 2.94 ± 0.24 cm/s (mean ± S.E.M.) for post-stimulation for SERT-Cre animals (**Figure 3.1L**). Furthermore, we observed a dose dependency of photostimulation frequency (5, 15 and 25 Hz) on speed, confirmed with a linear correlation (Pearson correlation coefficient, r = -0.992, **Figure 3.1N**). No significant effects were found in either measure for WT mice (**Figure 3.1F-H**, n = 9 mice). Finally, delta speed (difference between post- and pre-stimulation speed) was significantly different between SERT-Cre and WT animals (two-sample t test, $p = 7.45 \times 10^{-7}$, **Figure 3.1M**).

These results show that optical activation of DRN 5-HT neurons promotes a robust decrease in speed in SERT-Cre mice exploring an open field arena.

3.3.2 Effect of DRN 5-HT photostimulation is persistent regardless of previous speed

To further characterize the 5-HT result, we tested if the decrease in movement depended on the animal's previous speed. For that, we analyzed the effect of optical activation of DRN 5-HT neurons conditioned by the ongoing speed of the animal. To assess different speed states, ranging from immobility to running, we first divided the pre-stimulation speed distribution of each animal in four quartiles (**Figure 3.2A, D**).

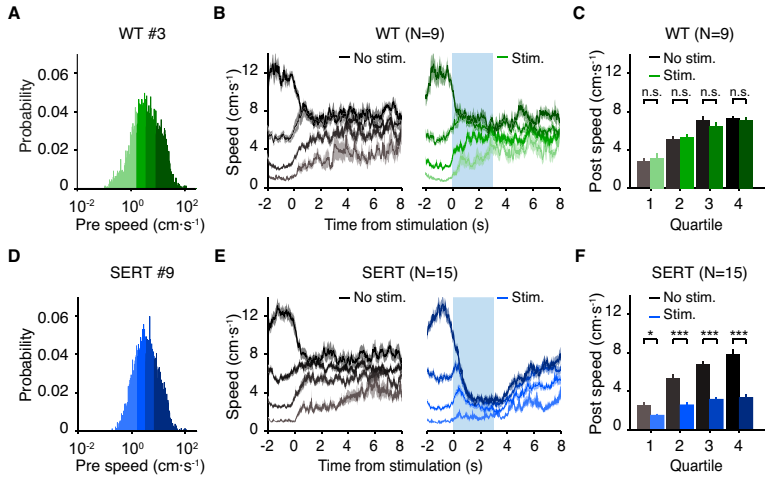

Figure 3.2. Effect of DRN 5-HT photostimulation is persistent regardless of previous speed of the animals
(A) Speed probability distribution of pre-stimulation intervals for both stimulated and non-stimulated trials for an example WT mouse. Different color gradients represent quartiles of the distribution. (**B**) Speed traces of all non-stimulated (black) and stimulated (green) trials, conditioned to previous speed of the animal, for the population of WT mice (n = 9). The four gradient colors represent quartiles of speed (showed in A). Averages across mice are shown. The shaded area indicates SEM. **(C)** Average speed of the post-stimulation interval (2 s during stimulation) in non-stimulated (black) and stimulated (green) trials, for each quartile of pre-stimulation speed for the population of WT mice (n = 9). Averages across mice are shown and error bars indicate SEM. n.s., not significant. (**D**) The same as (A) but for an example SERT-Cre mouse. **(E)** The same as (B) but for the population of SERT-Cre mice (n = 15). (**F**) The same as (C) but for the population of SERT-Cre mice (n = 15). Non-stimulated trials in black and stimulated trials in blue. * $p < 0.013$, ** $p < 0.003$, *** $p < 2.50 \times 10^{-4}$ (paired t test with Bonferroni correction for multiple comparisons).

We then looked at the 'post' speed, given the 'pre' speed in each quartile. We found a decrease in movement during photostimulation, in all quartiles of pre speed, for the population of SERT-Cre mice (**Figure 3.2E**, n = 15 mice). The effect was confirmed with a three-way ANOVA (subjects, stimulation, quartiles) on the average speed for SERT-Cre mice (stimulation,

$F_{(1,40)}$ = 77.451, p = 4.20 x 10^{-7}; quartile, $F_{(3,30)}$ = 63.867, p =5.48 x 10^{-16}; stimulation x quartile $F_{(1,40)}$ = 22.158, p = 1.29 x 10^{-8}), followed by a paired t test, comparing post-stimulation speed (2 s interval in stimulation period) between non-stimulated and stimulated trials across quartiles (p(quartile 1) = 0.009, p(quartile 2) = 3.95 x 10^{-5}, p(quartile 3) = 1.06 x 10^{-6}, p(quartile 4) = 3.34 x 10^{-7}, * p < 0.013, *** p < 2.50 x 10^{-4} (with Bonferroni correction), **Figure 3.2F**, SERT-Cre mice, n = 15). No significant changes were found for WT mice (**Figure 3.2B-C**, n = 9 mice).

These results show that DRN 5-HT photostimulation reduces movement of animals exploring an open field, regardless of their ongoing speed.

3.3.3 DRN 5-HT movement effect is not exclusive to specific spatial locations in the open field

Previous studies using ethological assessments of animal behavior showed that pharmacological drugs affect distinct behavioral states in the open field (Choleris 2001). To further characterize the movement effect in different states of the animal's behavior, we next investigated the effect of DRN 5-HT activation in different areas of the open field arena. We defined three spatial areas (**Figure 3.3A**) and measured their occupancy times. We found that both WT and SERT-Cre mice spend more time in corners and periphery and less in center (**Figure 3.3B**, WT not shown), as described previously in the literature (Prut and Belzung). The three spatial areas of the open field displayed

diverse speed probability distributions, consistent with distinct states of the animal's behavior (Choleris 2001).

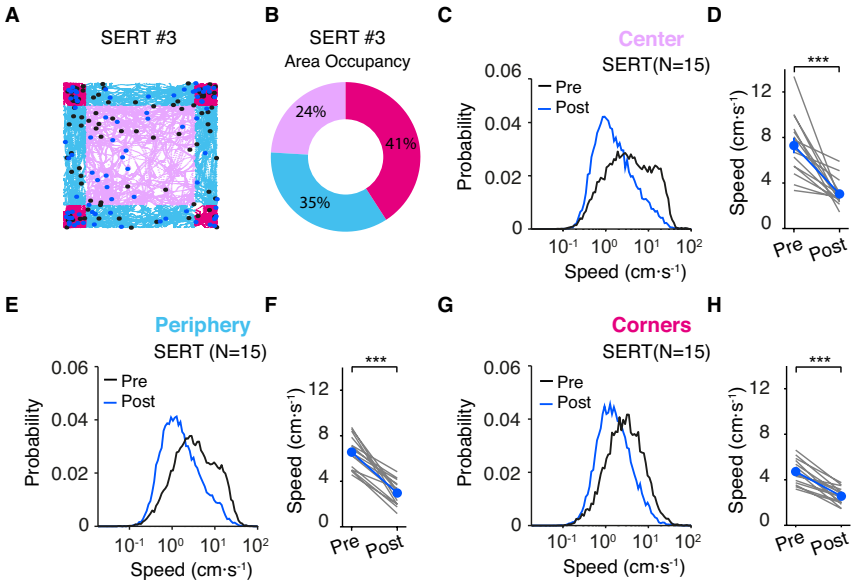

Figure 3.3. Effect of DRN 5-HT photostimulation is not exclusive to spatial areas of the open field

(A) Locomotion tracks of all positions visited for one example session of a SERT-Cre mouse, depicting the three main areas of the open field. In dark pink the corners, in light blue the periphery and in light pink the center. Filled circles represent beginning of each trial (blue for stimulated and black for non-stimulated trials). **(B)** Occupancy (%) in each area of the open field for one example session of a SERT-Cre mouse. In dark pink the corners, in light blue the periphery and in light pink the center. **(C)** Speed probability distribution of pre- and post-stimulation intervals in photostimulated trials in the center area of the open field for the population of SERT-Cre mice (n = 15). Non-stimulated trials in black and stimulated trials in blue. **(D)** Speed of pre- and post-stimulation intervals in all photostimulated trials that happened in the center area for the population of SERT-Cre mice (n = 15). Individual mice shown in grey lines. Averages across mice are shown in blue circles. Error bars indicate SEM. In some cases, the error bars are too small to be visible. **p < 0.01 with paired t test. **(E)** The same as (C) but for the periphery area of the open field. **(F)** The same as (D) but for the periphery area of the open field. **(G)** The same as (C) but for the corners area of the open field. **(H)** The same as (D) but for the corners area of the open field.

DRN 5-HT photostimulation in SERT-Cre mice caused a robust decrease in speed, regardless of the spatial area where the animal was located (center **Figure 3.3C**, periphery **Figure 3.3E** and corners **Figure 3.3G**). The effect was confirmed with a paired t test, comparing the mean speed of pre- and post-stimulation in the center (**Figure 3.3D**, $p = 6.19 \times 10^{-5}$, $n = 15$), periphery (**Figure 3.3F**, $p = 2.50 \times 10^{-7}$, $n = 15$) and corners (**Figure 3.3H**, $p = 6.08 \times 10^{-7}$, $n = 15$).

These results show that DRN 5-HT activation promotes a decrease in movement in the different areas of the open field, thus suggesting that 5-HT effect seems to be independent of the state of the animal.

3.3.4 Effect of DRN 5-HT photostimulation does not seem to affect anxiety-like behavior

The open field assay has been classically used to provide an initial screen for anxiety-related behavior in rodents (Bailey & Crawley 2009) and 5-HT has long been associated with anxiety. Previous studies, using pharmacological 5-HT agonists in the open field, described an increase in center avoidance, which is generally accepted to be a measure of anxiety-like behavior (reviewed in Prut & Belzung 2003). We next tested if optical activation of DRN 5-HT neurons promotes an increase in center avoidance. We found no significant difference in total time spent in the center between non-stimulated and stimulated five-minute blocks (**Figure 3.4D-E**) for SERT-Cre animals (n = 15). Also, we observed no change in the distance from the center of the open

field arena, between stimulated and non-stimulated trials (**Figure 3.4F**). No significant changes were observed in either measure for WT mice (**Figure 3.4A-C**).

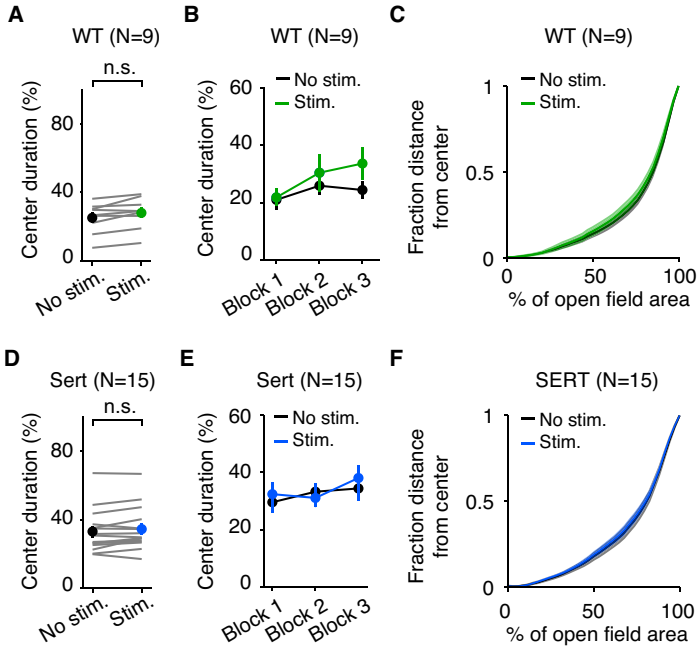

Figure 3.4. DRN 5-HT photostimulation does not affect anxiety-like parameters in the open field

(A) Total center area occupancy (%) of the open field in non-stimulated (black) and stimulated (green) 5 min blocks for the population of WT mice (n = 9). Individual mice shown in grey lines. Averages across mice are shown in filled circles. Error bars indicate SEM. In some cases, the error bars are too small to be visible. n.s., not significant. **(B)** Center area occupancy (%) of the open field in non-stimulated (black) and stimulated (green) across 5 min blocks for the population of WT mice (n = 9). Averages across mice are shown. Error bars indicate SEM. In some cases, the error bars are too small to be visible. **(C)** Distance from the center of the open field for stimulated vs non-stimulated blocks. Averages across mice are shown. The shaded area indicates SEM. **(D)** The same as (A) but for the population of SERT-Cre mice (n = 15). In blue, the stimulated 5 min blocks. **(E)** The same as (B) but for the population of SERT-Cre mice (n = 15). In blue, the stimulated 5 min blocks. **(F)** The same as (C) but for the population of SERT-Cre mice (n = 15). In blue, the stimulated 5 min blocks.

These results indicate that DRN 5-HT photostimulation has no effect in the preference for spatial locations in the open field arena, hence does not attenuate or enhance anxiety-related behavior.

3.3.5 Effect of DRN 5-HT photostimulation is not due to motor behavior impairment

We next investigated possible explanations for the movement effect. We first tested the hypothesis that DRN 5-HT photostimulation reduces movement via impairment of motor coordination. For that, we initially ran a subset of the animals in the accelerating rotarod test (**Figure 3.5A**), a widely used assay to assess drug effects on motor coordination in rodents (Carter et al. 2001). Mice were trained for two consecutive days on an accelerating rotarod and on the third day DRN 5-HT neurons were photostimulated (25 Hz at 10 ms pulses, 5 mW amplitude) in a random 50% of the trials (**Figure 3.5B**). We found no significant difference in latency to fall between stimulated and non-stimulated trials for WT (n = 2) and SERT-Cre mice (n = 3) or between WT and SERT-Cre mice, as exhibited in **Figure 3.5C**. To further investigate the effect of DRN 5-HT photostimulation in motor coordination, we then tested a subset of mice in the LocoMouse (**Figure 3.5D**), a linear track assay developed to assess fine motor coordination (Machado et al. 2015). DRN 5-HT photostimulation was delivered in randomly assigned trials, starting when the animal entered the corridor and finishing once it reached the other end.

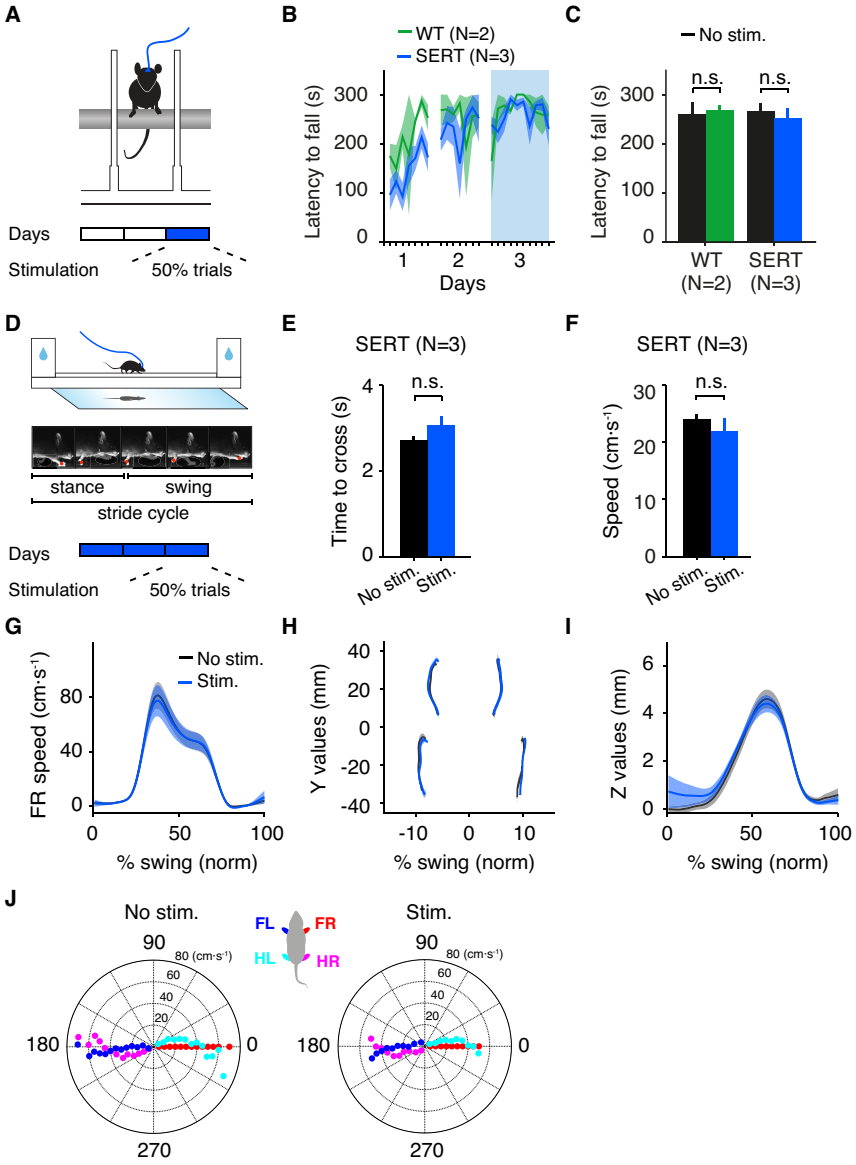

Figure 3.5. DRN 5-HT photostimulation does not affect motor coordination in the rotarod and LocoMouse assays

(A) Schematic drawing of the accelerating rotarod assay. **(B)** Motor skill learning in the accelerating rotarod task for the population of WT (green, n = 2) and SERT-Cre mice (blue, n = 3). Cyan bar indicates stimulation session (day 3). The shaded area indicates SEM. **(C)** Latency to fall on the accelerating rotarod task in stimulated and non-stimulated trials (black). Green represents stimulated trials for WT mice (n = 2) and blue for SERT-Cre mice (n = 3). n.s., not significant. **(D)** Schematic drawing of the LocoMouse apparatus. Water

deprived animals walk freely across a glass corridor connected to two boxes with water ports. A mirror below at 45º angle allows a single high-speed camera to capture side and bottom views. Individual strides were divided into swing and stance phases for further analysis. DRN 5-HT photostimulation happened randomly in 50 % of the trials. **(E)** Time to cross the linear track from one side to the other for non-stimulated (black) and stimulated (blue) trials for the SERT-Cre mice population (n = 3). Averages across mice are shown. Error bars indicate SEM. n.s., not significant. **(F)** Whole-body speed (center of mass) in non-stimulated (black) and stimulated (blue) trials for the SERT-Cre mice population (n = 3). Averages across mice are shown. Error bars indicate SEM. n.s., not significant. **(G)** Instantaneous forward speed of front-right paw during swing phase at stride speed of 15-20 cm/s. Stimulated trials in blue and non-stimulated trials in black. Averages across mice are shown. The shaded area indicates SEM. **(H)** x-y position of four paws relative to the body center during swing. Stimulated trials in blue and non-stimulated trials in black. Averages across mice are shown. The shaded area indicates SEM. **(I)** Vertical (z) position of front-right paw relative to ground during swing. Stimulated trials in blue and non-stimulated trials in black. Averages across mice are shown. The shaded area indicates SEM. (**J)** Polar plots indicating the phase of the step cycle in which each limb enters stance, aligned to stance onset of front-right paw (FR, red). Distance from the origin represents walking speed. Left, non-stimulated trials. Right, stimulated trials.

We observed no significant difference between stimulated and non-stimulated trials, both for average time to cross the track ($F_{(1,402)}$ = 2.424, p = 0.239, ANOVA, **Figure 3.5E**) and average speed ($F_{(1,402)}$ = 1.958, p = 0.272, ANOVA, **Figure 3.5F**, for the population of SERT-Cre mice (n = 3). It is important to note that mice moved in general with higher average speed in this task (24.08 ± 0.77 cm/s), when compared with the open field test (6.14 ± 0.31 cm/s, mean ± S.E.M.).

The setup was connected to a high-speed camera that allowed us to further characterize motor coordination of the animals, by tracking the position of the four paws, nose and tail (**Figure 3.5D**). We performed single-limb gait analyses, looking at continuous 3D paw trajectories in forward (x-axis), side-to-side (y-axis) and vertical (z-axis) movement, for different speed

intervals. We found no differences in any dimension for the animal paw's locomotion, between stimulated and non-stimulated trials (**Figure 3.5G-I**, speed bin example, 15-20 cm/s). Polar plots indicating the phase of the step cycle in which each limb enters stance, showed no differences with DRN 5-HT stimulation (**Figure 3.5J**). Furthermore, neither nose nor tail tracking were affected in stimulated trials (**Figure S 3.1**).

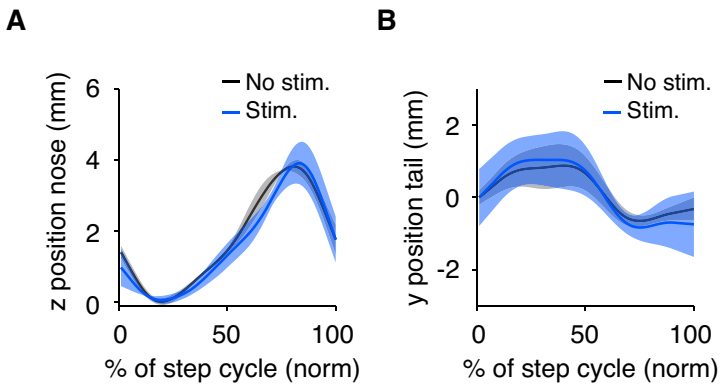

Figure S 3.1. DRN 5-HT activation in the LocoMouse test does not produce changes in the nose and tail movement
(A) Nose trajectory along the z-position, for the population of SERT-Cre mice (n = 3) walking at 15-20 cm/s. Stimulated trials in blue and non-stimulated trials in black. Averages across mice are shown. The shaded area indicates SEM. **(B)** Tail segment 8 trajectory along the y-position, for the population of SERT-Cre mice (n = 3) walking at 15-20 cm/s. Stimulated trials in blue and non-stimulated trials in black. Averages across mice are shown. The shaded area indicates SEM.

To ensure that the lack of effect was not explained by the time-course of virus infection, we re-tested the animals in the open field, after performing the LocoMouse assay, and confirmed the decrease in speed with DRN 5-HT photostimulation (Figure S 3.2, $p = 0.032$, paired t test, SERT-Cre mice, n = 3).

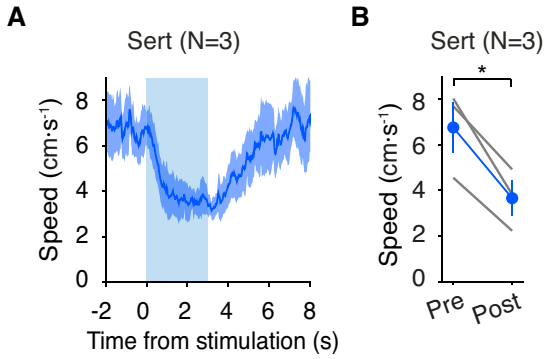

Figure S 3.2. DRN 5-HT photostimulation in the open field for a subset of SERT-Cre mice (n = 3), performed after LocoMouse experiment
(A) Speed traces of all stimulation trials, aligned to light onset, for a subset of SERT-Cre mice (n = 3), after performing Experiment 5. Averages across mice are shown. The shaded area indicates SEM. **(B)** Speed of pre- and post-stimulation intervals in all photostimulated trials for a subset of SERT-Cre mice (n = 3). Stimulation happened in the same conditions as Experiment 3, 20 mW, 25 Hz at 10 ms pulses. Averages across mice are shown. Error bars indicate SEM. n.s., not significant.

Overall, based in our results, it is unlikely that the effect of DRN 5-HT photostimulation is explained by impairment in motor coordination.

3.3.6 Effect of DRN 5-HT photostimulation in the open field is persistent across days and is not explained by novelty of the environment

Another possible explanation for the movement effect is connected with the novelty of the environment. Previous pharmacological studies reported that 5-HT affects locomotion, suggesting the effect is due to the exploration of a novel context (Prut and Belzung). We therefore investigated if the decrease in

speed observed in SERT-Cre mice diminished with habituation to the open field context.

Two subsets of the SERT-Cre and WT animals (G1 and G2) were exposed to the open field arena for consecutive days. Group 1, 'G1' (3 SERT-Cre and 2 WT mice) received DRN 5-HT photostimulation for 24 consecutive days. To control for habituation to the open field, group 2, 'G2' (3 SERT-Cre and 2 WT mice) was exposed to the arena for 23 days with no stimulation, being stimulated on the 24^{th} day and for six consecutive days (**Figure 3.6A**). Surprisingly, the effect of DRN 5-HT photostimulation on speed persisted throughout days in SERT-Cre mice (**Figure 3.6B**, G1, n = 3 mice), even for G2 after 23 days exposure to the open field (**Figure 3.6B**, n = 3 mice).

We observed no significant differences in the first stimulated sessions between SERT-Cre animals of G1 and G2 (2-way ANOVA with groups of mice and sessions as main factors, no significant effects). Therefore, we merged the two data sets to further explore the effect of DRN 5-HT stimulation across blocks for the first six sessions.

Optical activation of DRN 5-HT neurons in the open field happened with a blocks scheduled, as previously described (**Figure 3.1D**). We observed an overall persistency of delta speed decrease in all stimulated blocks, with a stronger effect in the first photostimulated 5 min block, for the population of SERT-Cre mice (**Figure 3.6D**, n = 6). The result was confirmed with a three-way ANOVA (subjects, stimulation, blocks) on the delta speed for SERT-Cre mice (stimulation, $F_{(1,28)} = 69.922$, $p = 8.15 \times 10^{-7}$;

blocks, $F_{(2,28)}$ = 3.360, p = 0.049; stimulation x blocks, $F_{(2,28)}$ =1.692, p = 0.202), followed by a paired t test for comparison between non-stimulated and stimulated trials across blocks (p(block 1) = 3.33 x 10^{-4}, p(block 2) = 0.001, p(block 3) = 0.001, **p<0.003, ***p<3.33x10^{-4} (with Bonferroni correction), **Figure 3.6E**, SERT-Cre mice, n = 15).

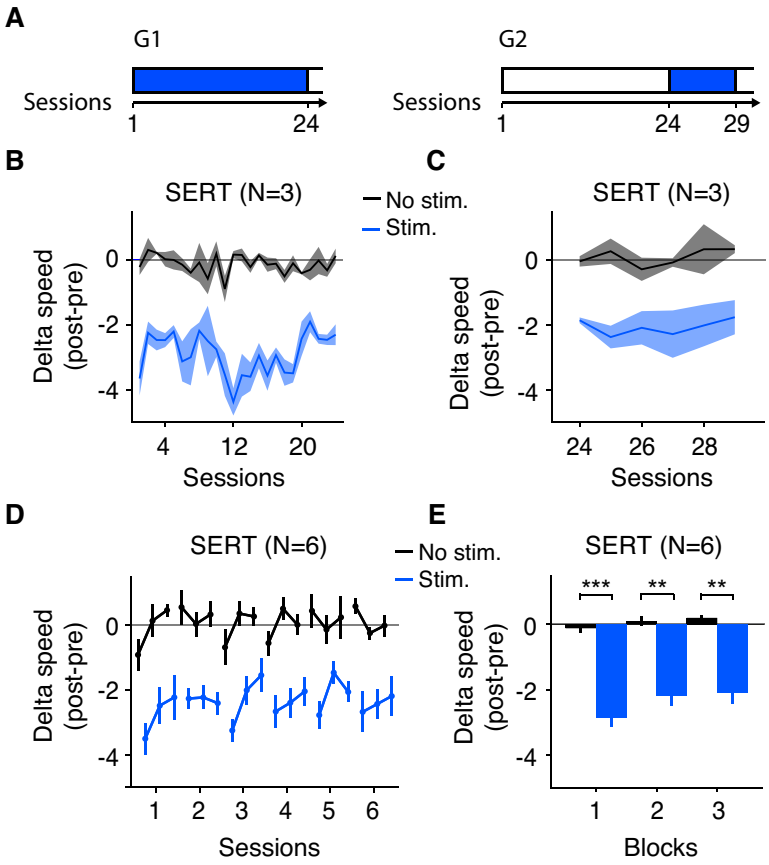

Figure 3.6. Effect of DRN 5-HT photostimulation is not explained by novelty and it is persistent across sessions and blocks

(A) Schematic drawing of open field novelty experiment. Two groups of mice were exposed to the same open field arena for consecutive days. G1 (3 SERT-Cre and 2 WT mice) received photostimulation starting from session 1 and until 24 days. G2 (3 SERT-Cre and 2 WT mice) was exposed to the arena for 23 days, receiving photostimulation only on the 24th day and for 6 consecutive

days. Stimulation was performed as described previously (see Figure 3.1). **(B)** Delta speed (difference between post- and pre-stimulation intervals) across 25 sessions for a subset of SERT-Cre mice (G1, n = 3). Non-stimulated trials in black and stimulated trials in blue. Averages across mice are shown. The shaded area indicates SEM. **(C)** Delta speed (difference between post- and pre-stimulation intervals) across 6 sessions for a subset of SERT-Cre mice that was previously exposed to the open field for 24 days, without receiving photostimulation (G2, n = 3). Non-stimulated trials in black and stimulated trials in blue. Averages across mice are shown. The shaded area indicates SEM. **(D)** Delta speed (difference between post- and pre-stimulation intervals) for each block of trials across the first six sessions for the population of SERT-Cre mice (n = 6). Non-stimulated trials in black and stimulated trials in blue. Averages across mice are shown. Error bars indicate SEM. **(E)** Delta speed (difference between post- and pre-stimulation intervals) for each block of the first six sessions for the population of SERT-Cre mice (n = 6). Non-stimulated trials in black and stimulated trials in blue. Averages across mice are shown. Error bars indicate SEM. $^{**}p<0.003$, $^{***}p<3.33x10^{-4}$ (paired t test with Bonferroni correction for multiple comparisons).

As expected, we found no significant changes in delta speed between stimulated and non-stimulated trials across sessions or blocks for WT animals (data not shown, n = 4). Our results show that the reduction in movement observed in SERT-Cre mice is persistent across days and blocks and it does not seem to be explained by novelty of the environment.

To further investigate if novelty of the context could have an effect on the 5-HT movement result, we ran the same animals in modified versions of the open field, testing different floors (corncob, plastic and paper) and geometry (rectangular and circular) in an interleaved way (**Figure 3.7A**). Surprisingly, we found that DRN 5-HT activation in the open field with plastic floor produced a smaller movement effect, when compared with the stimulation effect in the corncob floor (**Figure 3.7B**). Furthermore, geometry did not seem to change the 5-HT movement effect. This effect was confirmed with a three-way

ANOVA (subjects, floor and geometry) on delta speed of SERT-Cre mice (floor, $F_{(2,21)} = 7.824$, $p = 0.003$; geometry, $F_{(1,21)} = 0.374$, $p = 0.548$), followed by a post-hoc multiple comparison t test, using the Bonferroni method to compare between different floor conditions (corncob x plastic, $p < 0.05$; no other floor combinations were significant). No significant differences were found in delta speed of WT mice (data not shown).

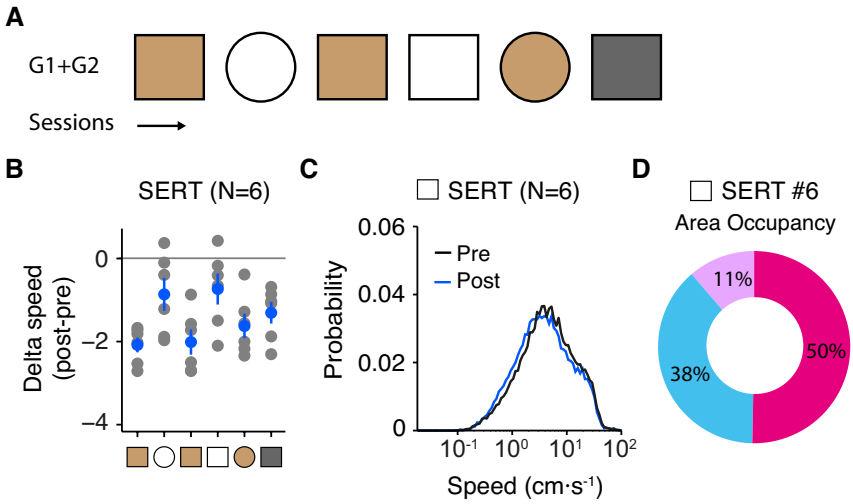

Figure 3.7. Effect of DRN 5-HT photostimulation is sensitive to open field floor, but not geometry

(A) Schematic drawing of open field texture and geometry test. A subset of mice (n = 6) were exposed to open field arenas with different texture floors and geometries for consecutive days. Different floors were corncob bedding (brown), plastic (white) and paper (grey). Geometries were rectangular and oval shape. **(B)** Delta speed (difference between post- and pre-stimulation intervals) for photostimulated trials for the population of SERT-Cre mice (blue) in the different conditions of open field (floor and geometry). Individual mice shown in grey filled circles. **(C)** Speed probability distribution of pre- and post-stimulation intervals in photostimulated trials for the population of SERT-Cre mice (n = 6) in the no-bedding rectangular condition. **(D)** Occupancy (%) in each area of the open field for one example session of a SERT-Cre mouse. In dark pink the corners, in light blue the periphery and in light pink the center.

We next further characterized the behavior of SERT-Cre mice exploring the rectangular plastic floor open field, to compare it with the corncob floor previously described (**Figure 3.1-3.3**). To note that the open field in this case was exactly the same, but instead of adding fresh corncob bedding, animals were placed directly in the plastic floor of the arena. We observed a smaller effect in the speed probability distributions between pre- and post-stimulation intervals (**Figure 3.7C**), when compared with the corncob case (**Figure 3.1L**). Animals in the plastic floor displayed higher average pre-stimulation speed (7.99 ± 0.38 cm/s) and spent less time in the center (11% center occupancy, **Figure 3.7E**, representative animal in the plastic floor), than in the corncob case (average pre-stimulation speed, 6.14 ± 0.31 cm/s, **Figure 3.1L**; 24 % center occupancy, **Figure 3.3B**).

Altogether, these results show that the effects of DRN 5-HT photostimulation are persistent across sessions, not specific to a novel environment, but seem to be decreased in a different open field floor.

3.3.7 DRN 5-HT Photostimulation Does Not Produce Aversive nor Appetite Responses

We next tested whether the decrease in movement was related to possible appetitive or aversive effects of DRN 5-HT activation. We ran an open field assay with photostimulation happening exclusively in a region of interest (ROI) of the arena (**Figure 3.8**).

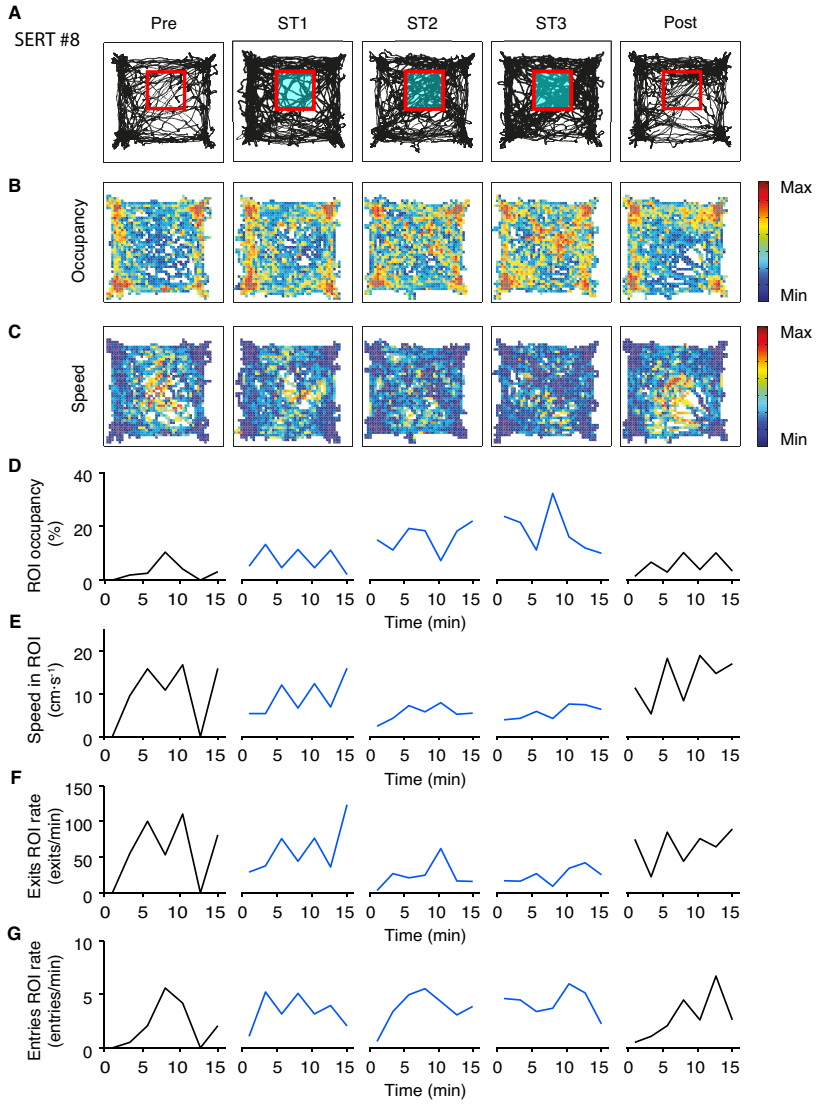

Figure 3.8. DRN 5-HT photostimulation in a specific region of interest of the open field

(A) Locomotion tracks illustrating the spatial exploration before (pre), during (T1-T3) and after (post) ROI photostimulation of an example SERT-Cre mouse. **(B)** Occupancy heatmaps illustrating the spatial exploration before (pre), during and after (post) ROI photostimulation of an example SERT-Cre mouse. The color scale at the right indicates the duration in a specific area. **(C)** Speed heatmaps before (pre), during and after (post) ROI photostimulation of an example SERT-Cre mouse. The color scale at the right indicates the average speed in a specific area. **(D)** Time spent inside ROI across sessions for one example SERT-Cre mouse (2 min per point). Blue for stimulated and black for

non-stimulated trials. **(E)** The same as (D) but for the entries ROI rate. **(F)** The same as (D) but for the exits ROI rate. **(G)** The same as (D) but for the average speed in ROI.

After one habituation session ('Pre'), mice were subjected to 3 days of conditioning ('T1-T3'), with DRN 5-HT photostimulation happening exclusively in the defined ROI with 10 ms pulses at 25Hz and 20mW amplitude. (We also ran a subset of mice in the standard open field protocol under the same amplitude and found similar magnitude results, **Figure S 3.3**). On day 5, mice were retested in the absence of optical activation ('Post').

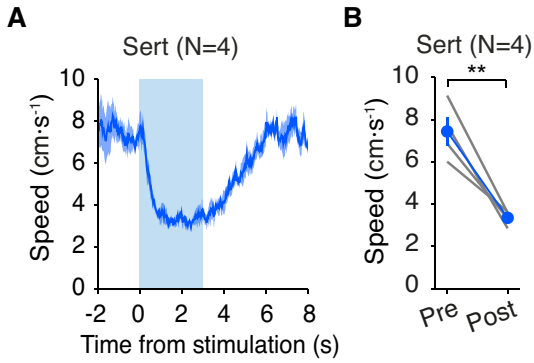

Figure S 3.3. DRN 5-HT photostimulation at 20mW slows down animals in the open field
(A) Speed traces of all stimulation trials, aligned to light onset, for a subset of SERT-Cre mice (n = 4). Stimulation happened in the same conditions as Experiment 3, 20 mW, 25 Hz at 10 ms pulses. Averages across mice are shown. The shaded area indicates SEM. **(B)** Speed of pre- and post-stimulation intervals in all photostimulated trials for a subset of SERT-Cre mice (n = 4). Stimulation happened in the same conditions as Experiment 3, 20 mW, 25 Hz at 10 ms pulses. Averages across mice are shown. Error bars indicate SEM. In some cases, the error bars are too small to be visible. n.s., not significant.

Based on the recent finding that activation of DRN 5-HT neurons positively reinforces behaviors (Liu et al. 2014) and on the observation that animals in general spend less time in the center

of the open field (**Figure 3.3B**), we defined the ROI as a sub-region of the center area (**Figure 3.8A**). For each day, animals had no visible cues for the ROI in the open field and they freely explored the arena for 15 min. Locomotion traces, occupancy and speed heatmaps for all five days of the assay for a representative SERT-Cre mouse are shown in **Figure 3.8A-C**. Furthermore, we analyzed the ROI occupancy (**Figure 3.8D**), rate of entries (**Figure 3.8E**) and exits (**Figure 3.8F**) to/from the ROI and average speed (**Figure 3.8G**) across time for each session. Photostimulation of DRN 5-HT neurons produced a significant increase in ROI occupancy across stimulated sessions ($F_{(4,15)}$ = 5.563, p = 0.006, ANOVA; **Figure 3.9G**), without affecting the total number of entries ($F_{(4,15)}$ = 0.032, p = 0.998, ANOVA; **Figure 3.9H**) or the rate of entries in the ROI ($F_{(4,15)}$ = 0.195, p = 0.937, ANOVA; **Figure 3.9I**) in SERT-Cre mice (n = 4). Based on the dramatic decrease of speed after optical activation of DRN 5-HT neurons that we report (**Figure 3.1-3.3**), our original prediction was that animals would spend more time in the ROI as a consequence of the movement effect. We found indeed a decrease in the rate of exits from ROI ($F_{(4,15)}$ = 26.612, p = 1.17 x 10^{-6}, ANOVA; **Figure 3.9J**), average interval of visits to ROI ($F_{(4,15)}$ = 24.657, p = 1.91 x 10^{-6}, ANOVA; **Figure 3.9K**) and average speed inside ROI ($F_{(4,15)}$ = 73.595, p = 1.80 x 10^{-9}, ANOVA; **Figure 3.9L**), across stimulated sessions for the population of SERT-Cre (n = 4). No significant differences were found for average speed outside the ROI across sessions for both SERT-Cre and WT mice (data not shown).

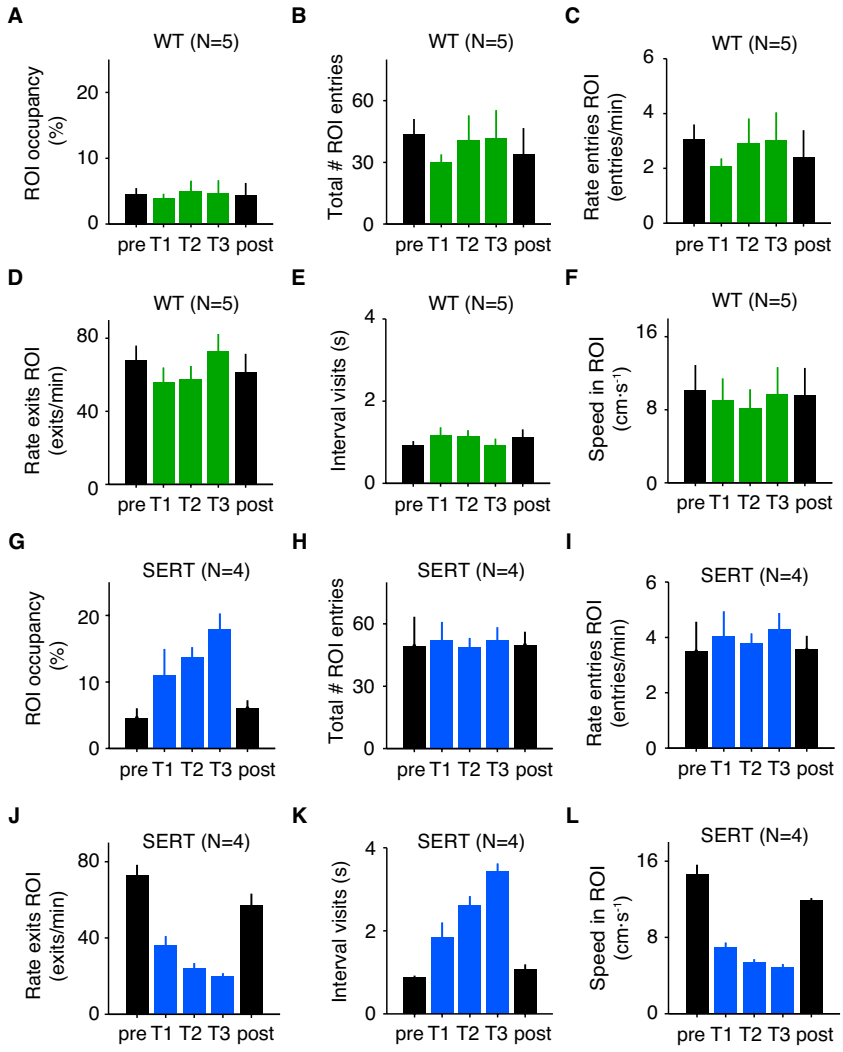

Figure 3.9. DRN 5-HT photostimulation in a specific region of interest does not produce aversive or appetitive responses

(A) Total occupancy of ROI across sessions for the population of WT mice (n = 5). Green for sessions with ROI stimulation. Error bars indicate SEM. **(B)** Same as (A) but for total number of entries in the ROI. **(C)** Same as (A) but for rate of entries in the ROI. **(D)** Same as (A) but for rate of exits in the ROI. **(E)** Same as (A) but for average interval of visits to the ROI. **(F)** Same as (A) but for average speed in the ROI. **(G)** Same as (A) but for the population of SERT-Cre mice (n = 4). Blue for sessions with ROI stimulation. **(H)** Same as (B) but for the population of SERT-Cre mice (n = 4). Blue for sessions with ROI stimulation. **(I)** Same as (C) but for the population of SERT-Cre mice (n = 4). Blue for sessions with ROI stimulation. **(J)** Same as (D) but for the population of SERT-Cre mice (n = 4). Blue for sessions with ROI stimulation. **(K)** Same

as (E) but for the population of SERT-Cre mice (n = 4). Blue for sessions with ROI stimulation. (**L**) Same as (F) but for the population of SERT-Cre mice (n = 4). Blue for sessions with ROI stimulation.

The results were confirmed with a post-hoc test comparing the effect of each significant variable across sessions for SERT-Cre animals (**Table 3.1**).

Table 3.1. Comparison of significant variables across sessions for ROI stimulation experiment
No light was delivered in sessions Pre and Post. In T1-T3 animals received 5-HT DRN stimulation. Post-hoc multiple comparison t test using the Bonferroni method was performed restricted to SERT-Cre mice and for each variable. * $p < 0.05$. n.s., not significant.

Sessions	ROI occupancy	Rate exits ROI	Interval visits	Speed ROI
Pre vs T1	n.s.	*	n.s.	*
Pre vs T2	n.s.	*	*	*
Pre vs T3	*	*	*	*
Pre vs Post	n.s.	n.s.	n.s.	*
T1 vs T2	n.s.	n.s.	n.s.	n.s.
T1 vs T3	n.s.	n.s.	*	n.s.
T2 vs T3	n.s.	n.s.	n.s.	n.s.
Post vs T1	n.s.	*	n.s.	*
Post vs T2	n.s.	*	*	*
Post vs T3	*	*	*	*

All analyzed variables showed a significant difference between non-stimulated (Pre / Post) and stimulated sessions (T1 / T2 / T3). Furthermore, we found no significant differences between Pre

and Post sessions in % time spent in ROI, rate of ROI entries and average interval visits to ROI. Thus confirming the absence of an appetitive or aversive conditioning effect for DRN 5-HT photostimulation, as suggested by Fonseca et al. 2015 and opposed to Liu et al. 2014. No significant changes were observed for either variable in WT mice (**Figure 3.9A-F**, n = 5).

Overall, these results demonstrate that activation of DRN 5-HT neurons promotes a decrease in movement, without causing appetitive or aversive responses.

3.4 Discussion

In the present study, we found that activation of DRN 5-HT neurons slows down mice in the open field without affecting motor coordination or inducing appetitive/aversive responses. This robust effect was also persistent throughout days and did not promote anxiogenic or anxiolytic effects.

3.4.1 Serotonin Decreases Movement

Our results in the open field are consistent with the proposed behavioral inhibition theory (Soubrié 1986). This hypothesis is supported by previous 5-HT studies showing inhibitory effects on the five choice serial reaction time task (Harrison et al. 1997; Winstanley et al. 2004), go/no-go tasks (Harrison et al. 1999) and waiting tasks (Miyazaki et al. 2014; Fonseca et al. 2015). We

extend these findings by disentangling the 5-HT inhibitory role from reward or punishment factors (included in the previous studies).

The open field assay was already tested before in 5-HT pharmacological studies, mainly focusing on anxiety-like effects, but the literature is inconsistent (reviewed in Prut & Belzung 2003). The variability of effects might be justified by the complexity of the serotonergic system (at least 15 sub-types of receptors, both inhibitory and excitatory) or the technical limitations of pharmaceutical agents, e.g., possibility of paradoxical effects due to autoreceptor-mediated negative feedback (Fornal et al. 1996). Our movement effect and the lack of anxiety-like behavior results are consistent with another optogenetics study showing a decrease in locomotor activity and no effect on anxiety-like parameters in the elevated plus maze test, after activation of DRN 5-HT neurons (Ohmura et al. 2014). In opposition to our findings, another study activated optogenetically DRN neurons in the open field and observed an increase in speed (Warden et al. 2012). However the authors claim a lack of 5-HT specificity, as their method also affected GABAergic neurons in the DRN. Our results show that selective activation of DRN 5-HT neurons is causally sufficient to decrease movement, without affecting anxiety-like behaviors in the open field.

3.4.2 Serotonin Does Not Decrease Movement via Motor Coordination Impairment

Jacobs suggested that one of the primary functions of the 5-HT system in the brain is the central control of motor function (Jacobs & Fornal 1993). In C. elegans, 5-HT has a prominent role in motor behavior control (Sawin et al. 2000; Flavell et al. 2013), with 5-HT optogenetic activation promoting dwelling states (Flavell et al. 2013). Our study clearly demonstrates that DRN 5-HT activation reduces movement, without affecting motor coordination in the rotarod and LocoMouse tasks (**Figure 3.5**).

Our results are consistent with previous studies showing no change in DRN 5-HT neuronal activity in response to diverse treadmill locomotor tasks (Veasey et al. 1997) and no effect in the rotarod after administration of 5-HT2 agonist (Hawkins et al. 2002). 5-HT motor control is mainly originated from a population of neurons in the brainstem nuclei – raphe pallidus and raphe obscurus – that strongly project to the spinal cord (Bowker 1986), as opposed to DRN that provides most of the 5-HT to the forebrain (Azmitia & Segal 1978).

The absence of a significant decrease in movement in the motor assays could be also explained by the different nature of the tasks or the time of stimulation relative to behavior. Both tests are driven by a meaningful goal, i.e., not falling in the rotarod or obtaining water reward in the LocoMouse (absent in the open field test) and the photostimulation is delivered when animals are already engaged in the behavior.

Regardless of the cause, the reduction in speed without motor impairment suggests that DRN 5-HT neurons are not directly involved in the regulation of motor coordination.

3.4.3 Serotonin Impairment of Movement is Not Due to Reinforcing Effects

The robust decrease in speed that we observed during activation of DRN 5-HT neurons could be potentially explained by an induction of pleasant or unpleasant effects. Liu et al. proposed that 5-HT DRN neurons positively reinforce actions (Liu et al. 2014), although others failed to reproduce the reinforcing effect (Miyazaki et al. 2014; Fonseca et al. 2015; reviewed in Luo et al. 2015). In our study, we activated DRN 5-HT neurons exclusively in a ROI in the open field for consecutive days and found no evidence for appetite or aversive effects (**Figure 3.8-3.9**). Our results contradict the findings obtained by Liu et al. in a similar task (Liu et al. 2014), but are consistent with Fonseca et al. that found no reinforcing effects in conditioned place preference, real-time preference or choice bias in a probabilistic choice task (Fonseca et al. 2015) and Miyazaki et al. that found no reinforcement in spontaneous nose poking and no enhancement in the ability of a natural reinforcer to promote waiting (Miyazaki et al. 2014).

The discrepancy between ours and Liu et al's results could be explained by different populations of DRN neurons being affected. In detail, the Cre-lines of mice used (SERT-Cre vs ePet1-Cre), or the precise targeting of stereotaxic injections could

result in different subsets of neurons being affected. Pet-1 neurons consist of 10% pure glutamate neurons, besides the 5-HT neurons (Liu et al. 2014). Furthermore, it was found that DRN reinforcing effects are originated from a population of DRN neurons that activate the dopaminergic system via a glutamatergic synapse, but it is not clear how much of these neurons are 5-HT-positive (Liu et al. 2014; McDevitt et al. 2014; Qi et al. 2014). Additional differences in protocol of stimulation or subtype of AAV or are less likely to be important, because we used a similar photostimulation protocol (10 ms at 25 Hz vs 15 ms at 20 Hz), with similar amplitude (20 mW) and the same AAV serotype (AAV2/9) as Liu et al. (Liu et al. 2014). In our study, there were no sensory cues displaced in the arena to identify the region of stimulation. Another possibility is that the visual cues defining the stimulated region in space facilitated learning and conditioning of the animals. This would not explain however the lack of rewarding effects observed in the other behavioral tests performed by others (Miyazaki et al. 2014; Fonseca et al. 2015).

The exact cause of the inconsistency in the studies remains an open question (reviewed in Luo et al. 2015), but our results establish that DRN 5-HT activation decreases movement, independently of reinforcing effects, consistent with Fonseca et al. and Miyazaki et al. (Fonseca et al. 2015; Miyazaki et al. 2014). Furthermore, it strengthens the finding that reinforcing effects of DRN stimulation are non-serotonergic (McDevitt et al. 2014; Qi et al. 2014).

3.4.4 Two distinct 5-HT mechanisms for movement reduction?

Our study demonstrates a clear reduction in movement in the open field with DRN 5-HT release, both when 5-HT activation happens randomly in space (**Figure 3.1**) or in a confined ROI (**Figure 3.8-3.9**). It caught our attention that the effect of 5-HT activation in the ROI experiment seems to build throughout the stimulated days (**Table 1**). This increasing/decreasing trend of the effect only reached significance between the 1st and 3rd stimulated sessions for ROI visits (**Table 1**), but the trend was present in all affected variables (occupancy, rate of exits and speed in ROI, **Figure 3.9**), for all tested mice. We did not observe this "building" effect in the random stimulation protocol in the open field, but instead an immediate (< 0.5 s) decrease in speed, with no significant changes throughout the course of many days (**Figure 3.6**). Our results suggest that 5-HT might act in downstream circuits with two distinct mechanisms, probably depending on the presence/absence of an association. In a contingent task, where mice learn an association (e.g. stimulation locked to a spatial ROI), the effect of 5-HT builds over time. On the other hand, in a non-contingent task (e.g. random stimulation in the open field) 5-HT has a direct and immediate effect. Further experiments will help elucidate the possibility of two distinct mechanisms for the 5-HT inhibitory role in movement.

As a side note, the ROI experiment was performed in the open field with plastic floor that did not produce significant effects in

the random stimulation condition (**Figure 3.7**). The reason for this discrepancy might be related with the different light amplitudes used (5 mW vs 20 mW), or the differences in the protocol of stimulation (3 s in random places vs ROI for the time inside ROI). Further experiments, testing the open field with plastic floor at 20 mW or testing the ROI experiment with corncob floor at 5 mW should help to clarify the reason for the difference in the results.

The present study demonstrates with optogenetic methods that DRN 5-HT activation is sufficient to reduce animal's speed, without affecting motor coordination or producing appetitive/aversive responses. High-resolution analysis of the behavior, including characterization of animal's states (grooming, digging, defaecation, climbing, rearing, etc), sensory responses (sniffing, whisking, etc) and physiological reactions (heart rate, respiration, etc) will allow a further understanding of the 5-HT movement reduction in the open field. The specific pathways connecting 5-HT DRN to other brain areas for the rapid decrease in movement remains an open question too. Given the heterogeneity of DRN and its projections, it is likely to expect that different subpopulations of 5-HT DRN neurons activate different pathways, influencing behaviors in a different way. In fact, preliminary results suggest that labeling a slightly more anterior area of DRN (+ 0.3 mm) leads to an absence of the movement effect in the open field. More refined targeting strategies, e.g. retrograde infection (Rothermel et al. 2013) or

intersectional genetics (Jensen et al. 2008), might allow the assessment of the pathways involved in the DRN 5-HT movement effect. Overall our results provide a new level of evidence for the 5-HT involvement in behavioral inhibition, with DRN 5-HT activation promoting a general reduction of speed, without inducing motor coordination or reinforcing responses.

3.5 Experimental procedures

3.5.1 Animal subjects

Twenty-five adult C57BL/6 mice (16 SERT-Cre mice and 9 wild-type (WT) littermates) were used in this study. Different subsets of these were used in the subsequent experiments, as described in **Table 3.2**.

Table 3.2. Summary of the animals used in this study

Mice		Experiment
SERT-Cre	**WT**	
16	**9**	Open field test
6	**4**	Open field novelty
6	**4**	Open field texture/geometry
4	**2**	ROI stimulation
3	**2**	Accelerating Rotarod
4	**-**	Locomouse

All procedures were carried out in accordance with the European Union Directive 86/609/EEC and approved by *Direcção-Geral de*

Veterinária of Portugal. The SERT-Cre mouse line (Gong et al. 2007) was obtained from the Mutant Mouse Regional Resource Centers (stock number: 017260- UCD). Male and female mice (18 – 26 g) were group-housed prior to surgery and individually housed post-surgery and kept under a normal 12 hour light/dark cycle (tested at light phase). Mice had free access to food and water, except when mentioned otherwise. Seven subjects used in the open field test (4 SERT and 3 WT) and the four SERT-Cre mice used in the LocoMouse assay were under water deprivation protocol. In the LocoMouse experiment, water availability was restricted to the behavioral sessions. Extra water was provided if needed to ensure that mice maintained no less than 85% of their original weight.

3.5.2 Stereotaxic adeno-associated virus injection and cannula implantation

Animals were anesthetized with isoflurane (4% induction and 0.5 – 1% for maintenance) and placed in a stereotaxic frame (David Kopf Instruments, Tujunga, CA). Lidocaine (2%) was injected subcutaneously before incising the scalp. The skull was covered with a layer of Super Bond C&B (Morita, Kyoto, Japan) to help stabilization of an implant. A craniotomy was drilled over lobule 4/5 of the cerebellum and a pipette filled with a viral solution (AAV2.9.EF1a.DIO.hChR2(H134R)-eYFP.WPRE.hGH, 10^{13} GC/mL, University of Pennsylvania) was lowered to the DRN (Bregma -4.7 AP, -2.9 DV) with a 32-33° angle toward the back of the animal. The viral solution (1 μL) was injected using a

Picospritzer II (Parker) or an hydraulic pump (UMP3-1, World Precision Instruments, Sarasota, FL), connected to a 5 µl Hamilton syringe (Hamilton, Reno, NV), at a rate of 0.05–0.1 μL/min. An optical fiber (200 µm core diameter, 0.48 NA, 4-5 mm) housed inside a connectorized implant (M3, Doric lenses, Quebec, Canada) was lowered into the brain, through the same craniotomy as the viral injection, and positioned 200 µm above the injection point. The implant was cemented to the skull using dental acrylic (Pi-Ku-Plast HP 36, Bredent, Senden, Germany). The skin was stitched at the front and rear of the implant. Mice were monitored until recovery from the surgery and returned to their home cage. Gentamicin (48760, Sigma-Aldrich, St. Louis, MO) was topically applied around the implant. Behavioral testing started at least 2 weeks after virus injection to ensure good levels of expression. Previous studies using the same method reported that 94% of ChR2-YFP positive neurons were serotonergic, assessed with tryptophan hydroxylase immunohistochemistry (Dugué et al.).

3.5.3 Optogenetic stimulation

Light from a 473 nm laser (LRS-0473-PFF-00800-03, Laserglow Technologies, Toronto, Canada or DHOM-M-473-200, UltraLasers, Inc., Newmarket, Canada) was controlled by an acousto-optical modulator (AOM; MTS110-A1-VIS or MTS110-A3- VIS, AA optoelectronic, Orsay, France), except for LocoMouse assay (controlled directly with custom written software using LabView). The AOM controlled the laser power

without any auditory noise and it was triggered by the behavioral control system (Bcontrol), developed by Carlos Brody (Princeton University) in collaboration with Calin Culianu, Tony Zador (Cold Spring Harbor Laboratory) and Z.F.M. Light exiting the AOM was collected (KT110/M, Thorlabs, Newton, NJ) into an optical fiber patchcord (200 μm, 0.22 NA, Doric lenses), connected to a second fiber patchcord through a rotatory joint (FRJ 1x1, Doric lenses), then to a chronically implanted optic fiber cannula through an M3 connector (Doric lenses). Laser power was calibrated for each targeted laser power using a powermeter (PM130D, Thorlabs) before and after each animal session. The optical fiber patchord was screwed to the M3 implanted connector with the animal freely moving, in the beginning of each experiment.

3.5.4 Behavioral procedures

3.5.4.1 Open field test

3.5.4.1.1 Apparatus

The open field apparatus was a 50x40x30 cm (LxWxH) white box (IKEA, Sweden) illuminated with LED white lights (IKEA, Sweden) to ensure uniform illumination (250-350 lux). The floor of the apparatus was covered with fresh corncob bedding. Mice were placed in the center of the open field arena and allowed to freely explore the environment for 30 min. A video camera (Flea3, Point Grey, CA) was placed directly above the open field, and the x and y position, body centroid and orientation of the animal was

continuously tracked in real-time with Bonsai software (Lopes et al. 2015). An infrared LED placed outside of the apparatus was synchronized with the stimulation protocol and detection time was collected. All data for the animal tracking, LED detection and video was saved for subsequent offline analysis of the behavior. The open field apparatus was cleaned with 50% ethanol and the bedding was changed between each animal.

3.5.4.1.2 Stimulation protocol

Optical stimulation consisted of a train of 10 ms pulses with 25 Hz at 5 mW amplitude, delivered during 3 s. Previous studies described a robust behavioral effect using these parameters (Dugué et al. 2014; Fonseca et al. 2015). Stimulation alternated between on and off in blocks of 5 min, starting with no stimulation, for the total length of the session (30 min). Each stimulation trial included 3 s of light on and 7 s of inter-trail interval light off. One open field session was performed with 20 mW amplitude and similar frequency conditions, to test the same stimulation conditions as used in ROI stimulation experiment.

3.5.4.2 Open field novelty experiment

Two groups of mice (G1 and G2) were exposed to the open field test for consecutive days. G1 (3 SERT-Cre and 2 WT mice) was exposed to the open field arena receiving photostimulation for 24 successive days. G2 (3 SERT-Cre and 2 WT mice) was exposed to the arena for 23 days, receiving photostimulation only on the

24th day and for six consecutive days. Stimulation was performed as described in open field section (see **Figure 3.1**).

3.5.4.3 Open field texture and geometry test

G1 and G2 of mice, used for open field novelty experiment test (6 SERT-Cre and 4 WT mice) were tested in the open field with different texture floors and geometries. Different floors were corncob bedding (brown), plastic (white) and paper (grey). Geometries were rectangular and oval shaped. See **Figure 3.7A** for a schematic diagram of the different sessions. Stimulation was performed as described in open field section (see **Figure 3.1**).

3.5.4.4 Accelerating rotarod assay

A rotarod (ENV-575M, Med- Associates, St Albans, VT, USA) was set to accelerate from 4 to 40 r.p.m. over a 5 min time period. Mice (3 SERT-Cre and 2 WT) were trained for two consecutive days, with one daily session consisting of 7 trials separated by 5 min resting periods. Mice were placed on the rotarod and trials were considered to have started when the rod began to turn. Trials ended when mice fell from the rod or after 5 min elapsed. The optical fiber patchcord was connected to the animal and latency to fall and video was recorded in all sessions. The third session (test day) consisted of 10 trials with stimulation randomly assigned to 5 trials. Light was delivered (10 ms pulses, 25 Hz, 5 mW) during 3 s on and 7 s off.

3.5.4.5 LocoMouse assay

The custom-designed setup used to assess whole body coordination during over-ground locomotion in mice was described previously in (Machado et al. 2015). Briefly, the LocoMouse apparatus consisted of a 66.5x4.5x20 cm (LxWxH) clear glass corridor connected to two boxes with water ports. Animals (4 SERT) were placed on the right-side box and allowed to freely walk across a glass corridor with a mirror below at 45º angle. A single high-resolution, high-speed camera (Bonito CL-400B, Allied Vision Technologies) captured side and bottom views at 400 fps. Acquisition software was written in Labview and used National Instruments PCIe 1433 to record and save the movies in real time. Infrared (IR) sensors placed in the beginning and end of the corridor detected initiation and termination of each trial. The automatic triggering system allowed mice to self-initiate trials. Animals were water deprived in order to increase their motivation to run from one side to the other of the corridor. Water was delivered (4 µl) in each box, in all trials. Mice performed 4 sessions with each one consisting of 15-60 trials. An infrared LED was synchronized with the stimulation protocol and detection time was collected. Light stimulation (15 ms pulses, 25 Hz, 5 mW) happened in 50% of the trials (randomly assigned) and lasted the time it took the animal to cross the track. All data for the animal tracking, video, LED and sensor detection was saved for subsequent offline analysis of the behavior. The behavioral apparatus was cleaned with 50% ethanol between each animal.

3.5.4.6 Real time stimulation conditioned to a region of interest in the open field

The behavioral apparatus was the same as described in the open field test. A region of interest (ROI, 13x10.5 cm, LxW) was defined using a custom Bonsai workflow (Lopes et al. 2015), in order to outline the area of stimulation. No visual cues were existent in the open field arena. The experiment consisted of five days, including one baseline session (pre), three sessions with stimulation (ST1-ST3) and a final session without stimulation (post). The optical fiber patchcord was connected to the animal and data for the tracking and video was saved in all sessions. For the stimulation sessions, a Python script was included in the custom Bonsai workflow (Lopes et al. 2015) to define the conditioning protocol of stimulation. A digital output signal was sent to a microcontroller board (Uno, Arduino, IT), each time the body centroid of the animal entered in the ROI, producing light stimulation (25 Hz at 10 ms pulses, 20 mW amplitude). The stimulation was immediately terminated when the centroid of the mouse body left the ROI.

We quantified the following parameters for each animal: ROI occupancy (time spent in ROI), number of entries in ROI, rate of entries in ROI (number of entries ROI / occupancy outside ROI), rate of exits from ROI (number of exits from ROI / occupancy inside ROI), time of visits to ROI and average speed in ROI.

3.5.5 Histology

Histological analysis were performed after photostimulation experiments to confirm viral expression of ChR2-YFP and optical fiber placement. Mice were deeply anesthetized with pentobarbital (Eutasil, CEVA Sante Animale, Libourne, France) and perfused transcardially with 4% paraformaldehyde (P6148, Sigma-Aldrich). The brain was removed from the skull, stored in 4% paraformaldehyde overnight and kept in cryoprotectant solution (PBS in 30% sucrose) for one week. Sagittal sections (50 mm) were cut in a cryostat (CM3050S, Leica, Germany), mounted on glass slides with mowiol mounting medium (81381, Sigma-Aldrich, St. Louis, MO). Scanning images for YFP, RFP and transmitted light were acquired with an upright fluorescence microscope (Axio Imager M2, Zeiss, Oberkochen, Germany) equipped with a digital CCD camera (AxioCam MRm, Zeiss) with a 5X or 10X objective. Three SERT-Cre mice were not included in the study due to absence of ChR2-YFP viral expression, assessed after photostimulation experiments by scanning microscopy YFP images.

3.5.6 Data analysis

All data analysis was performed with custom-written software using MATLAB (Mathworks, Natick, MA). Error bars represent standard error of the mean (S.E.M).

For the open field and ROI stimulation experiments, the animal's path was recorded by an automated tracking system (Bonsai, Lopes et al. 2015). The recorded x, y coordinates were transformed to the real coordinates of the animal's location. The

video camera recorded the position with a temporal resolution of 60 fps. Speed data was smoothened (Benjamini et al. 2010), applying a median filter size 5. Two interval bins were defined for the pre- and post-stimulation intervals, both of 2 s. Pre was the window of 2 s before light delivery and post included the interval 1-3 s of the stimulation period.

For the LocoMouse assay, both tracking algorithm and data analysis software were performed offline and written in MATLAB. Detailed description of the LocoMouse tracker system can be found in Machado et al. 2015. The algorithm's output was the set of 3D coordinates of the features of interest, which were: the center of each of the four paws, the snout, and the tail divided into 15 points, for each frame of the movies. The output of the tracking system was visually inspected for each trial. Fewer than 10% of the trials were excluded due to tracking failure (typically due to exploration or grooming behavior that resulted in erroneous swing and stance point detection). The stride cycles of individual paws were automatically broken down into swing and stance phases based on the first derivative of the paw position trajectories. Individual strides were defined from stance onset to subsequent stance onset. All data was sorted into speed bins (5 cm/s bin width) in a stridewise manner, with a minimum stride count criterion of 5 strides per bin, per animal. 15-20 cm/s bin was selected for presentation, as it included the higher number of trials, for both non-stimulated and stimulated trials. Individual limb movements were defined as: *swing velocity* – x displacement of single limb during swing phase divided by swing duration;

stride length – x displacement from touchdown to touchdown of single limb; *stance duration* – time in milliseconds that foot is on the ground during stride. Interlimb coordination parameters were calculated as follows: *stance phase* – relative timing of limb touchdowns during stride cycle of reference paw; *tail and nose phases* – for each speed bin we correlate the stridewise tail and nose trajectories with the trajectory given by the difference between the forward position of the hind right paw and the forward position of the hind left paw (also normalized to the stride). The phase is then calculated by the delay in which this correlation is maximized.

3.5.7 Statistical analysis

To compare pre- and post-stimulation speed intervals (**Figure 3.1G, K**; **Figure 3.3D, F, H**) and no stimulation vs stimulation trials (**Figure 3.4A, D**; **Figure 3.5C**) we used a paired t test (ttest, MATLAB). Comparison between independent groups of mice (SERT-Cre vs WT) was done with a two-sample t test (ttest2, MATLAB). To compare speed across quartiles (**Figure 3.2C, F**) and delta speed across bocks (**Figure 3.6E**) we performed a three-way ANOVA (anovan, MATLAB), followed by a paired t test (ttest, MATLAB). Bonferroni correction for multiple comparisons was applied to set the significance level. Two-way ANOVA (anova2, MATLAB) was used for comparison of the first six sessions between G1 and G2 of mice in the open field novelty experiment (**Figure 3.6B-C**). To compare delta speed across open field arenas with different textures and geometry

(**Figure 3.7B**) we used a three-way ANOVA (anovan, MATLAB), followed by post-hoc t test, using Bonferroni correction (multcompare, MATLAB). Comparison of different variables in the ROI stimulation experiment across sessions was done with one-way ANOVA (anova1, MATLAB) and post-hoc t test, using Bonferroni correction (multcompare, MATLAB). In the LocoMouse experiment, differences between stimulated and non-stimulated trials for time to cross (**Figure 3.5E**) and speed (**Figure 3.5F**) were assessed with a two-way ANOVA, using mice and stimulation as factors. For all the ANOVAs performed, when mice were included, they were considered as a random factor. Differences were considered significant at $*p < 0.05$, $**p < 0.01$ and $***p < 0.001$, unless when Bonferroni correction for multiple comparisons was applied. Frequency dose-dependency curve (**Figure 3.1N**) was fitted with a linear regression, using a least squares approach (polyfit, MATLAB).

4 Optogenetic activation of dorsal raphe serotonergic neurons does not impair sexual behavior in male mice

Manuscript in preparation: Correia PA, Valente SS, Lima SQ, Mainen ZF. Optogenetic activation of dorsal raphe serotonergic neurons does not impair sexual behavior in male mice.

Author contributions: Patrícia A. Correia (PAC), Susana S. Valente (SSV), Susana Q. Lima and Zachary F. Mainen designed the experiments. PAC and SSV performed the experiments and scored the videos. PAC analyzed the data.

4.1 Abstract

Serotonin (5-HT) is a major neuromodulator in the brain, involved in diverse functions and behaviors. One main theory suggests that 5-HT is involved in behavioral inhibition. In particular, microdialysis studies indicate that 5-HT concentration is low throughout sexual intercourse, rising significantly at sexual behavior termination (male ejaculation). This result, together with other pharmacological studies, suggest a role for 5-HT in sexual behavior termination, although the details of this process remain enigmatic.

In this study, we used an optogenetic approach to activate 5-HT neurons from the dorsal raphe nuclei (DRN) of male mice during copulation. We found that DRN 5-HT activation during sexual intercourse did not produce significant changes in number and duration of mounts, intromissions, inter-mount intervals and latency to ejaculation. 5-HT modulation of sexual behavior might involve other specific pathways, alternative forms of activation, or it might be that 5-HT affects more subtle aspects of sexual behavior. Further studies, including monitoring 5-HT neuronal activity, as well as manipulating alternative 5-HT-producing brain areas during mating, should help clarify the role of this neuromodulator in sexual behavior.

4.2 Introduction

Serotonin (5-HT) is a major neuromodulator in the brain, involved in diverse functions and behaviors. One main theory suggests that 5-HT is involved in behavioral inhibition (Soubrié 1986). In detail, 5-HT is thought to modulate brain and behavior in an opponent way of dopamine (Deakin & Graeff 1991; Cools et al. 2011; Daw & Daw 2002). One example of such opponency mechanism comes from the sexual behavior literature, suggesting that dopamine promotes, while 5-HT inhibits sexual motivation and performance (**Figure 4.1**, reviewed in Pfaus 2009).

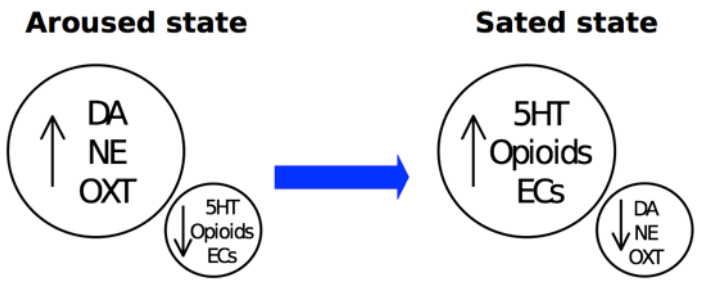

Figure 4.1. Schematic diagram of sexual behavior neuromodulatory mechanism
5-HT induces refractoriness and sexual satiety, whereas dopamine promotes sexual motivation. 5-HT levels are low in the aroused state and high in the sated state. The opposite is verified for dopamine (adapted from Pfaus 2009).

Sexual behavior in mammals can be described as a cycle of three main phases: arousal, copulation and satiety (reviewed in Hull & Dominguez 2007). In males, the arousal phase is characterized by investigation of the female's face and anogenital region. During the copulation phase, the male approaches the female with diverse mount attempts and mounting periods (including intromissions of the male penis into the female's vagina). The copulation phase

usually ends with male ejaculation, a very clear period in which the male becomes briefly immobile. The sated state comprises a post-ejaculatory refractory period, with variable time without sexual interactions, until eventually the male restarts the cycle (McGill 1962).

In the brain, both 5-HT and dopamine (amongst other neurotransmitters) play an important role in the modulation of sexual behavior (reviewed in Pfaus 2009). Microdialysis studies revealed that dopamine levels are high during arousal phase of the sexual encounter, but decrease significantly after ejaculation in males (Lorrain et al. 1999). Contrary to dopamine, 5-HT concentration is low when male and female rodents start interacting, but increases drastically after ejaculation (Lorrain et al. 1997). This result suggests a role for 5-HT in the sated phase of sexual behavior.

In humans, selective 5-HT re-uptake inhibitors (SSRIs) are commonly used to treat depression and some of the side effects include decrease in libido, longer time to reach ejaculation or anorgansmia (Normandin & Murphy 2011; reviewed in Kiser et al. 2012). Moreover, SSRIs are also prescribed for the treatment of premature ejaculation, proving to be efficient to the increase latency for males to ejaculate (Arafa & Shamloul 2007). Similar effects occur in male rats treated chronically with SSRIs (de Jong et al. 2005; Kita et al. 2006), including a decrease in sexual motivation and desire (Carter et al. 1992; Vega Matuszcyk et al. 1998). In mice, knockout animals for the 5-HT1B receptor (autoreceptor that acts by negative feedback inhibition, see

McDevitt & Neumaier 2011) show longer time to ejaculate and an increase in the number of mounts and intromissions (Rodríguez-Manzo et al. 2002). Furthermore, lesions in the dorsal raphe nuclei (DRN), the main source of serotonin to the forebrain, induce a decrease in both latency to ejaculation and post-ejaculatory period (Mclntosh & Barfield 1984). Many pharmacological, physiological and genetic studies have sketched out a general inhibitory function for 5-HT in sexual behavior, but exactly how and where in the brain this effect happens is still unclear.

To address these questions, in the present study, we used an optogenetic approach to activate 5-HT neurons from the DRN of male mice during copulation. Based on the literature, our initial prediction was that 5-HT activation of a sexually aroused animal would promote a decrease in its sexual motivation, thus increasing the time to ejaculate. Surprisingly, we found that DRN 5-HT activation specifically during the mounting period did not produce significant changes in number and duration of mounts, intromissions, inter-mount intervals and latency to ejaculate. These results suggest that rapid and specific DRN 5-HT activation during on-going sexual intercourse does not affect male sexual behavior.

4.3 Results

4.3.1 C57BL/6 male mice display high variability in sexual behavior

We first characterized the sexual behavior of C57BL/6 male mice. We trained males to have sexual intercourse with receptive females for successive sessions. For each session, males always interacted with a new receptive female. Male mice took on average 20.1 ± 12.7 min (mean ± SD) to ejaculate, but we found the behavior very variable across sessions (**Figure 4.2**).

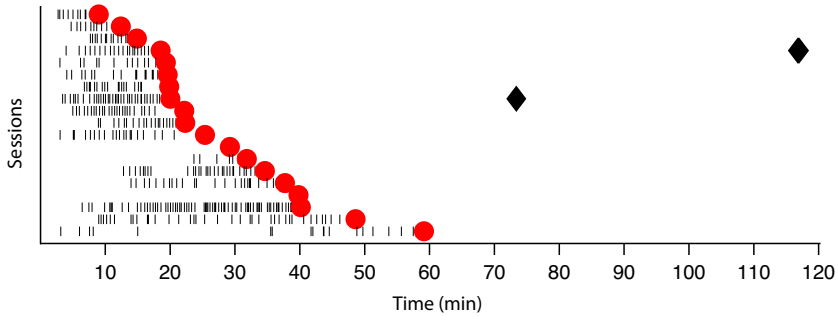

Figure 4.2. C57BL/6 male sexual behavior
Raster plots are aligned to the insertion of the female in the behavioral paradigm and depict mount events (black ticks), ejaculation (red circles) and the first mount event after ejaculation (black diamonds) for C57BL/6 male (n = 19) x C57BL/6 female (n = 19). Sessions finished 180 min after female insertion.

Furthermore, we observed that C57BL/6 male mice had very long (> 180 min) refractory periods (time between ejaculation and next mount), as opposed to what was previously described in rats (de Jong et al. 2006). Given this result, we next focused on the intra-sexual intercourse measurements, excluding the refractory period. For the 5-HT manipulation experiment, all sessions ended after the male ejaculated (or after 1h, if no ejaculation was reached).

4.3.2 Optogenetic approach to activate DRN 5-HT neurons during sexual behavior

To understand the role of 5-HT in male sexual behavior, we first trained male adult transgenic mice expressing CRE recombinase under the serotonin transporter promoter (SERT-Cre) to have sexual experience with receptive females. To manipulate 5-HT activity, we expressed the light-sensitive ion channel channelrhodopsin-2 (ChR2) using an AAV2/1 viral vector (AAV2/1-Dio-ChR2-EYFP) injected into the DRN of SERT-Cre mice (ChR2, n = 18) and implanted an optical fiber in the same location (**Figure 4.3A**, see Dugué et al. 2014). Control mice (YFP, n = 15) were SERT-Cre animals injected with an AAV2/1 viral vector lacking ChR2 (AAV2/1-Dio-EYFP). Histology was performed at the end of testing to confirm YFP expression localized to the DRN in SERT-Cre animals (**Figure 4.3B**).

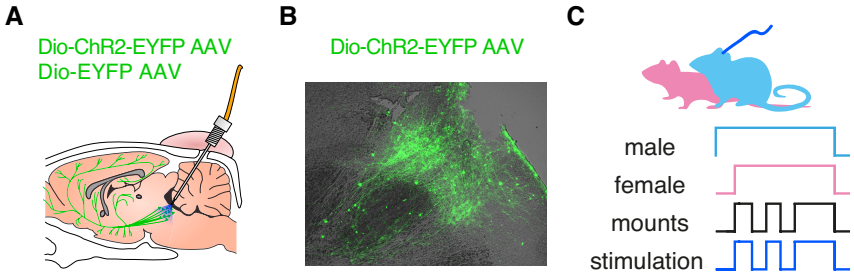

Figure 4.3. Optogenetic strategy to activate DRN 5-HT neurons during sexual behavior
(A) Schematic drawing of the optogenetic approach. DRN neurons are infected with AAV2/1-Dio-ChR2-EYFP (test group) or AAV2/1-Dio-EYFP (control group). In SERT-Cre mice injected with Dio-ChR2-EYFP, 5-HT neurons will express ChR2-YFP (green cells) and can be photoactivated with blue light delivered through an optical fiber implant. **(B)** Fluorescence image of a parasagittal section showing localized ChR2-YFP expression in the DRN. **(C)** Schematic diagram of photostimulation protocol in the sexual behavior experiment. Stimulation was locked to the male mounting periods. Light was manually controlled, being on for the full length of the mount.

After allowing 2–3 weeks for virus expression, we performed one baseline session, "pre" (no stimulation), followed by a photostimulation session, with light delivery at 10 Hz, 5 mW amplitude and 10 ms pulses locked to the mounting behavior (**Figure 4.3C**). Next, animals had another session without light delivery, "post". All sessions were spaced by one week and males always had an encounter with a novel receptive female. The experimenters were blind to the mice's identity throughout testing and offline video scoring. The main outcomes of the analysis were: time of ejaculation, number and duration of mounts, number of intromissions and inter-mount intervals.

4.3.3 Optical activation of DRN 5-HT neurons does not promote changes in sexual behavior of male mice

To test weather DRN 5-HT activation has an inhibitory effect in male sexual behavior, we compared "pre" and stimulation sessions for the population of ChR2 and YFP mice. Surprisingly, activation of DRN 5-HT neurons during sexual intercourse seemed to produce no changes in latency to ejaculate (**Figure 4.4A**), number and duration of mounts (**Figure 4.4B-C**), inter-mount intervals (**Figure 4.4D**) and number of intromissions (**Figure 4.4E**) for the population of ChR2 (n = 18) and YFP (n = 15) mice, comparing between "pre" and stimulation sessions. The absence of 5-HT significant effect in sexual behavior was confirmed with a three-way ANOVA, including virus as a factor for latency to ejaculation (virus x stimulation: $F_{(1,29)} = 1.37$, P = 0.197), number of mounts (virus x stimulation: $F_{(1,29)} = 0.43$, P =

0.517), duration of mounts (virus x stimulation: $F_{(1,29)} = 0.08$, P = 0.778), inter-mount intervals (virus x stimulation: $F_{(1,29)} = 0.71$, P = 0.407) and number of intromissions (virus x stimulation: $F_{(1,29)} = 0.06$, P = 0.812).

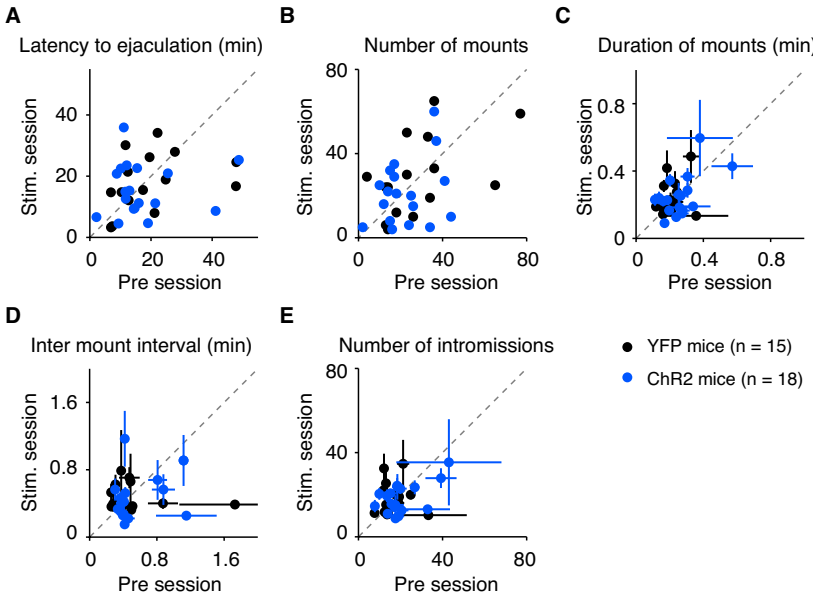

Figure 4.4. DRN 5-HT activation during sexual behavior for ChR2 and YFP mice

(A-E) Correlation of pre-stimulation versus stimulation sessions for latency to ejaculation (**A**), number (**B**) and duration of mounts (**C**), inter-mount intervals (**D**) and number of intromissions (**E**), for the population of ChR2 (n = 18, blue circles) and YFP mice (n = 15, black circles). Averages for each session are shown for duration of mounts, inter-mount intervals and number of intromissions. Error bars indicate SEM. In some cases, the error bars are too small to be visible.

We next compared the same behavioral outcomes, including also the post-stimulation session (**Figure 4.5A-E**) for the population of ChR2 mice (n = 18). We confirmed the absence of significant effects with two-way ANOVA restricted to ChR2 mice for

latency to ejaculation (stimulation: $F_{(1,16)} = 0.04$, $P = 0.846$), number of mounts (stimulation: $F_{(1,16)} = 0.76$, $P = 0.397$), duration of mounts (stimulation: $F_{(1,16)} = 2.92$, $P = 0.105$), inter-mount intervals (stimulation: $F_{(1,16)} = 0.35$, $P = 0.562$) and number of intromissions (stimulation: $F_{(1,16)} = 4.58$, $P = 0.046$).

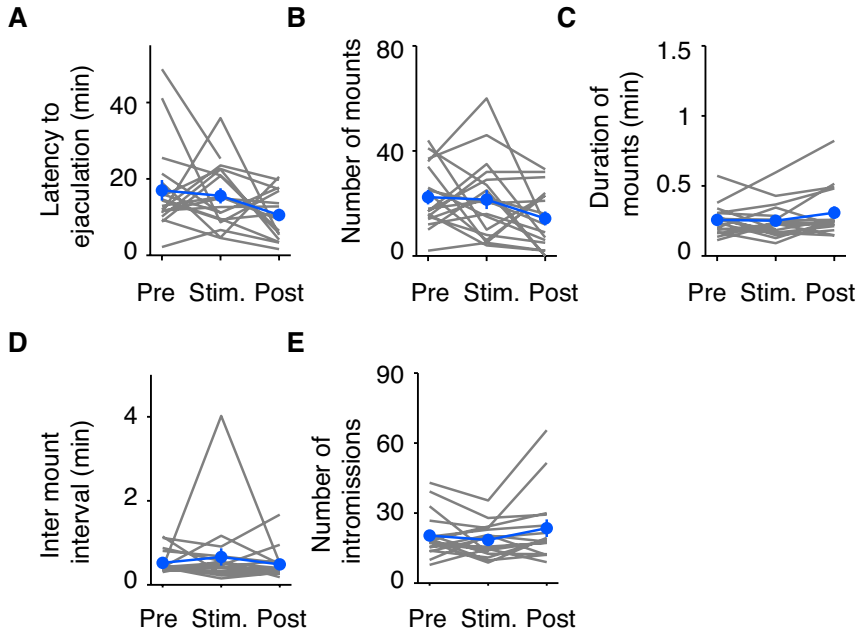

Figure 4.5. DRN 5-HT activation during mounts does not affect male sexual behavior in SERT-Cre mice
(A-E) Comparison between pre-stimulation, stimulation and post-stimulation sessions for latency to ejaculation (**A**), number (**B**) and duration of mounts (**C**), inter-mount intervals (**D**) and number of intromissions (**E**), for the population of ChR2 mice (n = 18). All sessions were spaced of one week. Individual mice shown in grey lines. Averages across mice are shown in filled circles. Error bars indicate SEM. In some cases, the error bars are too small to be visible.

The stimulation factor for the number of intromissions (**Figure 4.5E**) produced a significant effect ($p < 0.05$), however a post-hoc t-test with Bonferroni correction revealed no significant changes between stimulated and non-stimulated sessions.

Overall, our results show a high degree of variability in sexual behavior of SERT-Cre male mice. We found that DRN 5-HT activation during the mounting period did not induce any changes in the standard measures of male sexual behavior.

4.4 Discussion

Based on pharmacological, physiological and genetic studies, it has been previously proposed that 5-HT inhibits sexual behavior (reviewed in Pfaus 2009). Using optogenetic methods, we selectively activated DRN 5-HT neurons while male mice interacted with receptive females. Our main findings were that activation of DRN 5-HT neurons did not produce significant changes in the main male sexual behavior outcomes (latency to ejaculate, number and duration of mounts, inter-mount intervals and number of intromissions). Our results contradict the expected inhibitory role of 5-HT in sexual behavior, suggesting that 5-HT modulation might involve 1) different forms of activation, 2) alternative pathways, and/or 3) more subtle aspects of the behavior.

4.4.1 5-HT might need different forms of activation to modulate sexual behavior

One possibility for the lack of 5-HT effect is that the light delivery parameters used to activate DRN 5-HT neurons were not ideal to modulate sexual behavior. DRN 5-HT activation in mice

behaving in the open field induced a rapid decrease in movement (< 0.5 s onset from light delivery), and the effect persisted for the light period (3 s, **Figure 3.1**). Mount duration and consequently light stimulation in the sexual behavior experiment had the duration of 15.44 ± 1.77 s (mean ± S.E.M., **Figure 4.5C**). It is possible that the different temporal pattern of photostimulation would induce a diverse mechanism of 5-HT activity (Ranade & Mainen 2009).

Additional differences in the subtype of AAV (AVV2/1 versus AAV2/9 in the movement study) and frequency of light delivery (10 Hz versus 25 Hz in the movement study) should also be considered, although previous studies using similar parameters (AAV2/1 at 1, 5, 12.5 and 25 Hz) show a dose-dependency increase in waiting time of SERT-Cre mice after DRN 5-HT activation (Fonseca et al. 2015). Further experiments to test alternative forms of 5-HT light delivery, including at different moments in the behavior (e.g. outside the mounting periods), should help elucidate the role of 5-HT in sexual behavior.

4.4.2 5-HT regulation of sexual behavior may act via alternative pathways

Hypothalamic nuclei are critical for homeostatic regulation of basic physiological processes, including sexual behavior (Vaughan and Fisher, 1962; Davidson 1966). A variety of studies involving brain lesions, electrical stimulation, or intracranial hormone injection identify the hypothalamus as necessary and sufficient for both aggressive and sexual behaviors (reviewed in

Sternson 2013), but the precise circuit connectivity is poorly understood. More recently with optogenetic methods, it was identified a subset of ventromedial hypothalamus, ventrolateral subdivision neurons, that when weakly activated promoted mounting behavior, sniffing and close investigation (Lee et al. 2014). Increasing photostimulation intensity in the same neuronal subpopulation promoted a transition towards aggressive attacking behaviors (Lee et al. 2014). These results help pinpoint the circuits involved in sexual behavior, but the fundamental regulation of neuromodulators, specifically 5-HT, remains elusive. In our study we focused on the effect of DRN 5-HT activation, given the extensive 5-HT innervation to the forebrain, including a strong projection to the lateral hypothalamus (Vertes & Linley 2008; Pollak Dorocic et al. 2014). However, we cannot discard the possibility that other raphe nuclei (e.g. raphe obscurus) might have a determinant role modulating sexual behavior. Evidence to support this hypothesis comes from loss-of-functions studies in rats, where lesions in the raphe obscurus induced low levels of mounting, intromission and ejaculation frequencies, and prolonged mount latencies, as opposed to lesions in the raphe magnus, that produced no significant changes in sexual behavior (Yamanouchi & Kakeyama 1992).

4.4.3 DRN 5-HT activation may affect more subtle aspects of sexual behavior

Our results show that DRN 5-HT activation during mounts did not induce significant changes in latency to ejaculate, number and

duration of mounts, inter-mount-intervals and number of intromissions in SERT-Cre male mice. Nonetheless, we cannot discard the possibility that other behavioral measurements could be affected by light delivery. Further high-resolution automated analysis, including more detailed characterization of the states and physiological responses of the animal might help provide a reliable and more comprehensive capture of behavioral activity. Furthermore, the absence of a significant decrease in any standard measure of sexual behavior could also be explained by the nature of the task or the time of stimulation relative to the behavior. Male-female sexual interactions involve a high motivational state from the male (the female too, but in our study we imposed receptivity). At the time of DRN 5-HT stimulation (during mounts), the male is already engaged in the behavior, and maybe 5-HT is not able to inhibit such engaging on-going behavior. In order to contour this issue, stimulation would ideally happen in a short interval before the mount. However, when dealing with such natural and spontaneous behavior, it is indeed an experimental challenge to anticipate the animal's action. One alternative possibility would be to manipulate 5-HT activity after the male dis-mounts the female and observe how it would affect the inter-mount-intervals.

Overall, our results depict a novel approach to study sexual behavior. We found that activation of DRN 5-HT neurons was not sufficient to modify male sexual behavior. Additional studies, including monitoring 5-HT cell activity, as well as manipulating

alternative 5-HT-producing brain areas, during mating, could help clarify the role of 5-HT in sexual behavior.

4.5 Experimental procedures

4.5.1 Animal subjects

Fifty-two adult C57BL/6 male mice (19 wild type and 33 SERT-Cre) and fifty-five adult C57BL/6 female mice (wild type) were used in this study. All procedures were carried out in accordance with the European Union Directive 86/609/EEC and approved by *Direcção-Geral de Veterinária* of Portugal. The SERT-Cre mouse line (Gong et al. 2007) was obtained from the Mutant Mouse Regional Resource Centers (stock number: 017260- UCD). Male mice (22 – 26 g) were group-housed prior to surgery and individually housed post-surgery and female mice (18 – 23 g) were group-housed before and after surgery. Mice were kept under a reverse 12 h light/dark cycle (tested at dark phase) and had free access to food and water.

4.5.2 Stereotaxic adeno-associated virus injection and cannula implantation

Male mice were anesthetized with isoflurane (4% induction and 0.5 – 1% for maintenance) and placed in a stereotaxic frame (David Kopf Instruments, Tujunga, CA). Lidocaine (2%) was injected subcutaneously before incising the scalp. The skull was covered with a layer of Super Bond C&B (Morita, Kyoto, Japan)

to help stabilization of an implant. A craniotomy was drilled over lobule 4/5 of the cerebellum and a pipette filled with a viral solution (either AAV2.1.EF1a.DIO.hChR2(H134R)-eYFP.WPRE.hGH, 10^{13} GC/mL, for test group or AAV2.1.EF1a.DIO-eYFP.WPRE.hGH, 10^{13} GC/mL, for control group, University of Pennsylvania) was lowered to the DRN (Bregma -4.45: -4.75 AP, -2.9: -3.1 DV) with a 32-33° angle toward the back of the animal. The viral solution (1 μL) was injected using a Picospritzer II (Parker) at a rate of 0.05–0.1 μL/min. An optical fiber (200 μm core diameter, 0.48 NA, 5 mm) housed inside a connectorized implant (M3, Doric lenses, Quebec, Canada) was lowered into the brain, through the same craniotomy as the viral injection, and positioned 200 μm above the injection point. The implant was cemented to the skull using dental acrylic (Pi-Ku-Plast HP 36, Bredent, Senden, Germany). The skin was stitched at the front and rear of the implant. Mice were monitored until recovery from the surgery and returned to their home cage. Gentamicin (48760, Sigma-Aldrich, St. Louis, MO) was topically applied around the implant. Behavioral testing started at least 2 weeks after virus injection to ensure good levels of expression. Previous studies using the same method reported that 94% of ChR2-YFP positive neurons were serotonergic, assessed with tryptophan hydroxylase immunohistochemistry (Dugué et al. 2014).

4.5.3 Female mice preparation

In order to decrease the variability in female behavior and ensure sexual receptivity, all females were ovariectomized and treated with sexual hormones to induce a behavioral estrous (Agmo et al. 2004). In summary, females underwent a bilateral ovariectomy (surgeries were conducted under isofluorane anaesthesia) and were after primed with Estradiol Benzoate and Progesterone before the experiments. Females were injected with 5 µl of Estradiol Benzoate in 0.1 ml of Sesame oil, followed by 500 µl of progesterone in 0.1 ml sesame oil 4h before testing).

4.5.4 Optogenetic stimulation

Light from a 473 nm laser (DHOM-M-473-200, UltraLasers, Inc., Newmarket, Canada) was controlled by a Master-8 (A.M.P.I., Israel). Light was triggered manually by the experimenters at the moment where the male did the first intromission during the mount. Light was manually switched off when the male un-mounted the female. Light was collected (KT110/M, Thorlabs, Newton, NJ) into an optical fiber patchcord (200 µm, 0.22 NA, Doric lenses), connected to a second fiber patchcord through a rotatory joint (FRJ 1x1, Doric lenses), then to a chronically implanted optic fiber cannula through an M3 connector (Doric lenses). Laser power was calibrated for each targeted laser power using a powermeter (PM130D, Thorlabs) before and after each animal session. The optical fiber patchord was screwed to the M3 implanted connector with the animal freely moving, in the beginning of each experiment.

4.5.5 Behavioral procedures

4.5.5.1 Training

Male mice were allowed 2-3 training sessions of 2 h with receptive females before surgery. Males that were not able to complete two sessions until ejaculation were discarded from the study. All training and experiment sessions were separated of 1 week (at least).

4.5.5.2 Male-female interactions

All behavioral tests were performed in the male home cages (1145T, Techniplast, 369 x 156 x 132 mm). Lid, food and water were removed and mice were allowed 10 min habituation. Next, females were gently inserted in the center of the male home cage. Mice were allowed to interact until male reached ejaculation, or after 1h of session. In case of ejaculation, we allowed 10 min until removal of female. The table where the home cage was placed was cleaned with 70% ethanol in between mice. A video camera (Flea3, Point Grey, CA) was placed laterally and the video continuously recorded using Bonsai software (Lopes et al. 2015). An infrared LED placed outside of the apparatus was synchronized with the stimulation protocol and detection time was collected. Recorded video was saved for subsequent offline analysis of the behavior.

4.5.6 Stimulation protocol

Optical stimulation consisted of a train of 10 ms pulses with 10 Hz at 5 mW amplitude, delivered during the length of the mounting period. Previous studies described a robust behavioral effect using these parameters (Dugué et al., 2014 and Fonseca et al., 2015).

4.5.7 Histology

Histological analysis were performed after photostimulation experiments to confirm viral expression of ChR2-YFP and optical fiber placement. Mice were deeply anesthetized with pentobarbital (Eutasil, CEVA Sante Animale, Libourne, France) and perfused transcardially with 4% paraformaldehyde (P6148, Sigma-Aldrich). The brain was removed from the skull, stored in 4% paraformaldehyde overnight and kept in cryoprotectant solution (PBS in 30% sucrose) for one week. Sagittal sections (50 mm) were cut in a cryostat (CM3050S, Leica, Germany), mounted on glass slides with mowiol mounting medium (81381, Sigma-Aldrich, St. Louis, MO). Scanning images for YFP, RFP and transmitted light were acquired with an upright fluorescence microscope (Axio Imager M2, Zeiss, Oberkochen, Germany) equipped with a digital CCD camera (AxioCam MRm, Zeiss) with a 5X or 10X objective.

4.5.8 Video scoring

All video scoring was performed with custom-written Bonsai software. Manual annotations were done for female entrance,

mount attempts, mounts, intromissions and ejaculation. The experimenters were blind to the identity of the animals.

4.5.9 Data analysis

All data analysis was performed with custom-written software using MATLAB (Mathworks, Natick, MA). Error bars represent standard error of the mean (S.E.M). Latency to ejaculation was calculated as the time from the first mount until ejaculation. Mount attempts (mounts without intromissions) were not included in the analysis.

4.5.10 Statistical analysis

To compare ChR2 and YFP mice we performed a three-way ANOVA (anovan, MATLAB), using virus (ChR2 or YFP), subjects and stimulation as main factors. Subjects factor was set as a random factor and virus was nested inside subjects. Two-way ANOVA (anovan, MATLAB) restricted to CHR2 mice was used for comparison of the three sessions ("pre", stimulation and "post"). For the number of intromissions variable, a post-hoc t test, using Bonferroni correction (multcompare, MATLAB) was done. Alpha was set to 0.05.

5 General Discussion

5-HT is at once implicated in virtually everything, but responsible for nothing.

Barry L. Jacobs

The great variety of suggested roles (for serotonin) can be said to be a tribute to man's ingenuity and his unquestionable willingness to write papers.

Irvine Page

The primary duties of a conductor are to unify performers, set the tempo, execute clear preparations and beats, and to listen critically and shape the sound of the ensemble.

Michael Bowles

(*in* The Art of Conducting)

5.1 The role of 5-HT in behavior

The present series of studies aimed to explore the role of 5-HT in behavior. We started by validating and optimizing an optogenetic strategy to target and manipulate specifically 5-HT neurons in the DRN, the main source of 5-HT to the forebrain (Dugué et al. 2014). We then tested some theories concerning 5-HT function, focusing primarily in behavioral inhibition. First we found that DRN 5-HT photostimulation decreases tactile responses in a mechanosensory task (Dugué et al. 2014). Then, we demonstrated that DRN 5-HT activation dramatically slows mice in the open field, without impairing motor coordination. We found that the inhibitory effect was not caused by the novelty of the environment nor by appetitive or aversive effects. Moreover, optical activation of DRN 5-HT neurons did not seem to induce anxiety-like responses, contrary to what has been previously suggested by diverse pharmacological studies. Finally, we investigated the role of 5-HT in sexual behavior and found that DRN 5HT activation does not seem to affect on-going mating behavior in male mice.

In this section, speculations and thoughts will be presented, mentioning some caveats and proposing a tentative model for 5-HT action. In the end, future experiments to further explore the role of 5-HT in behavior will be suggested.

5.1.1 What is 5-HT *conducting*?

In this thesis we explored the role of 5-HT in behavior, testing its effects in sensory responses, sexual behavior, movement, anxiety, motor coordination and reward. It is a challenge to reconcile all results, unifying them in one single theory. In fact, this might even be a *mission impossible*, and the neuroscience community will have to accept that 5-HT *conducts* the brain with different *performances*, depending on the animal state and behavioral context. In this section, I will summarize our major findings and comment on different possibilities to explain 5-HT function in behavior. I will propose one tentative model, suggesting behavioral inhibition as a candidate theory to encapsulate the main results described in this thesis.

5.1.2 Is 5-HT modulating anxiety?

The open field is a widely used assay to perform an initial screening for anxiety-related behaviors in rodents (Bailey & Crawley 2009). Despite leading to inconsistent results, a vast set of pharmacological agents and anxiolytic drugs were already tested in the open field, suggesting a role for 5-HT in anxiety (Bailey & Crawley 2009). It was generally accepted that animals that spent the greatest time in the central region of the open field were less 'anxious' than those that preferred the periphery. Total distance travelled and entries in the central area of the arena are among the most extracted measures from this test (reviewed in Prut & Belzung 2003; Zangrossi & Graeff 2014). In our open field study, we found no evidence for an increase /decrease in

anxiety-like behaviors, after DRN 5-HT activation. Our results are consistent with Ohmura and colleagues, which also found no effect of DRN 5-HT stimulation in anxiety-like parameters in the elevated plus maze (Ohmura et al. 2014). The reason for the discrepancy between our studies and the previous anxiety literature might be related with the fact that pharmacological and lesion studies could not exclude the possibility of secondary and compensatory effects. DRN 5HT stimulation with optogenetic methods allows a specific, selective and very fast temporal scale activation. Furthermore, the putative effect of 5-HT in anxiety-like behaviors might be dependent on the activation/ inhibition of specific 5-HT receptor subtypes (Piszczek et al. 2013). In anxiety studies, the same group of mice is usually tested in different behavioral assays, including the open field, the elevated plus maze, the light dark test and the suspension tail test (Piszczek et al. 2015 for example). Additional experiments should be performed to confirm that specific activation of DRN 5-HT neurons does not induce anxiety.

5.1.3 Is 5-HT modulating exploration?

Despite being largely used in the literature (including different variations in sizes, shapes, lights, session duration, analysis, etc), the exact motivation for the animals to move in the open field is not fully understood. Broadhurst studied the effects of some environmental variables in detail and concluded that movement in the open field was mainly determined by exploratory drive (Broadhurst 1957; Broadhurst 1958). Based on this claim and on

the light of behavioral inhibition theory, we can hypothesize that 5-HT inhibits exploratory behavior in the open field. Consistent with this hypothesis, is the study in *C. elegans* (Flavell et al. 2013), where 5-HT induces exploitation (dwelling states), rather than exploration (roaming states). In the open field with mice, it is harder to categorize the exact state of the animal and there is no direct exploitation. Exploration itself is a cognitive term that implies "what" the animal is doing. High-resolution analysis of the open field behaviors, including video scoring of animal's states (grooming, digging, defecation, climbing, rearing, etc.) could provide a reliable and more comprehensive capture of behavioral activity (see review Walsh & Cummins 1976). A more ethological analysis in the open field has been tried before, though coupled only with anxiolytic drugs (Blanchard et al. 1993a; Blanchard, et al. 1993b; Griebel et al. 1995; Choleris 2001). Furthermore, measuring sensory responses (sniffing, whisking, etc) and physiological reactions (heart rate, respiration, etc) could help explain how 5-HT modifies the internal behavioral state of the animal. In addition, other behavioral tasks could be performed to address exploratory behavior, including the hole-board test (File 1985; Jackson & Nutt 1992; Takeda et al. 1998). Despite being a valid explanation for the effect of 5-HT in the open field, the exploration hypothesis does not directly translate to the motor coordination, mechanosensory and sexual behavior results.

5.1.4 5-HT inhibits behavior: a proposed model

Inhibition can be viewed as a critical control mechanism, fundamental to regulate diverse cognitive and motor processes, preventing the execution of any action, e.g. motor inhibition, impulse control, resisting temptation, etc. (Lister et al. 1996; Aron 2007; Eagle et al. 2008). Thus, inhibition is crucial to perform all everyday tasks. Increasing evidence in diverse animal models suggests a role for 5-HT only in some behavioral subtypes of inhibition (reviewed in Eagle et al. 2008).

Our findings demonstrated that activation of DRN 5-HT neurons is causally sufficient to decrease tactile responses in a sensory/nociceptive task (**Figure 2.3**) and reduce movement in the open field, both when 5-HT stimulation happens randomly in space (**Figure 3.1**) or in a confined ROI (**Figure 3.8-3.9**). A similar approach did not seem to inhibit or promote sexual behavior (**Figure 4.5**), motor coordination (**Figure 3.5**), anxiety (**Figure 3.4**) or reinforcing responses (**Figure 3.8-3.9**). Similarly, previous studies demonstrate that 5-HT is strongly implicated in inhibitory control on go/no-go tasks, but not in the stop-signal task (reviewed in Eagle et al. 2008). The main difference between these two tasks is the temporal location of the inhibitory signal within the main motor task (Schachar et al. 2007): before or contiguous (go/no-go task) versus after the signal to go (stop-signal task). Further evidence for the selective inhibitory role of 5-HT comes from recent waiting studies (Miyazaki et al. 2014; Fonseca et al. 2015), where DRN 5-HT photostimulation prolonged waiting time and slowed movement times, but did not affect the reaction time to the tone or the time mice spent

retrieving the reward. Altogether these data suggest that 5-HT has an inhibitory action, specifically when the response is not already in the process of being executed.

Based on the previous findings together with our results, I propose a model related with decision-making to reconcile the diverse 5-HT effects. 5-HT inhibits behavior in general, but not all types of behaviors. Depending on the available choices and motivation of the animal to perform certain actions, 5-HT will act differently in the brain to modulate behavior.

When the animal is faced with two or more decisions, 5-HT acts in the brain to bias its choice. Evidence for this hypothesis comes from the findings that 5-HT promotes waiting for reward (Miyazaki et al. 2014; Fonseca et al. 2015). In both studies, mice were trained to perform a delayed reward task and were faced with two options: waiting for delayed reward or aborting the trial to restart a new one. In these tasks, DRN 5-HT activation increased the animal's capacity of waiting for delayed reward delivery, thus biasing the animal's decision. One criticism of this experiment is the fact that animals are performing a task with the motivation of getting reward, and this might interfere with their decisions. The open field test overcomes this issue, as it is an unconstrained environment, where no direct reward or punishment affects the animal's choice. The animal is indeed faced with many "similar" decisions while wanders around: "Where to go next? Should I jump out? Do I dig under the bedding? Do I go to the center? Shall I just rest in the corner?

And there comes the light again…" I propose that DRN 5-HT activation inhibits movement, by biasing the animal to choose the low-cost action. In the open field experiments, 5-HT activation decreases movement, biasing the animal to stay in the same location.

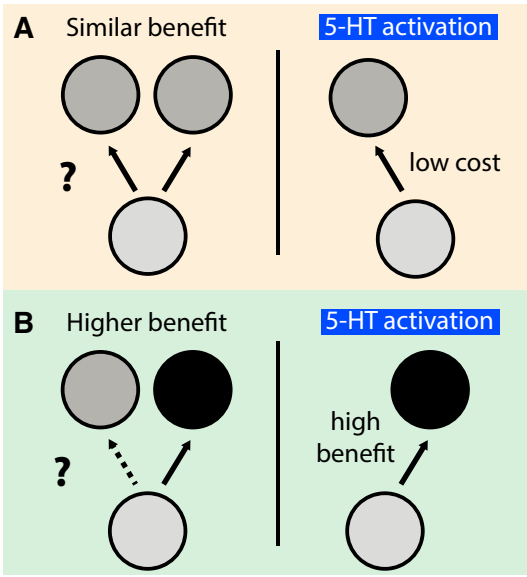

Figure 5.1. Schematic diagram for a proposed model of 5-HT action in behavior
(**A**) The animal is faced with two (or more) choices of similar benefit. 5-HT activation biases the animal to choose the low-cost option. (**B**) The animal has two (or more) choices, but one has higher benefit (black circle, e.g. reward or avoid punishment). The animal is already biased towards the high benefit option and 5-HT activation maintains that choice.

The hypothetical model being proposed for 5-HT inhibitory action assumes all choices are similar, i.e., have identical benefit (**Figure 5.1A**). However, in the situations where the animal is faced with different benefit (or value) choices and one of them is predominant, e.g. rewarding choices (mounting in sexual

behavior, drinking water, eating food, escaping from punishment, etc.), DRN 5-HT activation does not affect the animal's choice (**Figure 5.1B**). Our results with the motor coordination assays and sexual behavior are consistent with this hypothesis. We can consider two minimalistic choices for each task: 1) rotarod: fall down (aversive) or keep running; 2) locoMouse: run or not to get reward; 3) sexual behavior: mount or not to mate. In these situations, the state of the animal has already a very strong bias towards avoiding the aversive event or going to the rewarding event. Hence, 5-HT activation cannot further bias the choices of the animal.

In summary, the proposed model for 5-HT action depends on the animal's motivation and reason to perform a certain behavior. 5-HT system will in general inhibit the animal's preference, unless a strong motivation is present, in which case 5-HT will just keep the animal on track for that decision. The exact mechanism by which 5-HT bias the animal's decision remains to be explored. One possibility would be that 5-HT makes the animal choose the less active choice, i.e., that involves less cost. Another option would be that 5-HT is actually delaying the time to make the decision for the next action. To test these hypotheses it would be useful to score the different states of the animal in the open field, using high-resolution analysis. 5-HT activation might be 1) extending the time in every state, 2) increasing some states and decreasing others or 3) creating a new third state. In the first case, 5-HT would equally inhibit all states, thus affecting a global

higher state of the animal. On the second option, 5-HT would modulate decisions by inducing some specific states in the animal. Evidence for this option comes from a pharmacological study, where the authors applied an ethological analysis to describe how drugs induce specific behavioral states in the open field and not others (Choleris 2001). Finally, 5-HT could be inducing a new third state in animal's behavior, but in this case it would raise the possibility of an artifact of stimulation, as the new state would not be biologically relevant.

5.1.5 Two possible distinct mechanisms for 5-HT action

Now let us consider the case where the animal has equal value choices, as we assume it is the case of the open field and the ROI experiment. We proposed in **Chapter 3** that 5-HT acts with two distinct mechanisms based on the immediate and "direct" (< 0.5 s) effect in the open field (**Figure 3.1**) and the apparent build-up and "associative" effect in the ROI stimulation experiment (**Figure 3.9**). The main difference in these tasks is that in the ROI stimulation, the animal can learn to associate the light with a spatial region, while in the open field stimulation happens randomly in space. These putative "associative" and "direct" effects might activate the same downstream circuits in a different way or actually activate distinct downstream circuits.

Furthermore, our study suggests that DRN 5-HT neurons do not act like classical dopaminergic neurons. Optogenetic stimulation of dopaminergic neurons in the ventral tegmental area (VTA) induces a rewarding effect, shown with conditioned place-

preference or self-stimulation procedures (reviewed in Ikemoto et al. 2015). Based on our findings and previous studies it is unlikely that 5-HT has a rewarding associative effect. We did not observe an increase in the number of entries or rate of entries in the ROI and most of the variables tested did not show a significant difference between "pre" and "post" non-stimulated sessions (**Table 3.1**), in the ROI experiment (**Figure 3.9**). Furthermore, DRN 5-HT activation did not produce conditioned or real-time place preference and no choice bias in a probabilistic choice task (Fonseca et al. 2015). Further experiments will be needed to 1) confirm the associative mechanism of 5-HT behavioral inhibition, and 2) understand the circuitry connection between 5-HT and dopamine and how they modulate associative learning. Finally, it will also be interesting to understand the difference between spatial and temporal associations. In the open field experiment, photostimulation is delivered randomly in space, but with fixed blocks of time (**Figure 3.1D**). If there is an associative indirect effect of 5-HT, it seems not to affect temporal associations, as we do not see any build-up in speed, across multiple days of open field testing (**Figure 3.6**).

5.1.6 A (still) mysterious *instrument*: 5-HT effect in the different open field floors

With such a complex mysterious neuromodulator it is not surprising that some results are harder to justify. While asking if the 5-HT movement effect could be explained by the novelty of the environment, we found that different open field floor textures

seemed to influence the effect in a different way (**Figure 3.7**). In the plastic floor we observed a small decrease in speed after DRN 5-HT activation, contrasting with the dramatic decrease in the corncob case. The general differences observed with our available video resolution analysis were that animals moved at higher speeds (**Figure 3.7C**) and spent less time in the center of the arena in the plastic floor case (**Figure 3.7D**). As a first consideration, the plastic floor is a completely novel texture to the animals, as opposed to the corncob, the common floor of their home-cage. However it is unlikely that the difference in the effect is exclusively due to the novelty of the context, because 1) in the first open field test (with corncob) the environment is mostly entirely new to the animal and DRN 5-HT activation dramatically decreases speed and 2) when tested with paper floor (novel to the animals) the decrease in speed was more evident than with the plastic. Although not very studied, this question has been previously addressed and different textures revealed different patterns of activity in the open field (Dixon & Mayeda 1976). It is not inconceivable that a change in the floor would alter the internal dynamic state of the animal and/or the kinetics of its movement. The absence of the corncob might change the somatosensory perception of the animal, thus modifying its behavior. Among others, one example behavior that might be relevant for the distinct floors is digging. Visual inspection of open field videos revealed that digging is a very frequent behavior present in the corncob and paper floors, but absent in the plastic case. Further high-resolution analysis might be the key to

understand the states of the animal and characterize in detail its behaviors in both contexts.

5.2 Future directions to be explored

5.2.1 Optogenetics limitations

In the last decade, we have witnessed exciting technological developments with the potential of making neuroscience dreams come true and obtaining full knowledge about the functions and mechanisms of neural circuits. In detail for the 5-HT system, we are now able to activate and inhibit DRN 5-HT neurons in a fast and specific way, something unreachable with previous methods. The validation and optimization of the optogenetic conditions to target and manipulate DRN 5-HT neurons was a crucial step (Dugué et al. 2014, **Chapter 2**), but the heterogeneity of this neuromodulator, together with the complexity of the brain, poses some extra challenges, even for optogenetics.

Let us consider the example of the role of 5-HT in reward (recently reviewed in Luo et al. 2015). One group described that stimulation of DRN 5-HT neurons is reinforcing in several behaviors (Liu et al. 2014), while our study, together with others (Miyazaki et al. 2014; Fonseca et al. 2015) showed an absence of rewarding effects with DRN 5-HT activation. The DRN has a high percentage of 5-HT neurons, but it contains also a substantial number of other neurotransmitter neurons, including glutamate, GABA and dopamine. Indeed, this might be the key to

solve the discrepancy in the results: the reward study activated Pet-1 neurons, which contain 10% of pure glutamate neurons, besides 5-HT neurons (Liu et al. 2014). In fact, other two studies report that rewarding effects in the DRN are mainly due to the contribution of glutamate (McDevitt et al. 2014; Qi et al. 2014). Thus, it will be important to generate new tools to separate neuron subpopulations and further investigate this question.

Even when using a specific mouse line to optogenetically target 5-HT neurons, experimenters should be aware of the possible technical limitations. Different optogenetic tools, labeling efficiency and stimulation parameters (amplitude, frequency and duration) might lead to divergent results. Given the heterogeneity of DRN and its projections, it is likely to expect that different subpopulations of 5-HT DRN neurons activate different pathways, influencing behaviors in a different way. Additional efforts should be devoted to characterize DRN sub-regions, in order to dissect the circuit wiring and the pathways in the upstream and downstream stations of the DRN. Furthermore, it is likely that 5-HT neurons co-release other substances, similarly to what was demonstrated for GABA release from dopaminergic cells (Tritsch et al. 2012).

Optogenetic techniques allow us to access the effect of 5-HT transients in behavioral actions at a very fast timescale, but it is pertinent to consider also that these effects might have long-term consequences. In SSRIs mechanism, the presynaptic 5-HT1A autoreceptors in the raphe nuclei act to limit the increase in synaptic 5-HT, but this effect appears to be reduced with long-

term SSRI treatment, due to receptor desensitization (Blier & Ward 2003). It is not yet well-characterized how optogenetic activation of 5-HT neurons reconciles the effects of different receptors and in detail long-term desensitization mechanisms. One attempt to optically manipulate G-protein coupled receptors was the development of the "opto-receptors" (Airan et al. 2009), chimeric receptors able to regulate appropriate signaling cascades in response to blue light. Although this strategy has also been applied to control 5-HT1A receptors (Oh et al. 2010), we lack further testing in behavioral assays. Another alternative is the usage of designer receptors exclusively activated by designer drugs (DREADDs, Armbruster et al. 2007), GPCRs that are activated by organic compounds but not by the endogenous ligands such as 5-HT. The basic idea is to use these GPCRs to control the corresponding intracellular pathway by a drug, which specifically only activates the modified GPCR. This strategy, although not ideal for fast time-course manipulations (due to the slow application of chemical compounds to activate the GPCR), can be a good alternative to address longer-term changes in specific receptors (reviewed in Aston-Jones & Deisseroth 2013).
Our knowledge of the 5-HT system has undoubtedly increased in the past decade with optogenetic methods. These are the times to study 5-HT (and other neuromodulatory systems) and with the technological "opto-evolution", soon all limitations mentioned here would be (hopefully) overcome.

5.2.2 5-HT circuits and mechanisms

Since it was first discovered in 1937 (Vialli & Erspamer 1937), 5-HT has been an increasing target for research. The following decades of neuroscience investigations have sketched out the basis for a 5-HT theoretical framework. More recently, optogenetic methods have allowed to confirm and to further test prominent theories for the role of 5-HT in behavior. The set of studies described in this thesis suggest a major function for 5-HT in behavioral inhibition, but the exact nature and circuitry involved in the effect remain to be explored.

One very informative direction would be to pinpoint the pathways connecting DRN to the downstream areas involved in the movement effect. Neuroanatomical studies of humans, non-human primates and rodents have identified regions of the frontal cortex and basal ganglia that are critical for general action inhibition (Band & van Boxtel 1999). Moreover, available evidence supports a role for orbitofrontal cortex in action inhibition (reviewed in Eagle et al. 2008). One candidate pathway is a circuit connecting the orbital/inferior frontal cortex with striatum/caudate putamen (Chamberlain et al. 2006; Eagle et al. 2008; Penadés et al. 2007). DRN sends projections to all these areas in the brain (Törk 1990), however the exact connection of these pathways with 5-HT modulation of action inhibition is not clear. Warden et al. looked in detail to the projection of DRN to medial prefrontal cortex, and found that optogenetic stimulation of medial prefrontal cortex axons in the DRN changes animal's behavior in the forced swim test (Warden et al. 2012). This study

lacks 5-HT specificity, but illustrates a causal role for medial prefrontal cortex – DRN pathway in driving behavioral changes.

The amygdala has been previously suggested for the connection of 5-HT with anxiety (Deakin & Graeff 1991; reviewed in Cools et al. 2007). This brain area is known to be a mediator of aversive conditioning. In our open field study, we found no evidence for an increase or decrease in anxiety-like behaviors, consistent with another study using also optogenetic methods (Ohmura et al. 2014). A recent study showed that both amygdala 5-HT2C receptor activity during memory consolidation and 5-HT DRN activity during aversive reinforcement are necessary for stress enhancement of fear memory in stressed, but not unstressed mice (Baratta et al. 2015). Although proposing another role for 5-HT, this study provides further evidence for the connection between DRN and the amygdala.

Less likely to be directly involved in the circuit, but yet to consider given its role in spatial navigation, is the hippocampus. Animals navigate in the open field building a place-cell representation of the context (O'Keefe & Dostrovsky 1971; see Moser et al. 2008 for review). 5-HT projections to the hippocampus are mainly originated in the medial and not dorsal raphe nuclei, but DRN projects also to the medial raphe (Acsády et al. 1996). Additional retrograde and anterograde labeling experiments should provide important insights on the 5-HT circuitry responsible for behavioral responses.

5.2.3 Summary of future experiments

The *road* ahead of us is still long… To further understand the nature of the 5-HT effect in movement and its relation with behavioral inhibition, we summarize the following future experiments.

- Perform high-resolution analysis of the open field behavior, including characterization of animal's states (grooming, digging, defecation, climbing, rearing, etc.), sensory responses (sniffing, whisking, etc.) and physiological reactions (heart rate, respiration, etc.).

- Monitor DRN 5-HT activity, while animals move in the open field. This can be achieved with bulk imaging of genetically-encoded calcium indicators (Tecuapetla et al. 2014) to allow highly specific and long-term term recordings. This approach was already used in head-fixed mice preparations in our lab (Matias et al. submitted). Alternatively, it is possible to record DRN 5-HT neuronal activity using photostimulation-assisted identification of neuronal populations (Lima et al. 2009), a method that uses ChR2 as a tag to identify the genotype of electrophysiologically-recorded neurons.

- Perform extra behavioral tests to confirm that DRN 5-HT activation does not induce anxiety. Classical anxiety assays include (other than the open field) the elevated plus

maze, the light dark test and the suspension tail test (Piszczek et al. 2015 for example).

- Pinpoint target areas connected with DRN, using retrograde and anterograde labeling methods. Candidate areas are frontal and orbitrofrontal cortices, basal ganglia, amygdala and hippocampus.

- Perform loss of function studies, inhibiting optogenetically (Zhang et al. 2007; Han & Boyden 2007) the activity of DRN 5-HT neurons, while animals move in the open field.

- Explore the connection between 5-HT and dopamine, by manipulating also dopaminergic activity in the open field and ROI stimulation experiments. Perform circuit manipulation experiments to further understand how the two neuromodulatory systems are connected (e.g. silence dopaminergic neurons, while DRN 5-HT activation).

- Manipulate and characterize distinct DRN 5-HT subpopulations, by analyzing the movement effect in diverse ChR2-viral infection areas of DRN. Preliminary data from the open field experiments suggests that labeling a specific subpopulation in the DRN might be crucial to obtain the reduction effect in speed.

- Test the 5-HT associative mechanism hypothesis, by performing an ROI experiment with different probabilities of photostimulation. Two equivalent spatial ROI could be defined with different probabilities of light delivery (e.g. 70 and 30%). The prediction would be that the build-up decrease of speed in the ROI would be more evident in the highest probability ROI. Next, a contingency degradation could be done to extinct the association of light with space.

5.3 Final remarks

Our set of studies indicate for the first time that DRN 5-HT optical activation dramatically slows animals in the open field and does not seem to affect other behaviors, including male copulation, motor coordination and reward or aversive responses. Our findings suggest an inhibitory role for 5-HT in some behaviors, but not in "high value" on-going actions. We propose a model to explain how 5-HT can inhibit movement, by biasing animal's choices. We also propose two distinct mechanisms for serotonergic modulation, "direct" (happening when DRN 5-HT activation occurs randomly in space) and "associative" (when the animal learns to associate stimulation to a specific ROI in space). These models will hopefully help to motivate research to better understand the roles of 5-HT in behavioral inhibition.

5-HT is a bit less mysterious neuromodulator today, but the neuroscience community has a long list of experiments and analysis to do to help demystify it. It is important to remember that 5-HT does not probably work in a binary "on" and "off" mechanism and it is not alone in the role of *conducting* the brain; it is most likely working hand in hand with other neuromodulatory systems (dopamine, norepinephrine, acetylcholine). It is indeed a complex system, which was the most exciting yet sometimes frustrating feature of this *expedition*.

References

Abrams, J.K. et al., 2004. Anatomic and functional topography of the dorsal raphe nucleus. *Annals of the New York Academy of Sciences*, 1018, pp.46–57.

Acsády, L. et al., 1996. Topographic distribution of dorsal and median raphe neurons with hippocampal, septal and dual projection. *Acta biologica Hungarica*, 47(1-4), pp.9–19.

Agmo, A. et al., 2004. Preclinical models of sexual desire: conceptual and behavioral analyses. *Pharmacology, biochemistry, and behavior*, 78(3), pp.379–404.

Airan, R.D. et al., 2009. Temporally precise in vivo control of intracellular signalling. *Nature*, 458(7241), pp.1025–9.

Andersen, E. & Dafny, N., 1982. Dorsal raphe nucleus modulates sensory evoked responses in caudate and septum. *The International journal of neuroscience*, 17(3), pp.151–5.

Anstey, M.L. et al., 2009. Gregarization Underlying Swarm Formation in Desert Locusts. , (January), pp.627–630.

Arafa, M. & Shamloul, R., 2007. A randomized study examining the effect of 3 SSRI on premature ejaculation using a validated questionnaire. *Therapeutics and clinical risk management*, 3(4), pp.527–31.

Araneda, S. et al., 1980. Retrograde axonal transport following injection of [3H]-serotonin into the olfactory bulb. II. Radioautographic study. *Brain research*, 196(2), pp.417–27.

Aravanis, A.M. et al., 2007. An optical neural interface: in vivo control of rodent motor cortex with integrated fiberoptic and optogenetic technology. *Journal of neural engineering*, 4(3), pp.S143–56.

Arenkiel, B.R. et al., 2007. In vivo light-induced activation of neural circuitry in transgenic mice expressing channelrhodopsin-2. *Neuron*, 54(2), pp.205–18.

Armbruster, B.N. et al., 2007. Evolving the lock to fit the key to create a family of G protein-coupled receptors potently activated by an inert ligand. *Proceedings of the National Academy of Sciences of the United States of America*, 104(12), pp.5163–8.

Aron, A.R., 2007. The neural basis of inhibition in cognitive control. *The Neuroscientist : a review journal bringing neurobiology, neurology and psychiatry*, 13(3), pp.214–28.

Aston-Jones, G. & Deisseroth, K., 2013. Recent advances in optogenetics and pharmacogenetics. *Brain and Cognition*, (1511), pp.1–5.

Audero, E. et al., 2008. Sporadic Autonomic Dysregulation and Death Associated with Excessive Serotonin Autoinhibition. *Science*, 321(5885), pp.130–133.

Azmitia, E.C. & Segal, M., 1978. An autoradiographic analysis of the differential ascending projections of the dorsal and median raphe nuclei in the rat. *The Journal of comparative neurology*, 179(3), pp.641–67.

Bailey, K. & Crawley, J., 2009. Anxiety-Related Behaviors in Mice. In J. Buccafusco, ed. *Methods of Behavior Analysis in Neuroscience. 2nd edition*. CRC Press.

Band, G.P. & van Boxtel, G.J., 1999. Inhibitory motor control in stop paradigms: review and reinterpretation of neural mechanisms. *Acta psychologica*, 101(2-3), pp.179–211.

Baratta, M. V. et al., 2015. Stress enables reinforcement-elicited serotonergic consolidation of fear memory. *Biological Psychiatry*, pp.1–9.

Barrot, M., 2012. Tests and models of nociception and pain in rodents. *Neuroscience*, 211, pp.39–50.

Benjamini, Y. et al., 2010. Ten ways to improve the quality of descriptions of whole-animal movement. *Neuroscience and Biobehavioral Reviews*, 34(8), pp.1351–1365.

Benzekhroufa, K. et al., 2009. Adenoviral vectors for highly selective gene expression in central serotonergic neurons reveal quantal characteristics of serotonin release in the rat brain. *BMC biotechnology*, 9(1), p.23.

Benzekhroufa, K. et al., 2009. Targeting central serotonergic neurons with lentiviral vectors based on a transcriptional amplification strategy. *Gene therapy*, 16(5), pp.681–8.

Blanchard, R.J., Yudko, E.B., et al., 1993. Defense system psychopharmacology: an ethological approach to the pharmacology of fear and anxiety. *Behavioural brain research*, 58(1-2), pp.155–65.

Blanchard, R.J., Taukulis, H.K., et al., 1993. Yohimbine potentiates active defensive responses to threatening stimuli in Swiss-Webster mice. *Pharmacology, biochemistry, and behavior*, 44(3), pp.673–81.

Blier, P. & Ward, N.M., 2003. Is there a role for 5-HT1A agonists in the treatment of depression? *Biological psychiatry*, 53(3), pp.193–203.

Bockaert, J., Claeysen, S. & Martin, P., 2010. Classification and signaling characteristics of 5-HT receptors. In C. Muller & B. Jacobs, eds. *Handbook of Behavioral Neurobiology of serotonin*.

Borsini, F., 1995. Role of the serotonergic system in the forced swimming test. *Neuroscience and biobehavioral reviews*, 19(3), pp.377–95.

Boureau, Y.-L. & Dayan, P., 2011. Opponency revisited: competition and cooperation between dopamine and serotonin. *Neuropsychopharmacology : official publication of the American College of Neuropsychopharmacology*, 36(1), pp.74–97.

Bowker, R.M., 1986. Intrinsic 5HT-immunoreactive neurons in the spinal cord of the fetal non-human primate. *Brain research*, 393(1), pp.137–43.

Boyden, E.S., 2015. Optogenetics and the future of neuroscience. *Nature Neuroscience*, 18(9), pp.1200–1201.

Broadhurst, P.L., 1957. Determinants of emotionality in the rat. I. Situational factors. *British journal of psychology (London, England : 1953)*, 48(1), pp.12–20.

Broadhurst, P.L., 1958. Determinants of emotionality in the rat. II. Antecedent factors. *British journal of psychology (London, England : 1953)*, 49(1), pp.12–20.

Brodie, B.B. & Shore, P. a, 1957. A concept for a role of serotonin and norepinephrine as chemical mediators in the brain. *Annals of the New York Academy of Sciences*, 66(3), pp.631–642.

Bromberg-Martin, E.S., Hikosaka, O. & Nakamura, K., 2010. Coding of task reward value in the dorsal raphe nucleus. *The Journal of neuroscience : the official journal of the Society for Neuroscience*, 30(18), pp.6262–6272.

Carter, C.S. et al., 1992. Oxytocin and social bonding. *Annals of the New York Academy of Sciences*, 652, pp.204–11.

Carter, R.J., Morton, J. & Dunnett, S.B., 2001. Motor coordination and balance in rodents. *Current protocols in neuroscience / editorial board, Jacqueline N. Crawley ... [et al.]*, Chapter 8, p.Unit 8.12.

Cerrito, F. & Raiteri, M., 1979. Serotonin release is modulated by presynaptic autoreceptors. *European journal of pharmacology*, 57(4), pp.427–30.

Challis, C. et al., 2013. Raphe GABAergic neurons mediate the acquisition of avoidance after social defeat. *The Journal of neuroscience : the official journal of the Society for Neuroscience*, 33(35), pp.13978–88, 13988a.

Chamberlain, S.R. et al., 2006. Motor inhibition and cognitive flexibility in obsessive-compulsive disorder and trichotillomania. *The American journal of psychiatry*, 163(7), pp.1282–4.

Chen, C. & Regehr, W.G., 2003. Presynaptic modulation of the retinogeniculate synapse. *The Journal of neuroscience : the official journal of the Society for Neuroscience*, 23(8), pp.3130–5.

Chiang, C.Y. et al., 1989. Changes in mechanoreceptive field properties of trigeminal somatosensory brainstem neurons induced by stimulation of nucleus raphe magnus in cats. *Brain research*, 485(2), pp.371–81.

Choi, I.-S. et al., 2012. 5-HT(1B) receptors inhibit glutamate release from primary afferent terminals in rat medullary dorsal horn neurons. *British journal of pharmacology*, 167(2), pp.356–67.

Choleris, E., 2001. A detailed ethological analysis of the mouse open field test: effects of diazepam, chlordiazepoxide and an extremely low frequency pulsed magnetic field. *Neuroscience & Biobehavioral Reviews*, 25(3), pp.235–260.

Clark, L., Cools, R. & Robbins, T.W., 2004. The neuropsychology of ventral prefrontal cortex: Decision-making and reversal learning. *Brain and Cognition*, 55(1), pp.41–53.

Clark, T., Weissbach, H. & Udenfriend, S., 1954. 5-hydroxytryptophan decarboxylase: preparation and properties. *Journal of Biological Chemistry*, Sep(210(1)), pp.139–148.

Cohen, J., Amoroso, M. & Uchida, N., 2015. Serotonergic neurons signal reward and punishment on multiple timescales. *eLife*, pp.3–5.

Cools, R., Nakamura, K. & Daw, N.D., 2011. Serotonin and dopamine: unifying affective, activational, and decision functions.

Neuropsychopharmacology : official publication of the American College of Neuropsychopharmacology, 36(1), pp.98–113.

Cools, R., Roberts, A.C. & Robbins, T.W., 2007. Serotoninergic regulation of emotional and behavioural control processes. *Trends in Cognitive Sciences*, 12(1), pp.31–40.

Dahlstroem, A. & Fuxe, K., 1964. Evidence for the existence of monoamine-containing neurons in the central nervous sys- tem. I. Demonstration of monoamines in the cell bodies of brainstem neurons. *Acta physiologica Scandinavica. Supplementum*, p.SUPPL 232:1–55.

Davidson, J.M., 1966. Activation of the male rat's sexual behavior by intracerebral implantation of androgen. *Endocrinology*, 79(4), pp.783–94.

Davis, M. & Sheard, M.H., 1974. Habituation and sensitization of the rat startle response: effects of raphe lesions. *Physiology and Behavior*, 12(3), pp.425–431.

Davis, M., Strachan, D.I. & Kass, E., 1980. Excitatory and inhibitory effects of serotonin on sensorimotor reactivity measured with acoustic startle. *Science (New York, N.Y.)*, 209(4455), pp.521–523.

Daw, N.D. & Daw, N., 2002. Opponent Interactions between Serotonin and Dopamine Opponent Interactions between Serotonin and Dopamine. , 2582, pp.603–616.

Dayan, P. & Huys, Q., 2009. Serotonin in affective control. *Annual review of neuroscience*, 32, pp.95–126.

Dayan, P. & Huys, Q.J.M., 2008. Serotonin, inhibition, and negative mood. *PLoS Computational Biology*, 4(2).

Deakin, J.F.W. & Graeff, F.G., 1991. 5-HT and mechanisms of defence. Author's response. *Journal of Psychopharmacology*, 5(4), pp.339–341.

Deisseroth, K., 2015. Optogenetics : 10 years of microbial opsins in neuroscience. *Nature*, 18(9), pp.1213–1225.

Delgado, P.L. et al., 1991. Rapid serotonin depletion as a provocative challenge test for patients with major depression: relevance to antidepressant action and the neurobiology of depression. *Psychopharmacology bulletin*, 27(3), pp.321–30.

Depue, R.A. & Spoont, M.R., 1986. Conceptualizing a serotonin trait. A behavioral dimension of constraint. *Annals of the New York Academy of Sciences*, 487, pp.47–62.

Derkach, V., Surprenant, A. & North, R.A., 1989. 5-HT3 receptors are membrane ion channels. *Nature*, 339(6227), pp.706–709.

Descarries, L. et al., 1982. The serotonin neurons in nucleus raphe dorsalis of adult rat: a light and electron microscope radioautographic study. *The Journal of comparative neurology*, 207(3), pp.239–54.

Dewsbury, D.A. & Davis, H.N., 1970. Effects of reserpine on the copulatory behavior of male rats. *Physiology & behavior*, 5(11), pp.1331–3.

Dewsbury, D.A., Davis, H.N. & Jansen, P.E., 1972. Effects of monoamine oxidase inhibitors on the copulatory behavior of male rats. *Bulletin of the Menninger Clinic*, 36(1), pp.209–17.

Dixon, L.K. & Mayeda, D. V, 1976. Effects of floor textures on open-field behavior in selected lines of mice. *Behavior genetics*, 6(1), pp.87–92.

Dong, W. et al., 1991. Focal dorsal raphe stimulation and pinnal electrical stimulation modulate spontaneous and noxious evoked responses in thalamic neurons. *The International journal of neuroscience*, 57(1-2), pp.123–40.

Dugué, G.P. et al., 2014. Optogenetic recruitment of dorsal raphe serotonergic neurons acutely decreases mechanosensory responsivity in behaving mice. *PloS One*, 9(8), p.e105941.

Eagle, D. et al., 2008. Stop-signal reaction-time task performance: role of prefrontal cortex and subthalamic nucleus. *Cerebral cortex (New York, N.Y. : 1991)*, 18(1), pp.178–88.

Eagle, D.M. et al., 2009. Serotonin depletion impairs waiting but not stop-signal reaction time in rats: implications for theories of the role of 5-HT in behavioral inhibition. *Neuropsychopharmacology : official publication of the American College of Neuropsychopharmacology*, 34(5), pp.1311–1321.

Eagle, D.M., Bari, A. & Robbins, T.W., 2008. The neuropsychopharmacology of action inhibition: Cross-species translation of the stop-signal and go/no-go tasks. *Psychopharmacology*, 199(3), pp.439–456.

Evenden, J.L., 1999. Varieties of impulsivity. *Psychopharmacology*, 146(4), pp.348–361.

Fardin, V., Oliveras, J.L. & Besson, J.M., 1984. A reinvestigation of the analgesic effects induced by stimulation of the periaqueductal gray matter in the rat. I. The production of behavioral side effects together with analgesia. *Brain research*, 306(1-2), pp.105–23.

File, S.E., 1985. What can be learned from the effects of benzodiazepines on exploratory behavior? *Neuroscience and biobehavioral reviews*, 9(1), pp.45–54.

Flavell, S.W. et al., 2013. Serotonin and the neuropeptide PDF initiate and extend opposing behavioral states in C. Elegans. *Cell*, 154(5), pp.1023–1035.

Fonseca, M.S., Murakami, M. & Mainen, Z.F., 2015. Activation of Dorsal Raphe Serotonergic Neurons Promotes Waiting but Is Not Reinforcing. *Current Biology*, pp.1–10.

Fornal, C. a. et al., 1996. A subgroup of dorsal raphe serotonergic neurons in the cat is strongly activated during oral-buccal movements. *Brain Research*, 716(1-2), pp.123–133.

Fornal, C.A. et al., 1994. Single-unit responses of serotonergic dorsal raphe neurons to 5-HT1A agonist and antagonist drug administration in behaving cats. *The Journal of pharmacology and experimental therapeutics*, 270(3), pp.1345–58.

Gately, P.F. et al., 1985. Depletion of brain serotonin by 5,7-dihydroxytryptamine alters the response to amphetamine and the habituation of locomotor activity in rats. *Psychopharmacology*, 87(4), pp.400–5.

Geyer, M.A. et al., 2001. Pharmacological studies of prepulse inhibition models of sensorimotor gating deficits in schizophrenia: a decade in review. *Psychopharmacology*, 156(2-3), pp.117–54.

Glennon, R., Dukat, M. & Westkaemper, R., 1995. Serotonin Receptor Subtypes and Ligands. In F. Bloom & D. Kupfer, eds. *Psychopharmacology - 4th Generation of Progress*. Raven Press, New York.

Glennon, R. & Lucki, I., 1988. Behaviors associated with the activation of serotonin receptors. In E. Sanders-Bush, ed. *The Serotonin Receptors*. The Humana Press Inc.

Gong, S. et al., 2007. Targeting Cre recombinase to specific neuron populations with bacterial artificial chromosome constructs. *The Journal*

of neuroscience : the official journal of the Society for Neuroscience, 27(37), pp.9817–9823.

Graeff, F.G. et al., 1996. Role of 5-HT in stress, anxiety, and depression. *Pharmacology, biochemistry, and behavior*, 54(1), pp.129–41.

Gras, C. et al., 2002. A Third Vesicular Glutamate Transporter Expressed by Cholinergic and Serotoninergic Neurons. , 22(13), pp.5442–5451.

Griebel, G. et al., 1995. Further evidence that the mouse defense test battery is useful for screening anxiolytic and panicolytic drugs: effects of acute and chronic treatment with alprazolam. *Neuropharmacology*, 34(12), pp.1625–33.

Groome, J.R., Clark, M. & Lent, C.M., 1993. The behavioural state of satiation in the leech is regulated by body distension and mimicked by serotonin depletion. *The Journal of experimental biology*, 182, pp.265–70.

Hall, C.S., 1934. Emotional behavior in the rat. I. Defecation and urination as measures of individual differences in emotionality. *Journal of Comparative Psychology*, 18(3), pp.385–403.

Han, X. & Boyden, E.S., 2007. Multiple-color optical activation, silencing, and desynchronization of neural activity, with single-spike temporal resolution. *PloS one*, 2(3), p.e299.

Harrison, A.A., Everitt, B.J. & Robbins, T.W., 1997. Central 5-HT depletion enhances impulsive responding without affecting the accuracy of attentional performance: interactions with dopaminergic mechanisms. *Psychopharmacology*, 133(4), pp.329–42.

Harrison, A.A., Everitt, B.J. & Robbins, T.W., 1999. Central serotonin depletion impairs both the acquisition and performance of a symmetrically reinforced go / no-go conditional visual discrimination. , 100, pp.99–112.

Hawkins, M.F. et al., 2002. Behavioral responses to stress following central and peripheral injection of the 5-HT 2 agonist DOI. *Pharmacology, biochemistry, and behavior*, 73, pp.537–544.

Heninger, G.R., Delgado, P.L. & Charney, D.S., 1996. The revised monoamine theory of depression: a modulatory role for monoamines, based on new findings from monoamine depletion experiments in humans. *Pharmacopsychiatry*, 29(1), pp.2–11.

Hoyer, D. et al., 1994. International Union of Pharmacology classification of receptors for 5-hydroxytryptamine (Serotonin). *Pharmacological reviews*, 46(2), pp.157–203.

Hull, E.M. & Dominguez, J.M., 2007. Sexual behavior in male rodents. *Hormones and Behavior*, 52(1), pp.45–55.

Hurley, L., Devilbiss, D. & Waterhouse, B., 2004. A matter of focus: monoaminergic modulation of stimulus coding in mammalian sensory networks. *Current Opinion in Neurobiology*, 14(4), pp.488–495.

Ikeda, T. et al., 2009. Effects of intrathecal administration of newer antidepressants on mechanical allodynia in rat models of neuropathic pain. *Neuroscience research*, 63(1), pp.42–6.

Ikemoto, S., Yang, C. & Tan, A., 2015. Basal ganglia circuit loops, dopamine and motivation: A review and enquiry. *Behavioural Brain Research*, 290, pp.17–31.

Inaba, K. et al., 2013. Neurons in Monkey Dorsal Raphe Nucleus Code Beginning and Progress of Step-by-Step Schedule, Reward Expectation, and Amount of Reward Outcome in the Reward Schedule Task. *Journal of Neuroscience*, 33(8), pp.3477–3491.

Ito, H. et al., 2013. Analysis of sleep disorders under pain using an optogenetic tool: possible involvement of the activation of dorsal raphe nucleus-serotonergic neurons. *Molecular brain*, 6(1), p.59.

Iwayama, K. et al., 1989. Effect of midbrain raphe nucleus stimulation on somatosensory evoked potential in cat. *Neurological research*, 11(2), pp.105–8.

Jackson, H.C. & Nutt, D.J., 1992. Effects of benzodiazepine receptor inverse agonists on locomotor activity and exploration in mice. *European journal of pharmacology*, 221(2-3), pp.199–203.

Jacobs, B.L., Asher, R. & Dement, W.C., 1973. Electrophysiological and behavioral effects of electrical stimulation of the raphe nuclei in cats. *Physiology & Behavior*, 11(4), pp.489–495.

Jacobs, B.L. & Azmitia, E.C., 1992. Structure and function of the brain serotonin system. *Physiological reviews*, 72(1), pp.165–229.

Jacobs, B.L. & Fornal, C. a, 1993. 5-HT and motor control: a hypothesis. *Trends in neurosciences*, 16(9), pp.346–352.

Jacobs, B.L. & Fornal, C. a., 1997. Serotonin and motor activity. *Current Opinion in Neurobiology*, 7(6), pp.820–825.

Jensen, P. et al., 2008. Redefining the serotonergic system by genetic lineage. *Nature neuroscience*, 11(4), pp.417–9.

De Jong, T.R. et al., 2005. Effects of chronic selective serotonin reuptake inhibitors on 8-OH-DPAT-induced facilitation of ejaculation in rats: comparison of fluvoxamine and paroxetine. *Psychopharmacology*, 179(2), pp.509–15.

De Jong, T.R. et al., 2006. Serotonin and the neurobiology of the ejaculatory threshold. *Neuroscience and Biobehavioral Reviews*, 30(7), pp.893–907.

Katsuyama, S. et al., 2013. Effects of repeated milnacipran and fluvoxamine treatment on mechanical allodynia in a mouse paclitaxel-induced neuropathic pain model. *Biomedical research (Tokyo, Japan)*, 34(2), pp.105–11.

Kayama, Y. et al., 1989. Effects of stimulating the dorsal raphe nucleus of the rat on neuronal activity in the dorsal lateral geniculate nucleus. *Brain research*, 489(1), pp.1–11.

Kiser, D. et al., 2012. The reciprocal interaction between serotonin and social behaviour. *Neuroscience and Biobehavioral Reviews*, 36(2), pp.786–798.

Kita, I., Yoshida, Y. & Nishino, S., 2006. An activation of parvocellular oxytocinergic neurons in the paraventricular nucleus in oxytocin-induced yawning and penile erection. *Neuroscience research*, 54(4), pp.269–75.

Kostowski, W. et al., 1969. Electrical stimulation of midbrain raphe: biochemical, behavioral and bioelectrical effects. *European journal of pharmacology*, 7(2), pp.170–5.

Kravitz, E.A., 1988. Hormonal control of behavior: amines and the biasing of behavioral output in lobsters. *Science (New York, N.Y.)*, 241(4874), pp.1775–81.

Lai, Y.Y. & Siegel, J.M., 1988. Medullary regions mediating atonia. *The Journal of neuroscience : the official journal of the Society for Neuroscience*, 8(12), pp.4790–6.

Lee, H. et al., 2014. Scalable control of mounting and attack by Esr1+ neurons in the ventromedial hypothalamus. *Nature*, 509(7502), pp.627–32.

Leonard, B.E., 1987. Depression: A psychobiological Synthesis. *Human Psychopharmacology: Clinical and Experimental*, 2(4), pp.248–249.

Lima, S.Q. et al., 2009. PINP: a new method of tagging neuronal populations for identification during in vivo electrophysiological recording. *PloS one*, 4(7), p.e6099.

Lister, S. et al., 1996. Acquisition of conditioned inhibition in rats is impaired by ablation of serotoninergic pathways. *The European journal of neuroscience*, 8(2), pp.415–23.

Liu, Z. et al., 2014. Dorsal raphe neurons signal reward through 5-HT and glutamate. *Neuron*, 81(6), pp.1360–1374.

Lopes, G. et al., 2015. Bonsai: An event-based framework for processing and controlling data streams. *Frontiers in Neuroinformatics*, 8(April), pp.1–14.

Lorrain, D.S. et al., 1997. Extracellular serotonin in the lateral hypothalamic area is increased during the postejaculatory interval and impairs copulation in male rats. *The Journal of neuroscience : the official journal of the Society for Neuroscience*, 17(23), pp.9361–9366.

Lorrain, D.S. et al., 1999. Lateral hypothalamic serotonin inhibits nucleus accumbens dopamine: implications for sexual satiety. *The Journal of neuroscience : the official journal of the Society for Neuroscience*, 19(17), pp.7648–7652.

Lottem, E., Lorincz, M. & Mainen, Z., Optogenetic activation of dorsal raphe serotonin neurons rapidly inhibits spontaneous but not odor-evoked activity in olfactory cortex. *submitted*.

Lucki, I., 1998. The spectrum of behaviors influenced by serotonin. *Biological Psychiatry*, 44(3), pp.151–162.

Luo, M., Zhou, J. & Liu, Z., 2015. Reward processing by the dorsal raphe nucleus: 5-HT and beyond. *Learning & memory (Cold Spring Harbor, N.Y.)*, 22(9), pp.452–60.

Machado, A. et al., 2015. A quantitative framework for whole-body coordination reveals specific deficits in freely walking ataxic mice. *submitted*.

Maier, S.F. & Watkins, L.R., 2005. Stressor controllability and learned helplessness: the roles of the dorsal raphe nucleus, serotonin, and

corticotropin-releasing factor. *Neuroscience and biobehavioral reviews*, 29(4-5), pp.829–41.

Mantz, J. et al., 1990. Inhibition of spontaneous and evoked unit activity in the rat medial prefrontal cortex by mesencephalic raphe nuclei. *Brain research*, 524(1), pp.22–30.

Martín-Cora, F.J. et al., 2000. Single-unit responses of serotonergic medullary and pontine raphe neurons to environmental cooling in freely moving cats. *Neuroscience*, 98(2), pp.301–309.

Matias, S. et al., Modulation of dopamine and serotonin activity by expectation mismatches during reversal learning. *submitted*.

McDevitt, R.A. et al., 2014. Serotonergic versus Nonserotonergic Dorsal Raphe Projection Neurons: Differential Participation in Reward Circuitry. *Cell Reports*, 8(6), pp.1857–1869.

McDevitt, R.A. & Neumaier, J.F., 2011. Regulation of dorsal raphe nucleus function by serotonin autoreceptors: a behavioral perspective. *Journal of chemical neuroanatomy*, 41(4), pp.234–46.

McGill, T.E., 1962. Sexual Behavior in Three Inbred Strains of Mice. *Behaviour*, 19(4), pp.341–350.

Mclntosh, T.K. & Barfield, R.J., 1984. Mcintosh84. , 12, pp.1–11.

Miyazaki, K., Miyazaki, K. & Doya, K., 2011. Activation of dorsal raphe serotonin neurons underlies waiting for delayed rewards. *The Journal of neuroscience : the official journal of the Society for Neuroscience*, 31(2), pp.469–479.

Miyazaki, K.W. et al., 2014. Optogenetic Activation of Dorsal Raphe Serotonin Neurons Enhances Patience for Future Rewards. *Current Biology*, pp.1–8.

Miyazaki, K.W., Miyazaki, K. & Doya, K., 2012. Activation of Dorsal Raphe Serotonin Neurons Is Necessary for Waiting for Delayed Rewards.pdf. *The Journal of neuroscience*, 32(31), pp.10451–10457.

Moser, E.I., Kropff, E. & Moser, M.-B., 2008. Place cells, grid cells, and the brain's spatial representation system. *Annual review of neuroscience*, 31, pp.69–89.

Müller, C.P., De Souza Silva, M.A. & Huston, J.P., 2007. Double dissociating effects of sensory stimulation and cocaine on serotonin activity in the occipital and temporal cortices. *Neuropharmacology*, 52(3), pp.854–62.

Nagel, G. et al., 2003. Channelrhodopsin-2, a directly light-gated cation-selective membrane channel. *Proceedings of the National Academy of Sciences of the United States of America*, 100(24), pp.13940–5.

Nakamura, K., Matsumoto, M. & Hikosaka, O., 2008. Reward-dependent modulation of neuronal activity in the primate dorsal raphe nucleus. *The Journal of neuroscience : the official journal of the Society for Neuroscience*, 28(20), pp.5331–5343.

Normandin, J.J. & Murphy, A.Z., 2011. Serotonergic lesions of the periaqueductal gray, a primary source of serotonin to the nucleus paragigantocellularis, facilitate sexual behavior in male rats. *Pharmacology Biochemistry and Behavior*, 98(3), pp.369–375.

O'Keefe, J. & Dostrovsky, J., 1971. The hippocampus as a spatial map. Preliminary evidence from unit activity in the freely-moving rat. *Brain research*, 34(1), pp.171–5.

Ogawa, S. et al., 2014. Organization of Monosynaptic Inputs to the Serotonin and Dopamine Neuromodulatory Systems. *Cell Reports*, pp.1–14.

Oh, E. et al., 2010. Substitution of 5-HT1A receptor signaling by a light-activated G protein-coupled receptor. *The Journal of biological chemistry*, 285(40), pp.30825–36.

Ohmura, Y. et al., 2014. Optogenetic activation of serotonergic neurons enhances anxiety-like behaviour in mice. *The international journal of neuropsychopharmacology / official scientific journal of the Collegium Internationale Neuropsychopharmacologicum (CINP)*, 2, pp.1–7.

Penadés, R. et al., 2007. Impaired response inhibition in obsessive compulsive disorder. *European psychiatry : the journal of the Association of European Psychiatrists*, 22(6), pp.404–10.

Peroutka, S.J. & Howell, T.A., 1994. The molecular evolution of G protein-coupled receptors: focus on 5-hydroxytryptamine receptors. *Neuropharmacology*, 33(3-4), pp.319–24.

Petzold, G.C., Hagiwara, A. & Murthy, V.N., 2009. Serotonergic modulation of odor input to the mammalian olfactory bulb. *Nature neuroscience*, 12(6), pp.784–91.

Pfaus, J.G., 2009. Pathways of sexual desire. *Journal of Sexual Medicine*, 6(6), pp.1506–1533.

Piszczek, L. et al., 2015. Modulation of anxiety by cortical serotonin 1A receptors. *Frontiers in Behavioral Neuroscience*, 9(February), pp.1–10.

Piszczek, L. et al., 2013. Serotonin 1A auto-receptors are not sufficient to modulate anxiety in mice. *European Journal of Neuroscience*, 38(4), pp.2621–2627.

Pollak Dorocic, I. et al., 2014. A whole-brain atlas of inputs to serotonergic neurons of the dorsal and median raphe nuclei. *Neuron*, 83(3), pp.663–78.

Porsolt, R.D. et al., 1978. Behavioural despair in rats: a new model sensitive to antidepressant treatments. *European journal of pharmacology*, 47(4), pp.379–91.

Prut, L. & Belzung, C., 2003. The open field as a paradigm to measure the effects of drugs on anxiety-like behaviors: a review. *European journal of pharmacology*, 463(1), pp.3–33.

Pum, M.E. et al., 2008. Visual sensory-motor gating by serotonin activation in the medial prefrontal and occipital, but not in the rhinal, cortices in rats. *Neuroscience*, 153(2), pp.361–72.

Qi, J. et al., 2014. A glutamatergic reward input from the dorsal raphe to ventral tegmental area dopamine neurons. *Nature communications*, 5, p.5390.

Qiao, J.T. & Dafny, N., 1988. Dorsal raphe stimulation modulates nociceptive responses in thalamic parafascicular neurons via an ascending pathway: further studies on ascending pain modulation pathways. *Pain*, 34(1), pp.65–74.

Ranade, S.P. & Mainen, Z.F., 2009. Transient firing of dorsal raphe neurons encodes diverse and specific sensory, motor, and reward events. *Journal of neurophysiology*, 102(5), pp.3026–3037.

Rapport, M.M., Green, A.A. & Page, I.H., 1948. Crystalline Serotonin. *Science (New York, N.Y.)*, 108(2804), pp.329–30.

Reyes-Vazquez, C., Qiao, J.T. & Dafny, N., 1989. Nociceptive responses in nucleus parafascicularis thalami are modulated by dorsal raphe stimulation and microiontophoretic application of morphine and serotonin. *Brain research bulletin*, 23(6), pp.405–11.

Riad, M. et al., 2001. Agonist-induced internalization of serotonin-1a receptors in the dorsal raphe nucleus (autoreceptors) but not hippocampus (heteroreceptors). *The Journal of neuroscience : the official journal of the Society for Neuroscience*, 21(21), pp.8378–86.

Richerson, G.B., 2004. Serotonergic neurons as carbon dioxide sensors that maintain pH homeostasis. *Nature reviews. Neuroscience*, 5(6), pp.449–61.

Rodríguez-Manzo, G. et al., 2002. Participation of 5-HT(1B) receptors in the inhibitory actions of serotonin on masculine sexual behaviour of mice: pharmacological analysis in 5-HT(1B) receptor knockout mice. *British journal of pharmacology*, 136(8), pp.1127–1134.

Rogers, R.D. et al., 2003. Tryptophan depletion alters the decision-making of healthy volunteers through altered processing of reward cues. *Neuropsychopharmacology : official publication of the American College of Neuropsychopharmacology*, 28(1), pp.153–162.

Rothermel, M. et al., 2013. Transgene expression in target-defined neuron populations mediated by retrograde infection with adeno-associated viral vectors. *The Journal of neuroscience : the official journal of the Society for Neuroscience*, 33(38), pp.15195–206.

Sahley, C.L., 1995. What we have learned from the study of learning in the leech. *Journal of neurobiology*, 27(3), pp.434–45.

Sawin, E.R., Ranganathan, R. & Horvitz, H.R., 2000. C. elegans locomotory rate is modulated by the environment through a dopaminergic pathway and by experience through a serotonergic pathway. *Neuron*, 26(3), pp.619–631.

Schachar, R. et al., 2007. Restraint and cancellation: multiple inhibition deficits in attention deficit hyperactivity disorder. *Journal of abnormal child psychology*, 35(2), pp.229–38.

Schultz, W., Dayan, P. & Montague, P.R., 1997. A neural substrate of prediction and reward. *Science (New York, N.Y.)*, 275(5306), pp.1593–1599.

Scott, M.M., Krueger, K.C. & Deneris, E.S., 2005. A differentially autoregulated Pet-1 enhancer region is a critical target of the transcriptional cascade that governs serotonin neuron development. *The Journal of neuroscience : the official journal of the Society for Neuroscience*, 25(10), pp.2628–36.

Seibenhener, M.L. & Wooten, M.C., 2015. Use of the Open Field Maze to measure locomotor and anxiety-like behavior in mice. *Journal of visualized experiments : JoVE*, (96), p.e52434.

Seymour, B. et al., 2012. Serotonin selectively modulates reward value in human decision-making. *The Journal of neuroscience*, 32(17), pp.5833–5842.

Sheibani, V. & Farazifard, R., 2006. Dorsal raphe nucleus stimulation modulates the response of layers IV and V barrel cortical neurons in rat. *Brain research bulletin*, 68(6), pp.430–5.

Soubrié, P., 1986. Reconciling the role of central serotonin neurons in human and animal beh. *The behavioral and brain sciences*, (9), pp.319–364.

Stark, K.L. et al., 2007. A novel conditional knockout strategy applied to serotonin receptors. *Handbook of experimental pharmacology*, (178), pp.347–63.

Steinbusch, H.W.M., 1981. Distribution of serotonin-immunoreactivity in the central nervous system of the rat—Cell bodies and terminals. *Neuroscience*, 6(4), pp.557–618.

Sternson, S.M., 2013. Hypothalamic survival circuits: Blueprints for purposive behaviors. *Neuron*, 77(5), pp.810–824.

Takeda, H., Tsuji, M. & Matsumiya, T., 1998. Changes in head-dipping behavior in the hole-board test reflect the anxiogenic and/or anxiolytic state in mice. *European journal of pharmacology*, 350(1), pp.21–9.

Tecuapetla, F. et al., 2014. Balanced activity in basal ganglia projection pathways is critical for contraversive movements. *Nature communications*, 5, p.4315.

Tenen, S.S., 1967. The effects of p-chlorophenylalanine, a serotonin depletor, on avoidance acquisition, pain sensitivity and related behavior in the rat. *Psychopharmacologia*, 10(3), pp.204–219.

Törk, I., 1990. Anatomy of the serotonergic system. *Annals of the New York Academy of Sciences*, 600, pp.9–34.

Tritsch, N.X., Ding, J.B. & Sabatini, B.L., 2012. Dopaminergic neurons inhibit striatal output through non-canonical release of GABA. *Nature*, 490(7419), pp.262–266.

Trudeau, L.-E., 2004. Glutamate co-transmission as an emerging concept in monoamine neuron function. *Journal of psychiatry & neuroscience : JPN*, 29(4), pp.296–310.

Varga, V. et al., 2009. Fast synaptic subcortical control of hippocampal circuits. *Science (New York, N.Y.)*, 326(5951), pp.449–53.

Veasey, S. et al., 1997. Single-unit responses of serotonergic dorsal raphe neurons to specific motor challenges in freely moving cats. *Neuroscience*, 79(1), pp.161–169.

Vega Matuszcyk, J., Larsson, K. & Eriksson, E., 1998. The selective serotonin reuptake inhibitor fluoxetine reduces sexual motivation in male rats. *Pharmacology, biochemistry, and behavior*, 60(2), pp.527–32.

Vergnes, M., Depaulis, A. & Boehrer, A., 1986. Parachlorophenylalanine-induced serotonin depletion increases offensive but not defensive aggression in male rats. *Physiology & Behavior*, 36(4), pp.653–658.

Vertes, R. & Linley, S., 2008. Efferent and afferent connections of the dorsal and median raphe nuclei in the rat. In B. L. Jacobs & D. J. Nutt, eds. *Serotonin and Sleep: Molecular, Functional and Clinical Aspects*.

Vialli, M. & Erspamer, V., 1937. Ricerche sul secreto delle cellule enterocromaffini. *Zeitschrift for Zellforschung und Mikroskopische Anatomie*, 27(1), pp.81–99.

Walletschek, H. & Raab, A., 1982. Spontaneous activity of dorsal raphe neurons during defensive and offensive encounters in the tree-shrew. *Physiology & behavior*, 28(4), pp.697–705.

Walsh, R.N. & Cummins, R.A., 1976. The open-field test: A critical review. *Psychological bulletin*, 83(3), p.482.

Wang, H. et al., 2007. High-speed mapping of synaptic connectivity using photostimulation in Channelrhodopsin-2 transgenic mice. *Proceedings of the National Academy of Sciences of the United States of America*, 104(19), pp.8143–8.

Wang, Q.P. & Nakai, Y., 1994. The dorsal raphe: an important nucleus in pain modulation. *Brain research bulletin*, 34(6), pp.575–85.

Warden, M.R. et al., 2012. A prefrontal cortex-brainstem neuronal projection that controls response to behavioural challenge. *Nature*, 492(7429), pp.428–32.

Waterhouse, B.D. et al., 1990. Modulation of rat cortical area 17 neuronal responses to moving visual stimuli during norepinephrine and serotonin microiontophoresis. *Brain research*, 514(2), pp.276–92.

Weissbourd, B. et al., 2014. Presynaptic Partners of Dorsal Raphe Serotonergic and GABAergic Neurons. *Neuron*, 83(3), pp.645–662.

Willner, P., 1990. Animal models of depression: an overview. *Pharmacology & therapeutics*, 45(3), pp.425–55.

Winstanley, C.A. et al., 2004. Fractionating Impulsivity : Contrasting Effects of Central 5-HT Depletion on Different Measures of Impulsive Behavior. *Neuropsychopharmacology*, pp.1–13.

Xu, W.J. et al., 2013. Involvement of ventrolateral orbital cortex 5-HT 1-7 receptors in 5-HT induced depression of spared nerve injury allodynia. *Neuroscience*, 238, pp.252–7.

Yamanouchi, K. & Kakeyama, M., 1992. Effect of medullary raphe lesions on sexual behavior in male rats with or without treatments of p-chlorophenylalanine. *Physiology & behavior*, 51(3), pp.575–579.

Yokogawa, T., Hannan, M.C. & Burgess, H.A., 2012. The dorsal raphe modulates sensory responsiveness during arousal in zebrafish. *The Journal of neuroscience : the official journal of the Society for Neuroscience*, 32(43), pp.15205–15.

Yoshida, M., Sasa, M. & Takaori, S., 1984. Serotonin-mediated inhibition from dorsal raphe nucleus of neurons in dorsal lateral geniculate and thalamic reticular nuclei. *Brain research*, 290(1), pp.95–105.

Zangrossi, H. & Graeff, F.G., 2014. Serotonin in anxiety and panic: Contributions of the elevated T-maze. *Neuroscience and Biobehavioral Reviews*, 46, pp.397–406.

Zhang, F. et al., 2007. Multimodal fast optical interrogation of neural circuitry. *Nature*, 446(7136), pp.633–9.

Zhuang, X. et al., 2005. Targeted gene expression in dopamine and serotonin neurons of the mouse brain. *Journal of Neuroscience Methods*, 143(1), pp.27–32.